Appendix 2

Supporting Information for Chapter 3
Accelerating Ni(II) Precatalyst Initiation using Reactive Ligands and
Its Impact on Chain-Growth Polymerizations

I. Materials

Flash chromatography was performed on SiliCycle silica gel (40-63 μm) and thin layer chromatography was performed on Merck TLC plates pre-coated with silica gel 60 F254. *i*-PrMgCl (2 M in THF) was purchased in 100 mL quantities from Aldrich. Bis(cyclooctadiene)nickel (Ni(cod)$_2$) and 1,2-bis(diphenylphosphino)ethane (dppe) were purchased from Strem. All other reagent grade materials and solvents were purchased from Aldrich, Acros, EMD, or Fisher and used without further purification unless otherwise noted. THF was dried and deoxygenated using an Innovative Technology (IT) solvent purification system composed of activated alumina, copper catalyst, and molecular sieves. *N*-Bromosuccinimide (NBS) was recrystallized from hot water and dried over P$_2$O$_5$. Compounds **1a-d**,[1] **2**,[2] **S1**,[3] **S2**,[4] **S3**,[1] **S4**,[4] **S5**,[5] **S6**,[1] **S7**,[5] **S8**,[1] **S9**,[5] **S10**,[1] **S11**,[6] were prepared from modified literature procedures.

II. General Experimental

NMR Spectroscopy: Unless otherwise noted, ^{1}H, ^{13}C, ^{19}F and ^{31}P NMR spectra for all compounds were acquired at rt in acetone-d_6 or $CDCl_3$ on a Varian vnmrs 700 operating at 700, 176, 660, and 283 MHz, Varian vnmrs 500 operating at 500, 126, 470, and 202 MHz or a Varian MR 400 operating at 400, 100, 376 and 162 MHz, respectively. For ^{1}H and ^{13}C spectra in deuterated solvents, the chemical shift data are reported in units of δ (ppm) relative to tetramethylsilane (TMS) and referenced with residual solvent. ^{19}F NMR spectra were referenced to $CFCl_3$ and ^{31}P NMR spectra were referenced to H_3PO_4. For ^{1}H, ^{19}F and ^{31}P NMR spectra in non-deuterated THF, the chemical shift data are reported in units of δ (ppm) and referenced with the THF peak at 3.58 ppm in the ^{1}H NMR spectrum which is then applied to all nuclei. Multiplicities are reported as follows: singlet (s), doublet (d), doublet of doublets (dd), triplet (t), quartet (q), multiplet (m), broad resonance (br), and apparent triplet (at).

Mass Spectrometry: HRMS data were obtained on a Micromass AutoSpec Ultima Magnetic Sector mass spectrometer.

IR Spectroscopy: Samples were recorded using a Mettler Toledo ReactIR iC10 fitted with a Mercury Cadmium Telluride (MCT) detector, and AgX probe (9.5 mm x 1.5 mm) with a SiComp tip. The spectra were processed using icIR 4.0 software and raw absorbances were exported into Microsoft Excel or Sigma Plot 10 for analysis.

MALDI-TOF MS: MALDI-TOF mass spectra were recorded using Waters Tofspec-2E in reflectron mode at a unit mass resolution of 4000. The matrix, α-cyano-4-hydroxy-cinnamic acid (CHCA), was prepared at a concentration of 10 mg/mL in a solution of 50/50 (v/v) CH_3CN/EtOH. The instrument was mass calibrated with a mixture of peptides in the CHCA matrix. The polymer sample was dissolved in CH_2Cl_2 to obtain a ~1 mg/mL solution. A 3 μL aliquot of polymer solution was mixed with 3 μL of the matrix solution. This mixture (1 μL) was placed on the target plate and then air-dried.

Gel-Permeation Chromatography: Polymer molecular weights were determined by comparison with polystyrene standards (Varian, EasiCal PS-2 MW 580-377,400) on a Waters 1515 HPLC instrument equipped with Waters Styragel® (7.8 x 300 mm) THF HR 0.5, THF HR 1, and THF HR 4 type columns in sequence and analyzed with Waters 2487 dual absorbance detector (254 nm). Samples were dissolved in THF (with mild heating) and passed through a 0.2 μm PTFE filter prior to analysis.

Titrations of the Grignard Reagents: An accurately weighed sample of salicylaldehyde phenylhydrazone[7] (typically between 290-310 mg) was dissolved in 5.00 mL of THF. A 0.50 mL aliquot of this solution was stirred at rt while ArMgCl was added dropwise using a 500 μL syringe. The initial solution is yellow
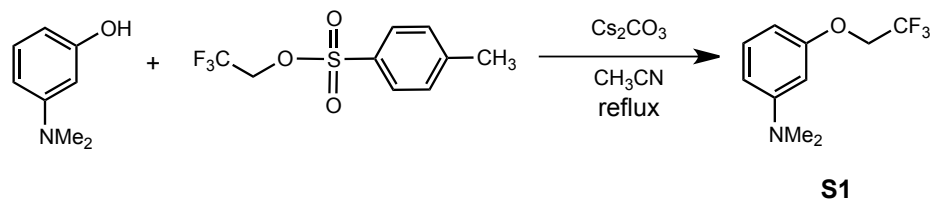
and turns bright orange at the end-point.

Statistical Analysis: Reported quantitative data represents the average of 2-3 experiments and the error bars represent the standard deviation in these measurements.

III. Synthetic Procedures

S1. A 100 mL round-bottom flask was equipped with a stir bar. Sequentially, 3-(dimethylamino)phenol (756 mg, 5.51 mmol, 1.0 equiv), CH_3CN (40 mL), Cs_2CO_3 (3.81 g, 11.7 mmol, 2.0 equiv) and 2,2,2-trifluoroethyl tosylate (1.81 g, 7.12 mmol, 1.3 equiv) were added to the flask. The mixture was refluxed for 4 d. The reaction mixture was cooled and concentrated in vacuo. The resulting mixture was washed with brine (40 mL), extracted with CH_2Cl_2 (3 x 30 mL). The combined organic layers were washed with water (2 x 30 mL) and brine (1 x 30 mL), dried over $MgSO_4$, filtered, and concentrated in vacuo. The resulting oil was purified with silica gel chromatography, using 10/90 (v/v) ethyl acetate/hexanes as the eluent to give 499 mg of **S1** as a clear liquid (41% yield). HRMS (EI): [M+] Calcd. for $C_{10}H_{12}F_3NO$, 219.0871; found, 219.0868. ^{19}F NMR (470 MHz, CDCl$_3$) δ -74.03 (t, J_{H-F} = 8.2 Hz).
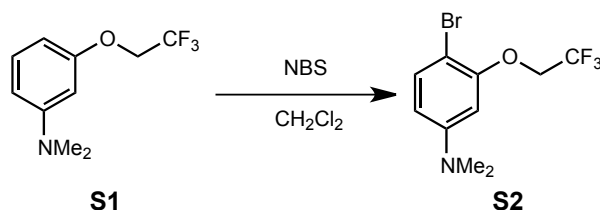

S2. A 10 mL oven-dried round-bottom flask was equipped with a stir bar. Sequentially, **S1** (210 mg, 0.96 mmol, 1.0 equiv), CH_2Cl_2 (3 mL), and NBS (180 mg, 0.99 mmol, 1.0 equiv) were added to the flask. The solution turned from clear to blue in 10 min. The solution was stirred at rt under N_2 overnight. The reaction was quenched with water (5 mL) and extracted with CH_2Cl_2 (3 x 10 mL). The combined organic layers were washed with water (2 x 20 mL) and brine (1 x 20 mL), then dried over $MgSO_4$, filtered, and concentrated in vacuo. The resulting oil was purified with prep HPLC, using 5/95 (v/v) ethyl acetate/hexanes as the eluent to give 114 mg of **S2** as a clear liquid (40% yield). HRMS (EI): [M+] Calcd. for $C_{10}H_{11}BrF_3NO$, 296.9976; found, 296.9975. ^{19}F NMR (470 MHz, CDCl$_3$) δ -73.93 (t, J_{H-F} = 8.2 Hz).

Ni(cod)$_2$ + PPh$_3$ + (S2) → (S3)

Toluene

S2

S3
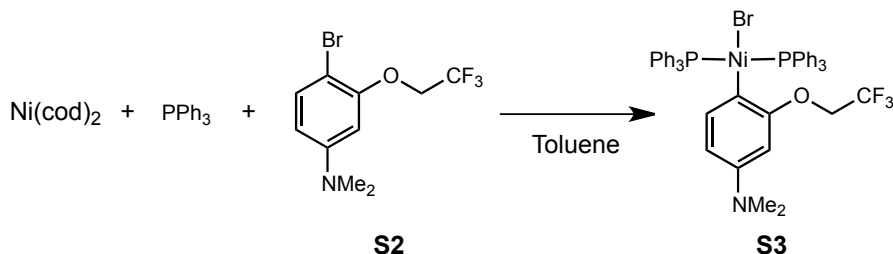
S3. A 20 mL vial was equipped with a stir bar in the glovebox. Sequentially, Ni(cod)$_2$ (70.1 mg, 0.255 mmol, 1.0 equiv), PPh$_3$ (135 mg, 0.515 mmol, 2.0 equiv), **S2** (83.7 mg, 0.281 mmol, 1.1 equiv), and toluene (2.5 mL) were added. The solution was stirred at rt overnight. The reaction was removed from the glovebox. Addition of hexanes (18 mL) led to a yellow orange precipitate. The solid was filtered and washed with hexanes (20 mL) and cold MeOH (5 mL). The resulting solid was recrystallized in THF/hexanes to give 85 mg of **S3** as a yellow solid (39% yield). ^{19}F NMR (470 MHz, CD$_2$Cl$_2$) δ -72.72.

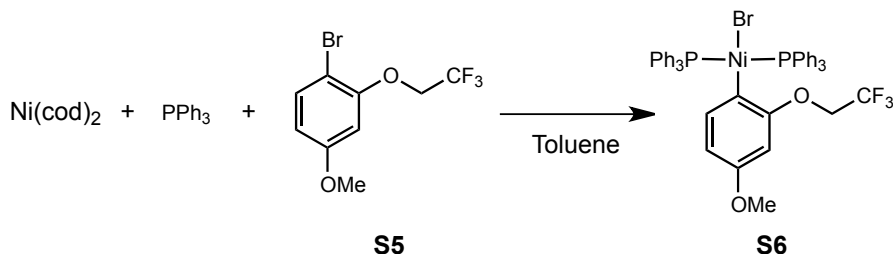**S3** + (dppe) → **1a**

THF

S3

1a
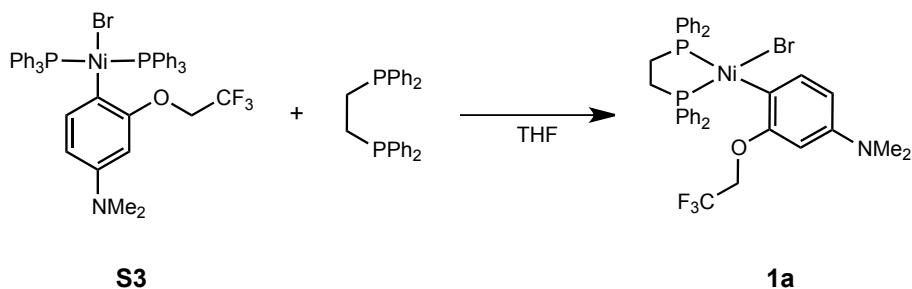
1a. A 20 mL vial was equipped with a stir bar in the glovebox. Sequentially, **S3** (222 mg, 0.252 mmol, 1.0 equiv), dppe (112 mg, 0.281 mmol, 1.1 equiv), and THF (5 mL) were added. The solution was stirred at rt for 2 h. The deep red solution was concentrated in vacuo until ~2 mL of solution was left. Addition of hexanes (18 mL) led to a yellow orange precipitate. The solid was filtered and washed with hexanes (20 mL). The resulting solid was recrystallized in THF/hexanes to give 153 mg of **1a** as an orange solid (81% yield). ^{19}F NMR (376 MHz, acetone-d_6) δ -73.64 (t, J_{H-F} = 9.5 Hz).
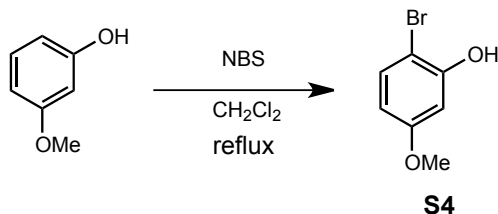
S4. A 100 mL round-bottom flask was equipped with a stir bar. Sequentially, 3-methoxyphenol (1.3 mL, 12 mmol, 1.0 equiv), CH_2Cl_2 (36 mL), and NBS (2.15 g, 12.1 mmol, 1.0 equiv) were added to the flask. The flask was connected to condenser and the reaction was refluxed under N_2 for 2 d. The reaction was cooled to rt and quenched with water (40 mL). The organic layer was washed with water (1 x 40 mL) and brine (1 x 40 mL), then dried over $MgSO_4$, filtered, and concentrated in vacuo. The resulting oil was purified with silica gel chromatography, using 10/90 (v/v) ethyl acetate/hexanes as the eluent to give 1.167 g of **S4** as a clear liquid (48% yield). HRMS (EI): [M+] Calcd. for $C_{10}H_{11}BrF_3NO$, 201.9629; found, 201.9637.
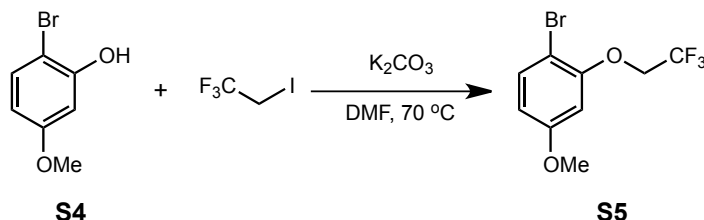

S5. A 35 mL bomb flask was equipped with a stir bar. Sequentially, **S4** (812 mg, 4.00 mmol, 1.0 equiv), DMF (12 mL), K_2CO_3 (1.66 g, 12.0 mmol, 3.0 equiv) and 2-iodo-1,1,1-trifluoroethane (1.6 mL, 16 mmol, 4.0 equiv) were added to the flask. The flask was capped and the reaction was heated to 70 °C for 6 d. Once cooled to rt, the reaction mixture was quenched with water (30 mL) and extracted with CH_2Cl_2 (3 x 30 mL). The combined organic layers were washed with water (2 x 50 mL) and brine (1 x 50 mL), dried over $MgSO_4$, filtered, and concentrated in vacuo. The resulting oil was purified with silica gel chromatography, using 5/95 (v/v) ethyl acetate/hexanes as the eluent to give 865 mg of **S5** as a clear liquid (76% yield). HRMS (EI): [M+] Calcd. for $C_9H_8BrF_3O_2$, 283.9660; found, 283.9662. ^{19}F NMR (470 MHz, $CDCl_3$) δ -73.87 (t, J_{H-F} = 8.3 Hz).

S5 → **S6** (via Ni(cod)$_2$ + PPh$_3$, Toluene)

S6. A 20 mL vial was equipped with a stir bar in the glovebox. Sequentially, Ni(cod)$_2$ (281.5 mg, 1.023 mmol, 1.0 equiv), PPh$_3$ (537.5 mg, 2.049 mmol, 2.0 equiv), **S5** (314.0 mg, 1.102 mmol, 1.1 equiv), and toluene (10 mL) were added. The solution was stirred at rt for 2 h. The reaction was removed from the glovebox and transferred to a 100 mL round-bottom flask. The deep red solution was concentrated in vacuo until ~3 mL of solution was left. Addition of hexanes (50 mL) led to a yellow orange precipitate. The solid was filtered and washed with hexanes (20 mL) and cold MeOH (5 mL). The resulting solid was recrystallized in THF/hexanes to give 431.6 mg of **S6** as a yellow solid (50% yield). Elemental Analysis: Calcd for C$_{45}$H$_{38}$BrF$_3$NiO$_2$P$_2$, C, 62.24; H, 4.41; F, 6.56; Found C, 62.19; H, 4.47; F, 6.77. ^{19}F NMR (470 MHz, CD$_2$Cl$_2$) δ -72.66.


S6 + dppe → **1b** (via THF)
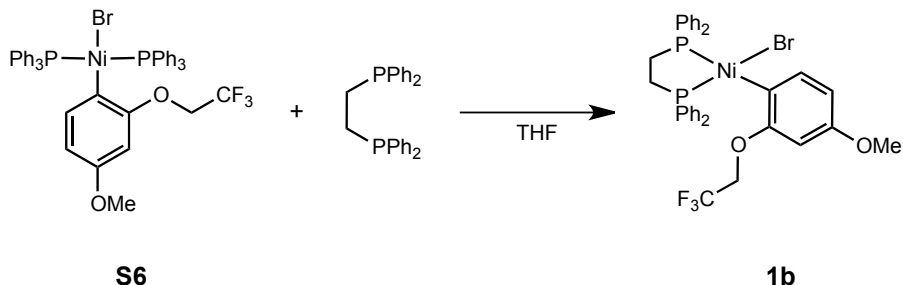
1b. A 20 mL vial was equipped with a stir bar in the glovebox. Sequentially, **S6** (347.4 mg, 0.4001 mmol, 1.0 equiv), dppe (178.1 mg, 0.4470 mmol, 1.1 equiv), and THF (8 mL) were added. The solution was stirred at rt for 2 h. The deep red solution was concentrated in vacuo until ~2 mL of solution was left. Addition of hexanes (18 mL) led to a yellow orange precipitate. The solid was filtered and washed with hexanes (20 mL). The resulting solid was recrystallized in THF/hexanes to give 214.3 mg of **1b** as an orange solid (72% yield). Elemental Analysis: Calcd for C$_{35}$H$_{32}$BrF$_3$NiO$_2$P$_2$, C, 56.64; H, 4.35; F, 7.68; Found C, 56.75; H, 4.64; F, 7.41. ^{19}F NMR (470 MHz, acetone-d_6) δ -73.57 (t, J_{H-F} = 6.7 Hz).
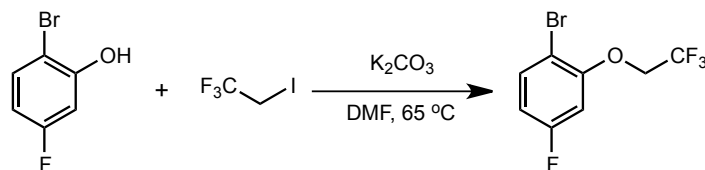
S7. A 35 mL bomb flask was equipped with a stir bar. Sequentially, 2-bromo-5-fluorophenol (0.92 mL, 8.2 mmol, 1.0 equiv), DMF (18 mL), K_2CO_3 (3.40 g, 24.6 mmol, 3.0 equiv) and 2-iodo-1,1,1-trifluoroethane (3.2 mL, 33 mmol, 4.0 equiv) were added to the flask. The flask was capped and the reaction mixture was heated to 65 °C for 14 d. Once cooled to rt, the reaction mixture was quenched with water (40 mL) and extracted with CH_2Cl_2 (3 x 40 mL). The combined organic layers were washed with water (2 x 100 mL) and brine (1 x 100 mL), dried over $MgSO_4$, filtered, and concentrated in vacuo. The resulting oil was purified with silica gel chromatography, using 2/98 (v/v) ethyl acetate/hexanes as the eluent to give 1.67 g of **S7** as a clear liquid (75% yield). HRMS (EI): [M+] Calcd. for $C_8H_5BrF_4O$, 271.9460; found, 271.9456. ^{19}F NMR (470 MHz, $CDCl_3$) δ -74.24 (t, J_{H-F} = 8.3 Hz), -111.54 (q, J_{H-F} = 8.2 Hz).
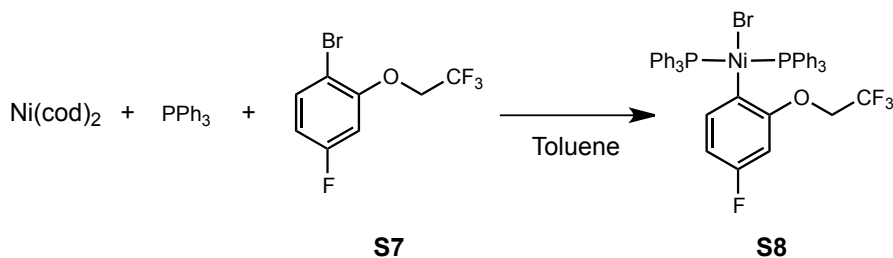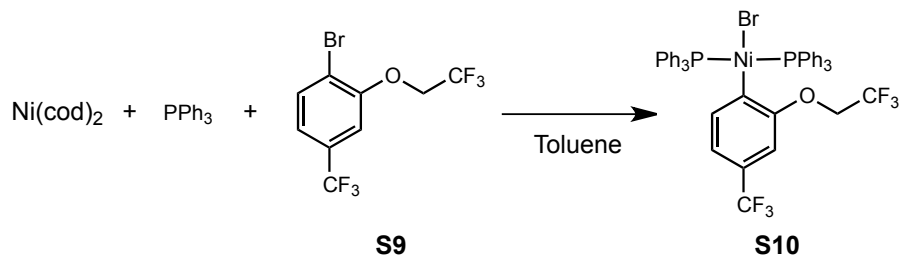

S8. A 20 mL vial was equipped with a stir bar in the glovebox. Sequentially, $Ni(cod)_2$ (276.2 mg, 1.004 mmol, 1.0 equiv), PPh_3 (525.3 mg, 2.003 mmol, 2.0 equiv), **S7** (410.8 mg, 1.505 mmol, 1.5 equiv), and toluene (10 mL) were added. The solution was stirred at rt for 3 h. The reaction was removed from the glovebox and transferred to a 100 mL round-bottom flask. Addition of hexanes (50 mL) led to a yellow orange precipitate. The solid was filtered and washed with hexanes (20 mL) and cold MeOH (5 mL). The resulting solid was dried in vacuo to give 663.6 mg of **S8** as a yellow solid (78% yield). Elemental Analysis: Calcd for $C_{44}H_{35}BrF_4NiOP_2$, C, 61.72; H, 4.12; F, 8.87; Found C, 61.99; H, 4.32; F, 8.97. ^{19}F NMR (470 MHz, $CDCl_3$) δ -72.28 (t, J_{H-F} = 7.0 Hz), -123.50.
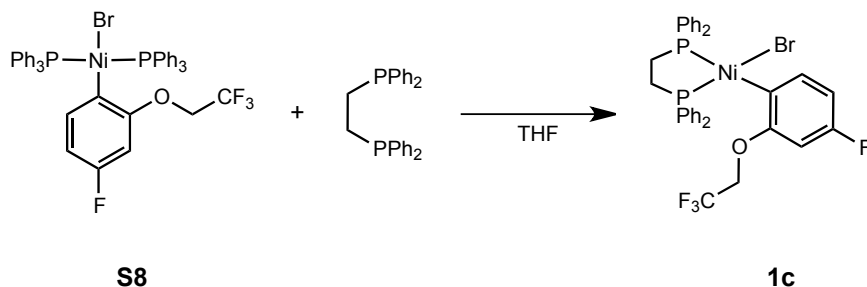
1c. A 20 mL vial was equipped with a stir bar in the glovebox. Sequentially, **S8** (428.5 mg, 0.5004 mmol, 1.0 equiv), dppe (219.3 mg, 0.5504 mmol, 1.1 equiv), and THF (10 mL) were added. The solution was stirred at rt for 2 h. The deep red solution was concentrated in vacuo until ~1 mL of solution was left. Addition of hexanes (18 mL) led to a yellow orange precipitate. The solid was filtered and washed with hexanes (20 mL). The resulting solid was recrystallized in THF/hexanes to give 181.7 mg of **1c** as an orange solid (50% yield). Elemental Analysis: Calcd for $C_{34}H_{29}BrF_4NiOP_2$, C, 55.93; H, 4.00; F, 10.41; Found C, 56.04; H, 4.18; F, 10.16. ^{19}F NMR (470 MHz, acetone-d_6) δ -73.53 (t, J_{H-F} = 8.2 Hz), -123.65 (q, J_{H-F} = 8.6 Hz).
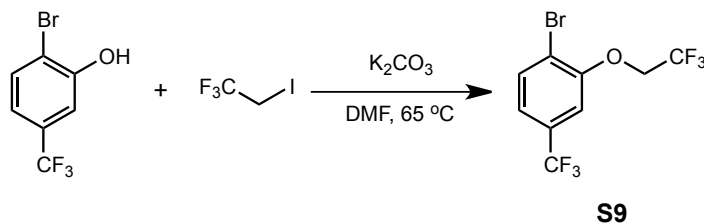

S9. A 35 mL bomb flask was equipped with a stir bar. Sequentially, 2-bromo-5-trifluoromethylphenol (1.98 g, 8.22 mmol, 1.0 equiv), DMF (18 mL), K_2CO_3 (3.40 g, 24.6 mmol, 3.0 equiv) and 2-iodo-1,1,1-trifluoroethane (3.2 mL, 33 mmol, 4.0 equiv) were added to the flask. The flask was capped and the reaction mixture was heated to 65 °C for 14 d. Once cooled to rt, the reaction mixture was quenched with water (40 mL) and extracted with CH_2Cl_2 (3 x 40 mL). The combined organic layers were washed with water (2 x 100 mL) and brine (1 x 100 mL), dried over $MgSO_4$, filtered, and concentrated in vacuo. The resulting oil was purified with silica gel chromatography, using 2/98 (v/v) ethyl acetate/hexanes as the eluent to give 1.39 g of **S9** as a clear liquid (53% yield). HRMS (EI): [M+] Calcd. for $C_9H_5BrF_6O$, 321.9428; found, 321.9428. ^{19}F NMR (470 MHz, CDCl$_3$) δ -62.80, -73.82 (t, J_{H-F} = 8.2 Hz).

S10. A 20 mL vial was equipped with a stir bar in the glovebox. Sequentially, Ni(cod)$_2$ (140.1 mg, 0.5093 mmol, 1.0 equiv), PPh$_3$ (262.9 mg, 1.002 mmol, 2.0 equiv), **S9** (194.1 mg, 0.6008 mmol, 1.2 equiv), and toluene (5 mL) were added. The solution was stirred at rt for 3 h. The reaction was removed from the glovebox and transferred to a 100 mL round-bottom flask. The deep red solution was concentrated in vacuo until ~2 mL of solution was left. Addition of hexanes (40 mL) led to a yellow orange precipitate. The solid was filtered and washed with hexanes (20 mL) and cold MeOH (5 mL). The resulting solid was dried in vacuo to give 226.1 mg of **S10** as a yellow solid (50% yield). Elemental Analysis: Calcd for C$_{45}$H$_{35}$BrF$_6$NiOP$_2$, C, 59.64; H, 3.89; F, 12.58; Found C, 59.94; H, 3.91; F, 12.29. ^{19}F NMR (470 MHz, CDCl$_3$) δ -61.82, -72.18 (t, $J_{H\text{-}F}$ = 8.4 Hz).
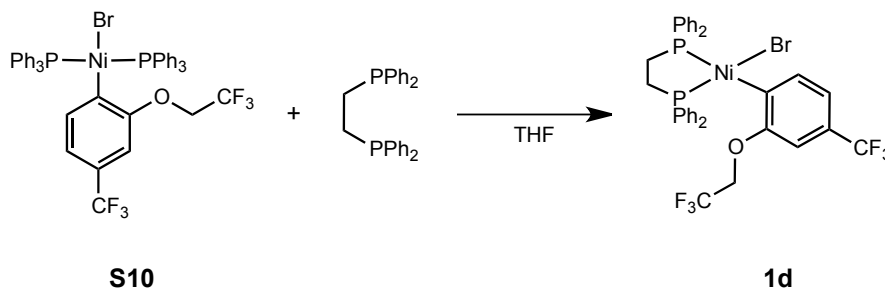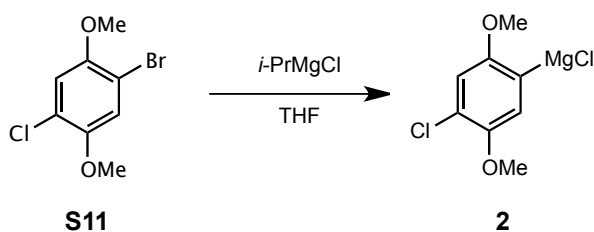

1d. A 20 mL vial was equipped with a stir bar in the glovebox. Sequentially, **S10** (383.1 mg, 0.4227 mmol, 1.0 equiv), dppe (186.2 mg, 0.4673 mmol, 1.1 equiv), and THF (10 mL) were added. The solution was stirred at rt for 2 h. The deep red solution was concentrated in vacuo until ~1 mL of solution was left. Addition of hexanes (18 mL) led to a yellow orange precipitate. The solid was filtered and washed with hexanes (20 mL). The resulting solid was recrystallized in THF/hexanes to give 241.9 mg of **1d** as an orange solid (74% yield). Elemental Analysis: Calcd for C$_{35}$H$_{29}$BrF$_6$NiOP$_2$, C, 53.88; H, 3.75; F, 14.61; Found C, 54.40; H, 4.01; F, 14.21. ^{19}F NMR (470 MHz, acetone-d_6) δ –61.93, -73.51.
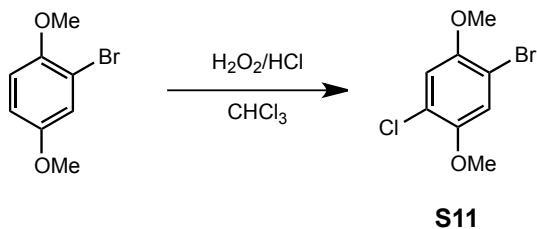
S11. A 100 mL round-bottom flask was equipped with a stir bar. Sequentially, 2-bromo-1,4-dimethoxybenzene (1.90 g, 8.75 mmol, 1.0 equiv) and $CHCl_3$ (7.5 mL) were added to the flask. Then, HCl (6 mL, 12 M) was added slowly. While stirring the reaction mixture vigorously, 30% H_2O_2 in H_2O (3.75 mL, 36.3 mmol, 4.0 equiv) was added via syringe pump over 45 min. The solution was stirred at rt overnight. The reaction mixture was extracted with $CHCl_3$ (3 x 25 mL). The combined organic layers were washed with 5% $NaHCO_3$ solution (1 x 50 mL), dried over $MgSO_4$, filtered, and concentrated in vacuo. The resulting solid was purified with silica gel chromatography, using 50/50 (v/v) hexanes/CH_2Cl_2 as the eluent to give 1.495 g of **S11** as a off-white solid (68% yield). HRMS (EI): [M+] Calcd. for $C_8H_8BrClO_2$, 249.9396; found, 249.9403.


2. All actions were performed in a glovebox under N_2 atmosphere. A 20 mL vial was equipped with a stir bar. Sequentially, **S11** (240 mg, 0.955 mmol, 1.0 equiv), THF (1.0 mL), and *i*-PrMgCl (0.43 mL, 0.86 mmol, 0.9 equiv) were added to the flask. The reaction mixture was stirred at rt for 8 h.
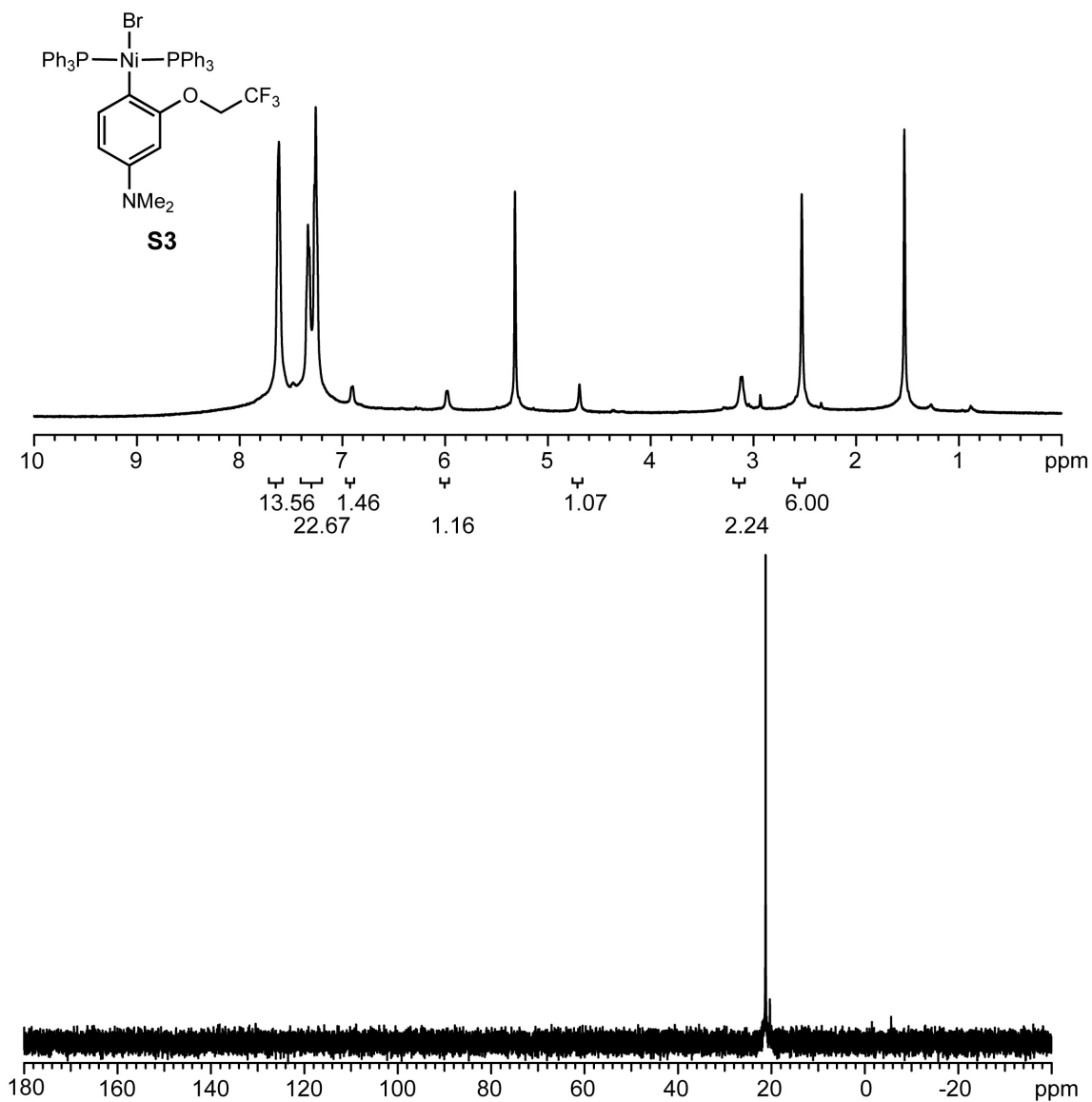
IV. NMR Spectra
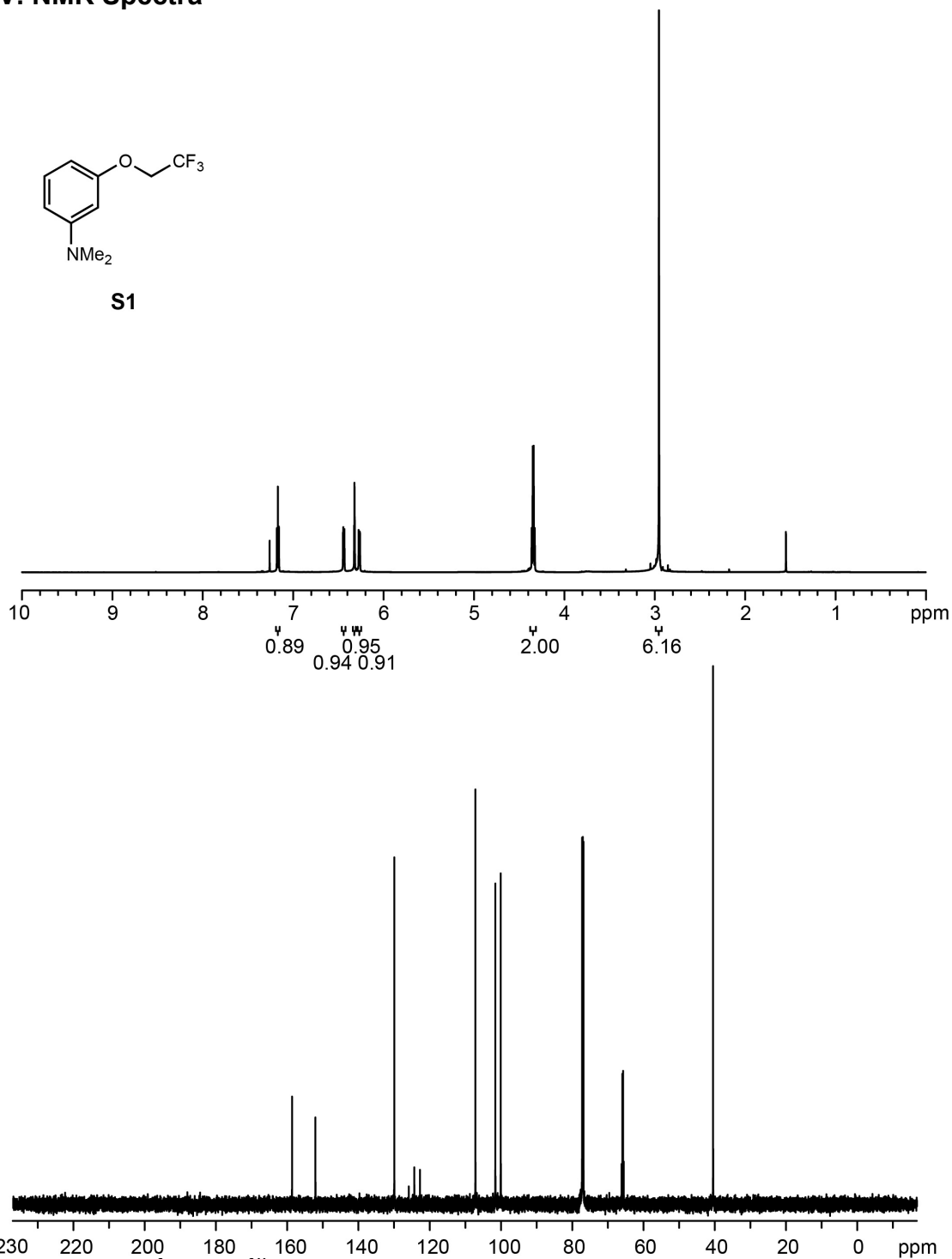
Figure S2-1. ^{1}H and ^{13}C NMR spectra of **S1**.
^{1}H NMR (700 MHz, CDCl$_3$) δ 7.17 (t, *J* = 8.3 Hz, 1H), 6.44 (dd, *J* = 8.3, 2.3 Hz, 1H), 6.32 (t, *J* = 2.4 Hz, 1H), 6.27 (dd, *J* = 8.0, 2.4 Hz, 1H), 4.34 (q, $J_{H\text{-}F}$ = 8.1 Hz, 2H), 2.95 (s, 6H). ^{13}C NMR (176 MHz, CDCl$_3$) δ 158.76, 152.20, 130.06, 123.65 (q, $J_{C\text{-}F}$ = 277.9 Hz), 107.30, 101.71, 100.19, 65.97 (q, $J_{C\text{-}F}$ = 35.7 Hz), 40.59.
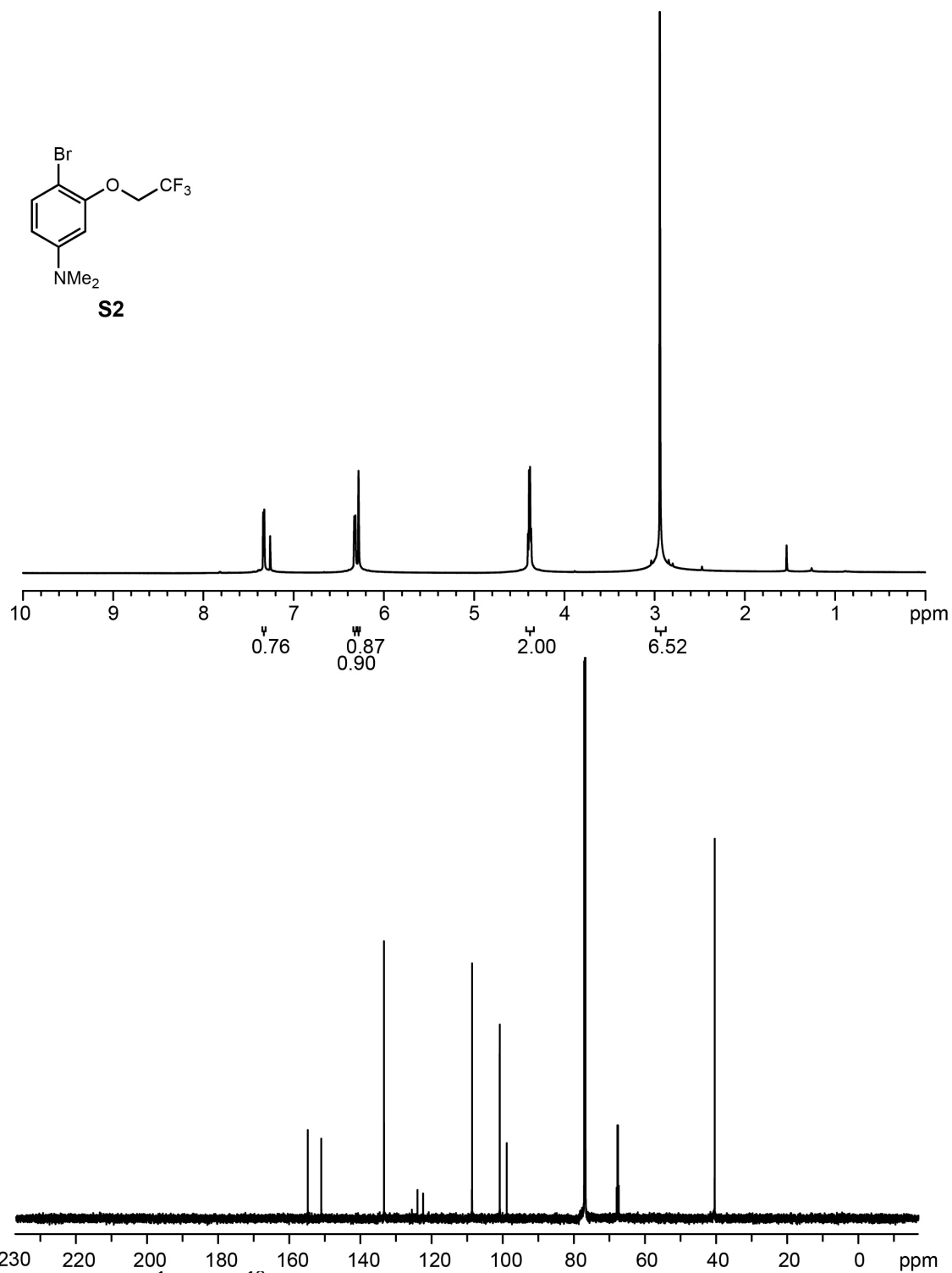
Figure S2-2. ^{1}H and ^{13}C NMR spectra of **S2**.

^{1}H NMR (700 MHz, CDCl$_3$) δ 7.33 (d, J = 8.6 Hz, 1H), 6.32 (d, J = 8.5 Hz, 1H), 6.28 (s, 1H), 4.39 (q, $J_{H\text{-}F}$ = 8.0 Hz, 2H), 2.94 (s, 6H). ^{13}C NMR (176 MHz, CDCl$_3$) δ 155.05, 151.27, 133.63, 123.42 (q, $J_{C\text{-}F}$ = 278.3 Hz), 108.87, 101.08, 99.13, 67.93 (q, $J_{C\text{-}F}$ = 35.4 Hz), 40.66.

Figure S2-3. ^{1}H and ^{31}P NMR spectra of **S3**.

^{1}H NMR (500 MHz, CD$_2$Cl$_2$) δ 7.62 (bs, 12H), 7.34-7.26 (m, 18H), 6.90 (d, *J* = 5.9 Hz, 1H), 5.97 (t, *J* = 5.9 Hz, 1H), 4.69 (s, 1H), 3.11 (q, *J* = 7.2 Hz, 2H), 2.53 (s, 6H). ^{31}P NMR (202 MHz, CD$_2$Cl$_2$) δ 21.22.
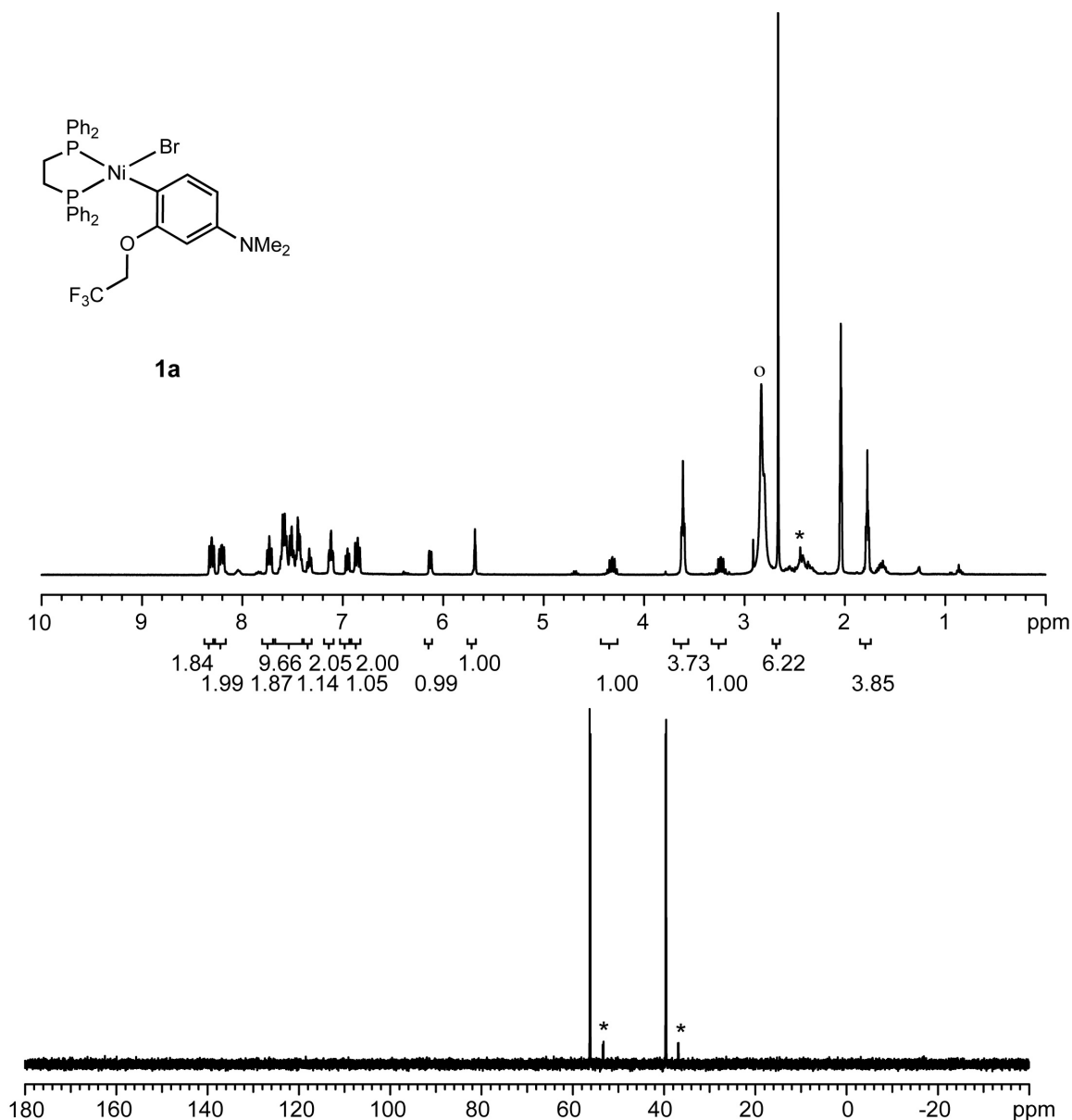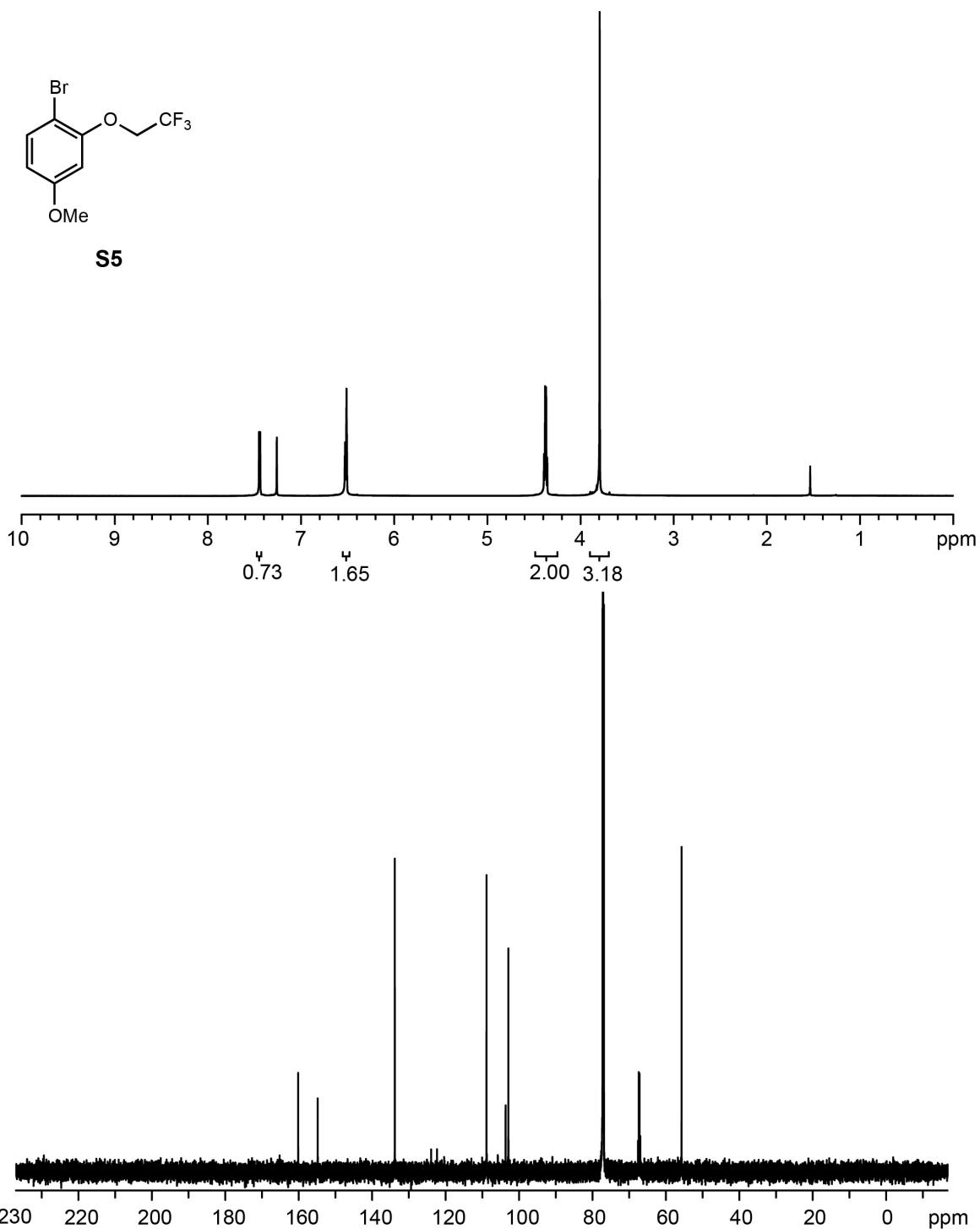
Figure S2-4. ^{1}H and ^{31}P NMR spectra of **1a**.
^{1}H NMR (400 MHz, acetone-d_6) δ 8.31 (at, J = 8.8 Hz, 2H), 8.23-8.18 (m, 2H), 7.73 (at, J = 8.5 Hz, 2H), 7.62-7.41 (m, 9H), 7.33 (at, J = 7.0 Hz, 1H), 7.14-7.10 (m, 2H), 6.95 (at, J = 6.8 Hz, 1H), 6.88-6.83 (m, 2H), 6.12 (d, J = 8.3 Hz, 1H), 5.68 (s, 1H), 4.32 (m, 1H), 3.61 (t, J = 6.0 Hz, 3H), 3.24 (m, 1H), 2.67 (s, 6H), 1.79-1.76 (m, 4H). residual °H$_2$O and *impurity. ^{31}P NMR (162 MHz, acetone-d_6) δ 56.21 (d, J = 26.5 Hz), 39.60 (d, J = 26.5 Hz).
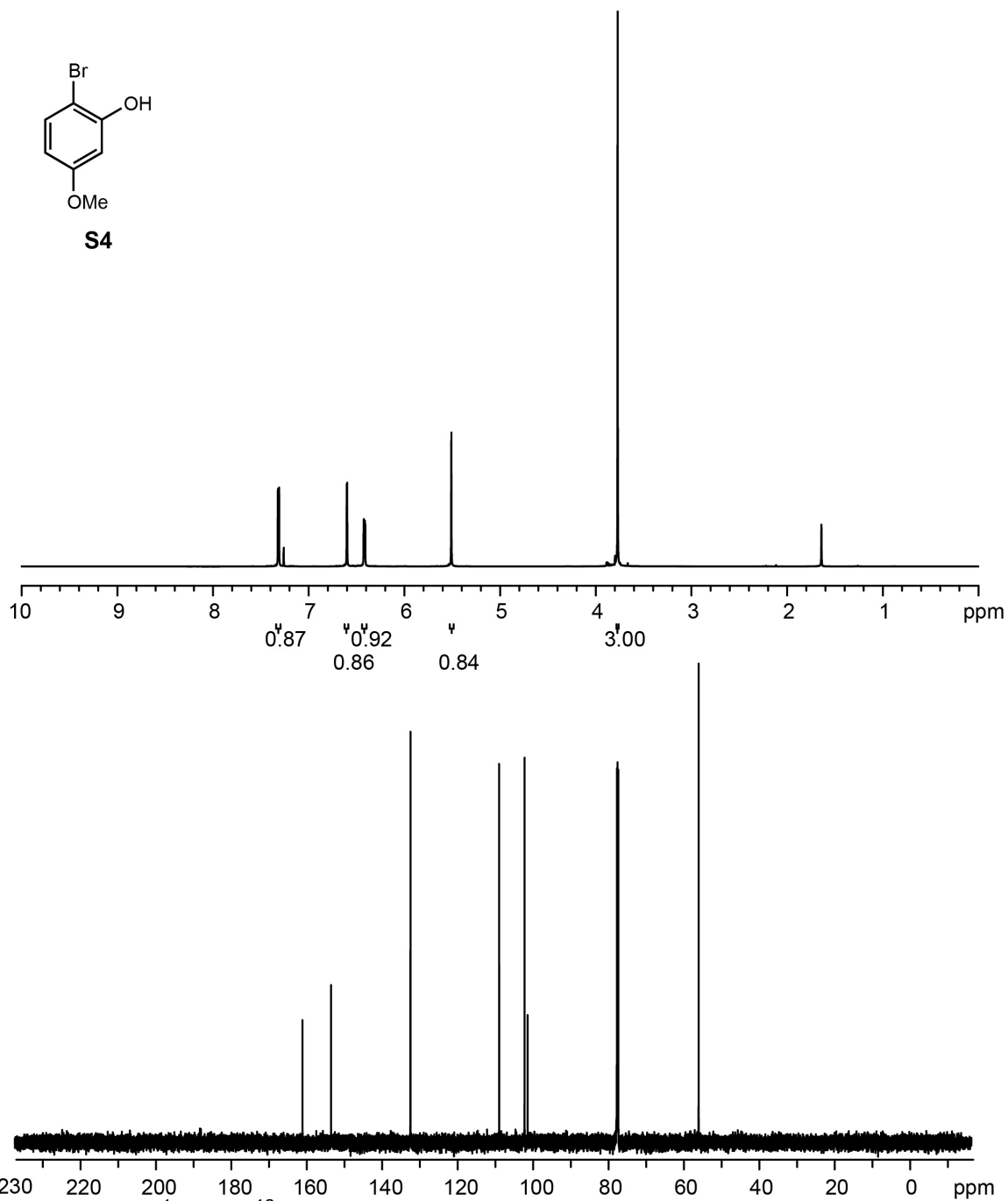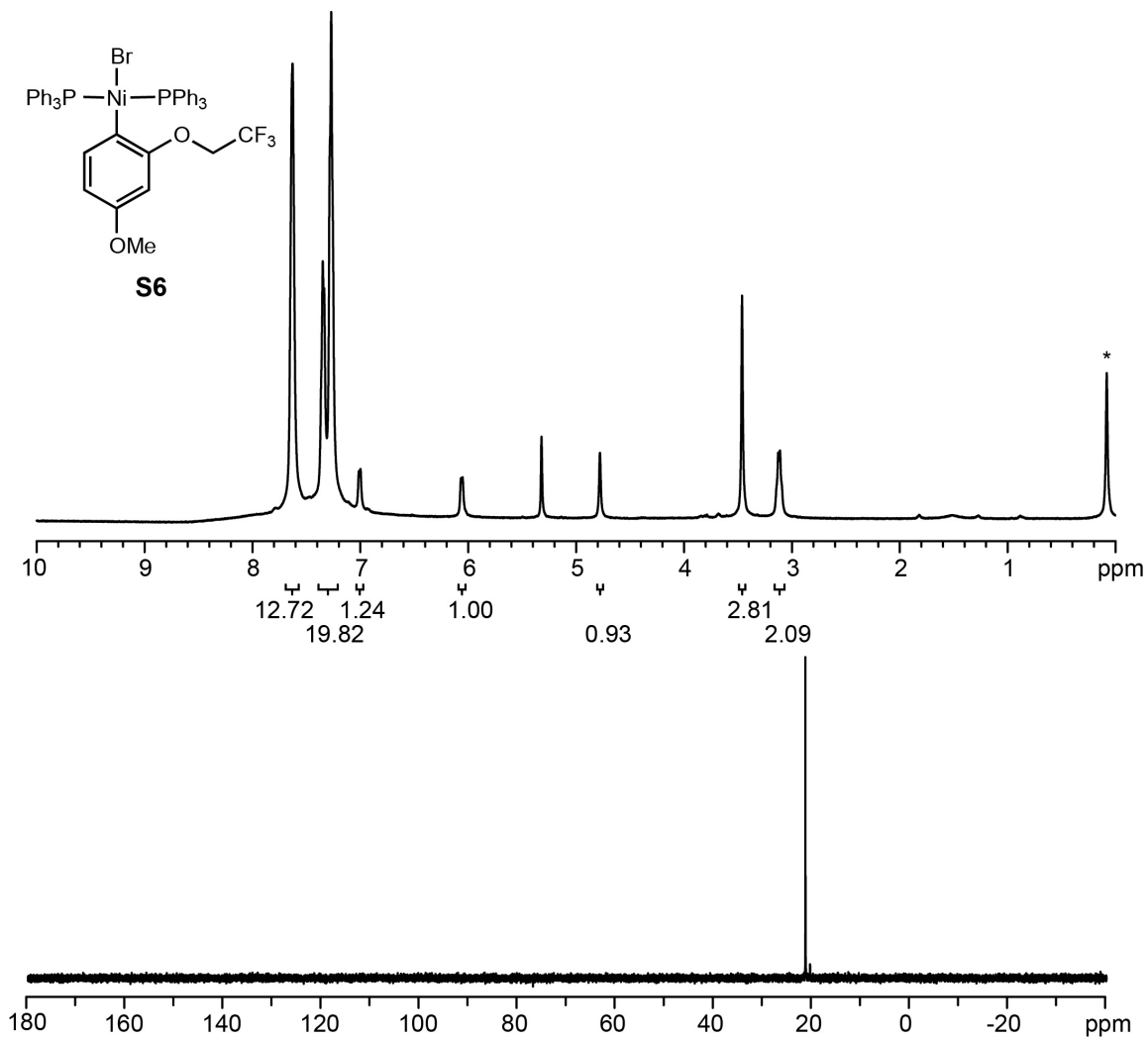
Figure S2-5. ^{1}H and ^{13}C NMR spectra of **S4**.
^{1}H NMR (700 MHz, CDCl$_3$) δ 7.31 (d, J = 8.8 Hz, 1H), 6.60 (d, J = 2.9 Hz, 1H), 6.42 (dd, J = 8.8, 2.9 Hz, 1H), 5.51 (s, 1H), 3.77 (s, 3H). ^{13}C NMR (176 MHz, CDCl$_3$) δ 160.73, 153.14, 132.09, 108.57, 101.82, 101.02, 55.67.

**Figure S2-6.** ^{1}H and ^{13}C NMR spectra of **S5**.

^{1}H NMR (700 MHz, CDCl$_3$) δ 7.44 (d, J = 8.5 Hz, 1H), 6.53 (m, 2H), 4.37 (q, $J_{H\text{-}F}$ = 8.1 Hz, 2H), 3.79 (s, 1H). ^{13}C NMR (176 MHz, CDCl$_3$) δ 160.26, 154.92, 133.93, 123.23 (q, $J_{C\text{-}F}$ = 278.5 Hz), 108.97, 103.76, 103.01, 67.39 (q, $J_{C\text{-}F}$ = 35.9 Hz), 55.82.
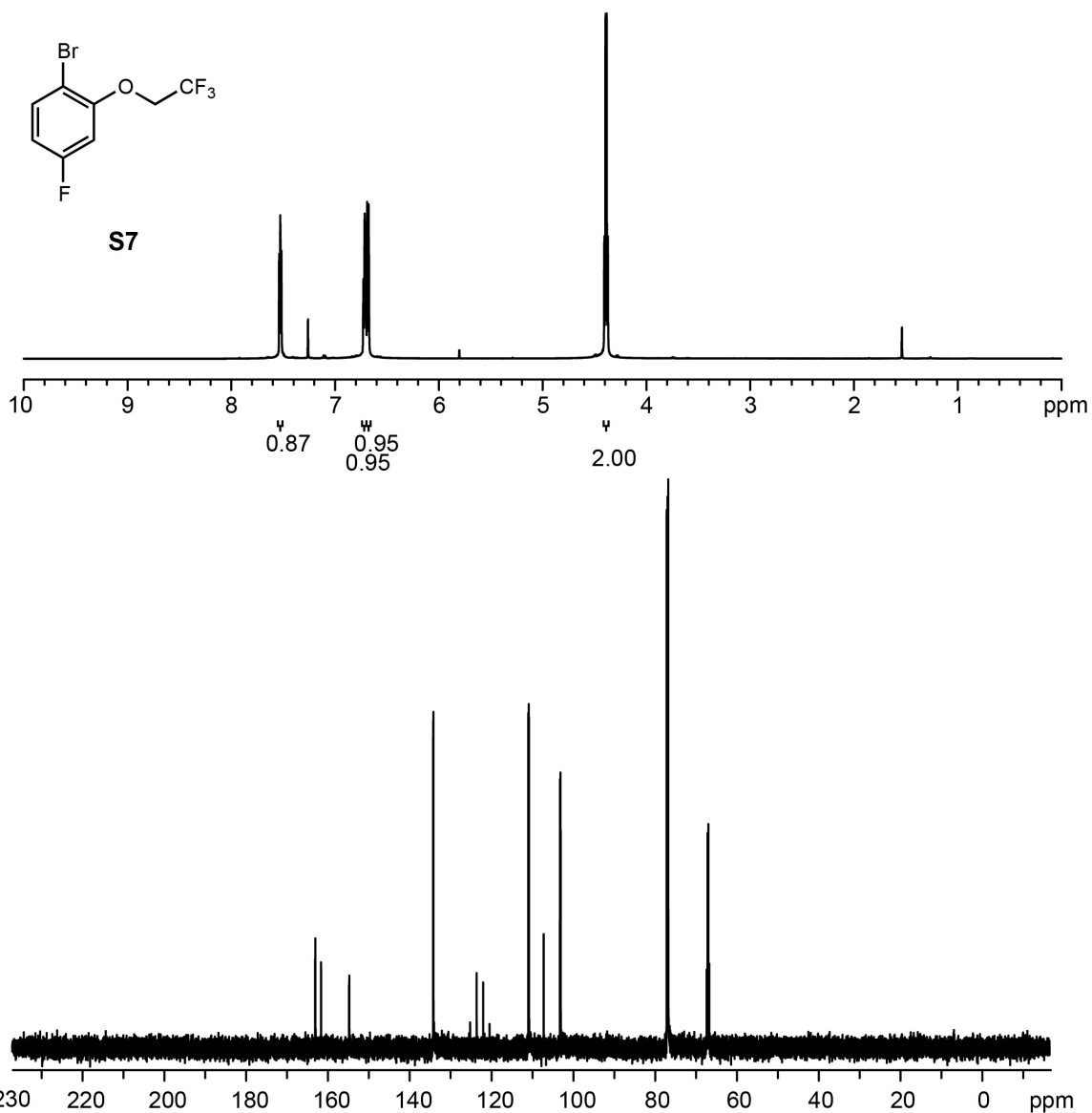
Figure S2-7. ^{1}H and ^{31}P NMR spectra of **S6**.
^{1}H NMR (500 MHz, CD$_2$Cl$_2$) δ 7.63 (bs, 12H), 7.36-7.26 (m, 18H), 7.01 (d, J = 7.7 Hz, 1H), 6.06 (at, J = 7.7 Hz, 1H), 4.78 (s, 1H) 3.46 (s, 3H), 3.12 (q, J_{H-F} = 8.4 Hz, 2H). *residual grease. ^{31}P NMR (202 MHz, CD$_2$Cl$_2$) δ 21.43.
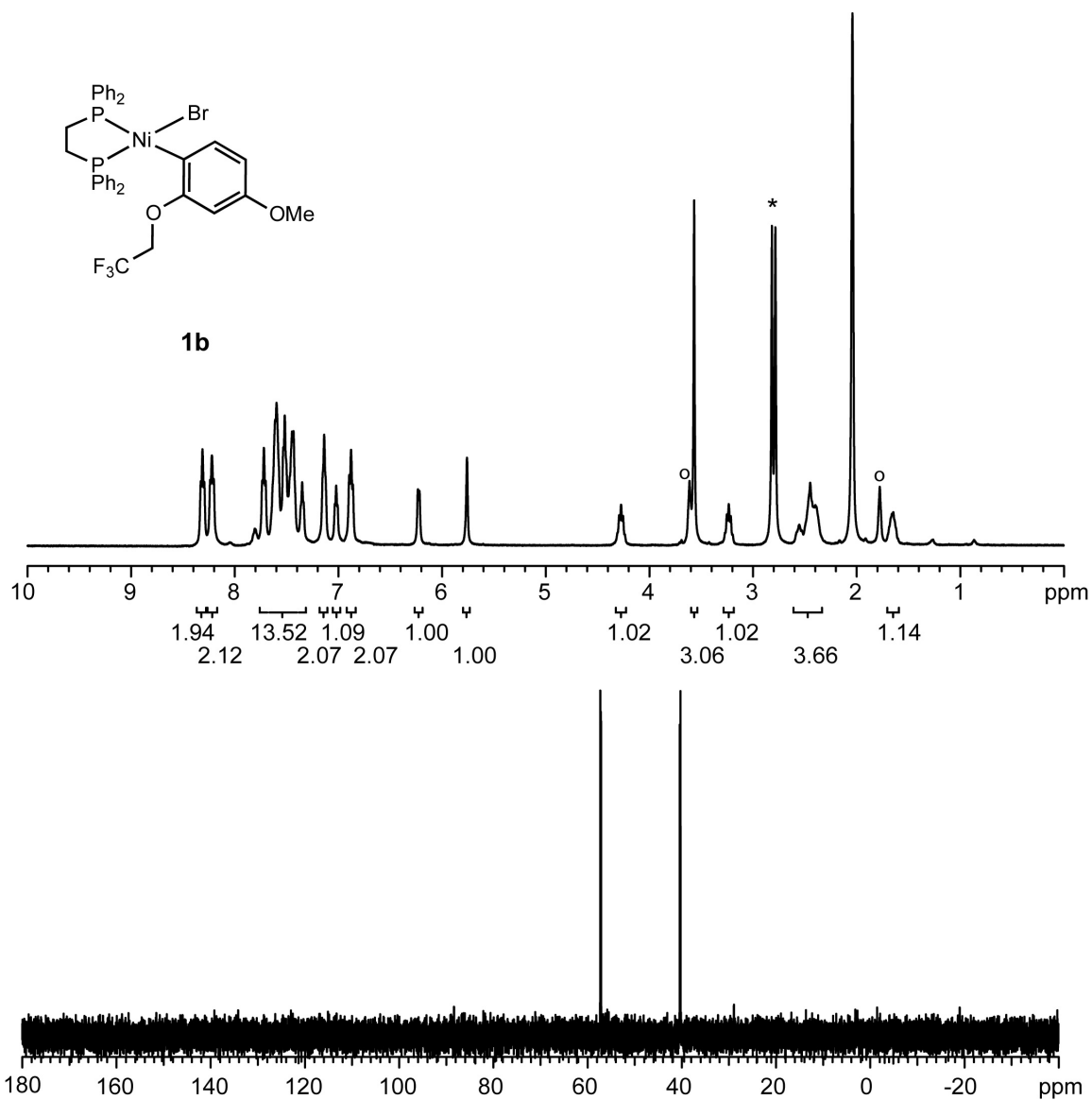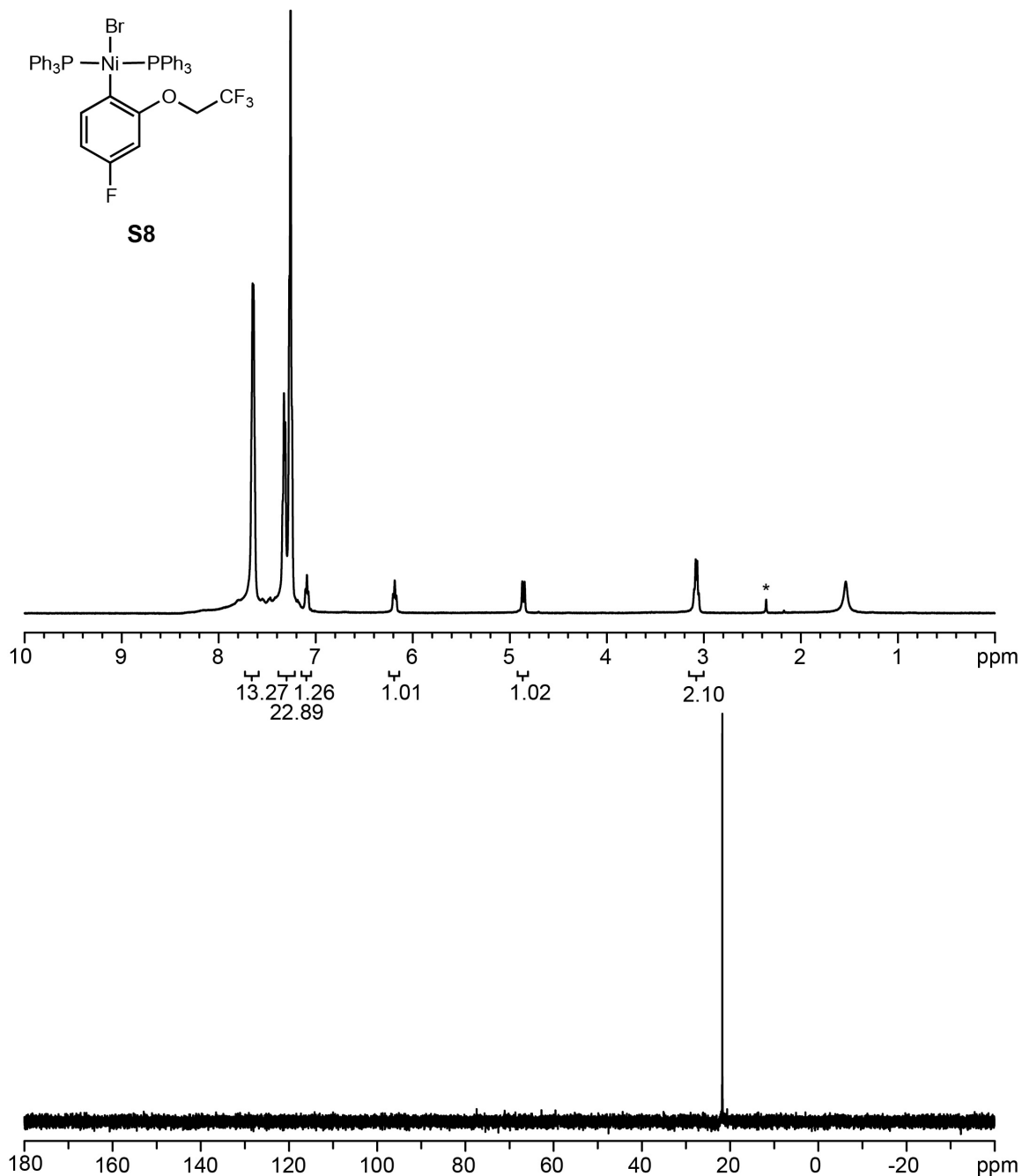
Figure S2-8. ^{1}H and ^{31}P NMR spectra of **1b**.
^{1}H NMR (500 MHz, acetone-d_6) δ 8.31 (at, J = 8.6 Hz, 2H), 8.22 (at, J = 8.6 Hz, 2H), 7.72-7.35 (m, 13H), 7.15-7.12 (m, 2H), 7.02 (at, J = 6.3 Hz, 1H), 6.88 (at, J = 9.0 Hz, 2H), 6.23 (d, J = 7.0 Hz, 1H), 5.76 (s, 1H), 4.27 (m, 1H), 3.57 (s, 3H), 3.23 (m, 1H), 2.55-2.40 (m, 3H), 1.78 (s, 1H), 1.62 (m, 1H). residual *H_2O and °THF. ^{31}P NMR (200 MHz, acetone-d_6) δ 57.23 (d, J = 28.9 Hz), 40.34 (d, J = 28.9 Hz).

139

Figure S2-9. ^{1}H and ^{13}C NMR spectra of **S7**.
^{1}H NMR (700 MHz, CDCl$_3$) δ 7.53 (at, J = 7.4 Hz, 1H), 6.71 (at, J = 8.1 Hz, 1H), 6.68 (d, J = 9.8 Hz, 1H), 4.39 (q, J_{H-F} = 8.1 Hz, 2H). ^{13}C NMR (176 MHz, CDCl$_3$) δ 162.55 (d, J_{C-F} = 248.0 Hz), 154.96 (d, J_{C-F} = 9.5 Hz), 134.41 (d, J_{C-F} = 9.7 Hz), 123.02 (q, J_{C-F} = 278.6 Hz), 111.11 (d, J_{C-F} = 21.9 Hz), 107.42, 103.37 (d, J_{C-F} = 26.5 Hz), 67.27 (q, J_{C-F} = 36.0 Hz).

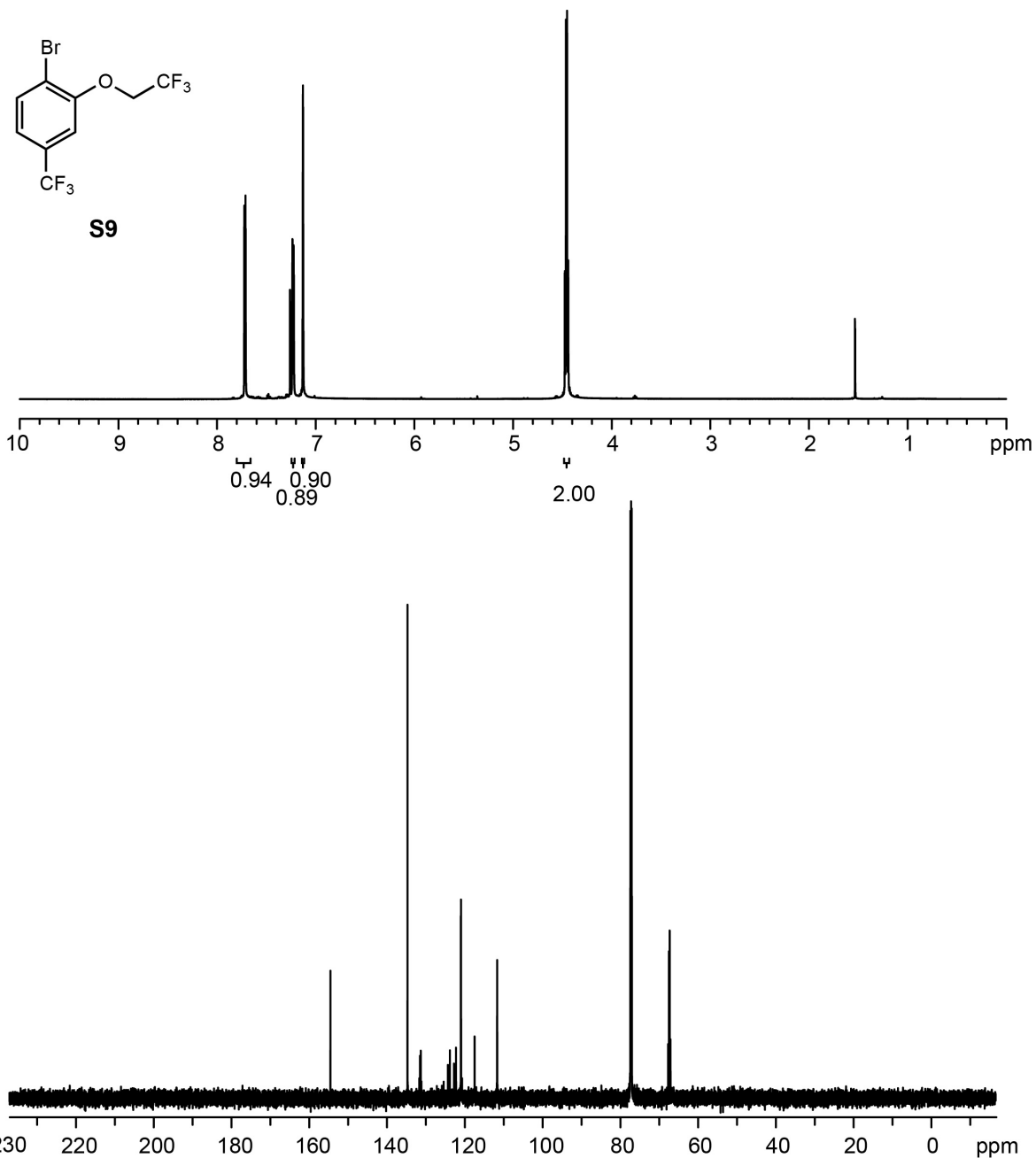**Figure S2-10.** ^{1}H and ^{31}P NMR spectra of **S8**.
^{1}H NMR (500 MHz, CDCl$_3$) δ 7.65 (bs, 12H), 7.34-7.24 (m, 18H), 7.09 (at, J = 7.8 Hz, 1H), 6.19 (at, J = 8.7 Hz, 1H), 4.86 (d, J = 11.9 Hz, 1H), 3.08 (q, $J_{H\text{-}F}$ = 8.4 Hz, 2H). *residual toluene. ^{31}P NMR (202 MHz, CDCl$_3$) δ 21.76.
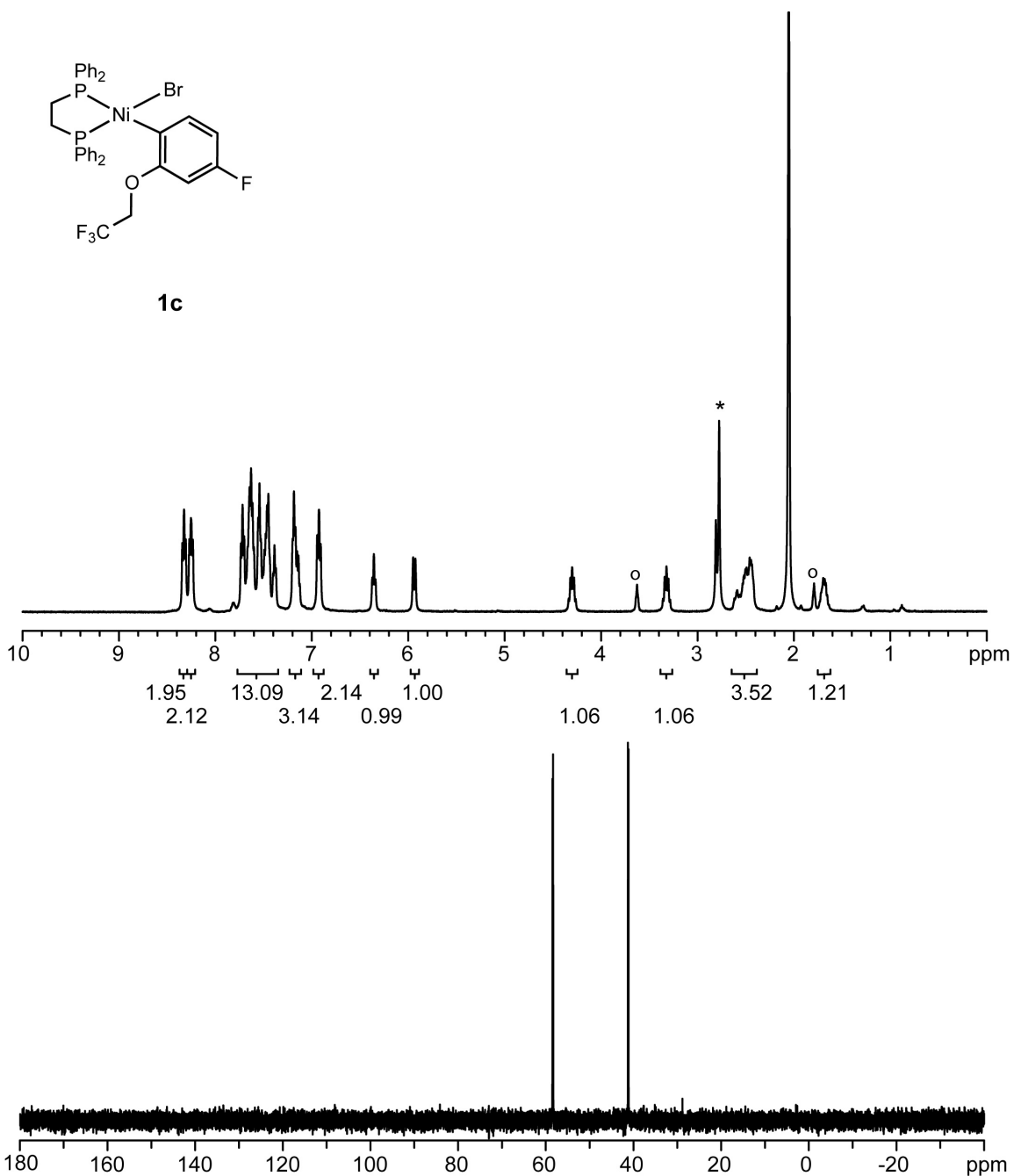
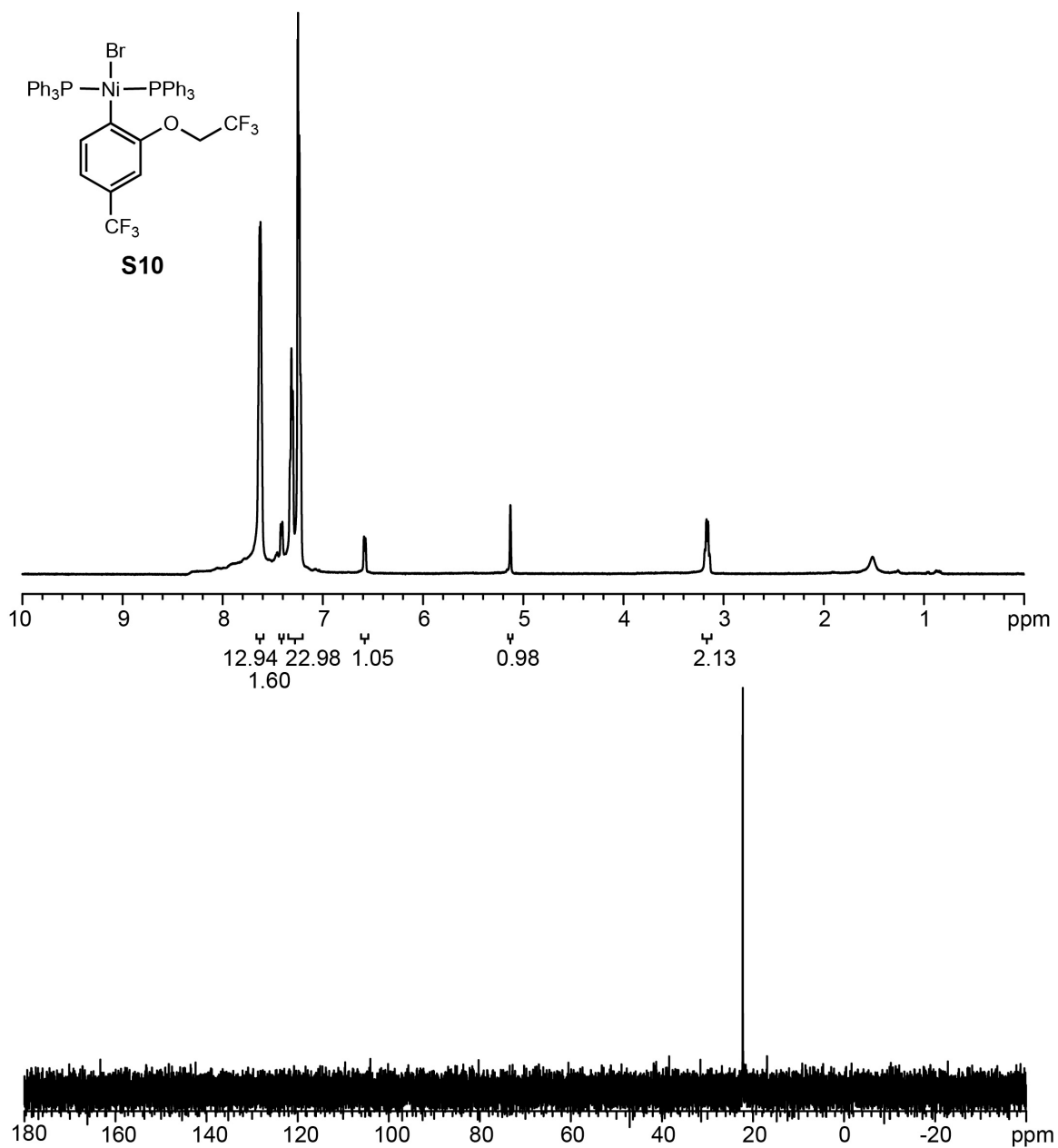**Figure S2-11.** ^{1}H and ^{31}P NMR spectra of **1c**.
^{1}H NMR (500 MHz, acetone-d_6) δ 8.33 (at, J = 8.9 Hz, 2H), 8.25 (at, J = 8.3 Hz, 2H), 7.72-7.39 (m, 13H), 7.20-7.12 (m, 3H), 6.93 (at, J = 9.1 Hz, 2H), 6.36 (at, J = 7.7 Hz, 1H), 5.94 (d, J = 12.3 Hz, 1H), 4.30 (m, 1H), 3.32 (m, 1 H), 2.59-2.43 (m, 3H), 1.79-1.66 (m, 1H). residual *H_2O and °THF. ^{31}P NMR (200 MHz, acetone-d_6) δ 58.46 (d, J = 30.5 Hz), 41.26 (d, J = 30.5 Hz).

Figure S2-12. ^{1}H and ^{13}C NMR spectra of **S9**.

^{1}H NMR (700 MHz, CDCl$_3$) δ 7.72 (d, J = 8.3 Hz, 1H), 7.23 (d, J = 8.2 Hz, 1H), 7.13 (s, 1H), 4.46 (q, $J_{H\text{-}F}$ = 7.8 Hz, 2H). ^{13}C NMR (176 MHz, CDCl$_3$) δ 154.48, 134.66, 131.34 (q, $J_{C\text{-}F}$ = 33.2 Hz), 123.48 (q, $J_{C\text{-}F}$ = 272.5 Hz), 122.97 (q, $J_{C\text{-}F}$ = 277.8 Hz), 120.91 (q, $J_{C\text{-}F}$ = 4.1 Hz), 117.39, 111.59 (q, $J_{C\text{-}F}$ = 3.38 Hz), 67.33 (q, $J_{C\text{-}F}$ = 36.6 Hz).

Figure S2-13. ^{1}H and ^{31}P NMR spectra of **S10**.
^{1}H NMR (500 MHz, CDCl$_3$) δ 7.63 (bs, 12H), 7.41 (d, J = 7.3 Hz, 1H), 7.33-7.22 (m, 18H), 6.58 (d, J = 6.7 Hz, 1H), 5.13 (s, 1H), 3.16 (q, J_{H-F} = 8.2 Hz, 2H). ^{31}P NMR (202 MHz, CDCl$_3$) δ 22.23.
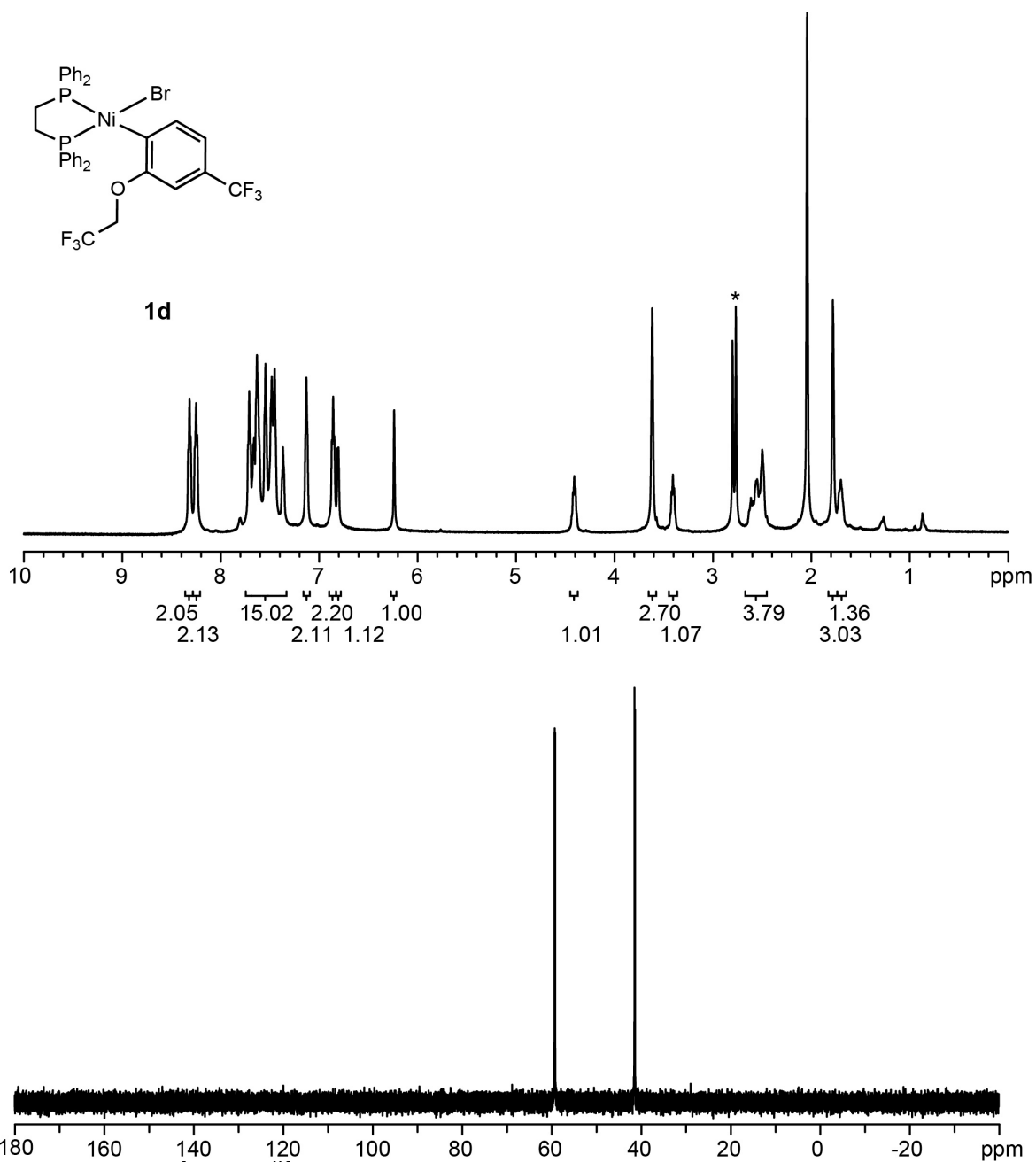
Figure S2-14. ^{1}H and ^{31}P NMR spectra of **1d**.
^{1}H NMR (500 MHz, acetone-d_6) δ 8.32 (at, J = 7.6 Hz, 2H), 8.25 (at, J = 7.6 Hz, 2H), 7.71-7.37 (m, 15H), 7.13 (s, 2H), 6.86 (at, J = 8.0 Hz, 2H), 6.81 (d, J = 6.9 Hz, 1H), 6.24 (s, 1H), 4.41 (m, 1H), 3.62 (s, 3H), 3.41 (m, 1H), 2.61-2.50 (m, 4H), 1.78-1.70 (m, 4H). *residual H$_2$O. ^{31}P NMR (200 MHz, acetone-d_6) δ 59.25 (d, J = 32.7 Hz), 41.40 (d, J = 32.7 Hz).
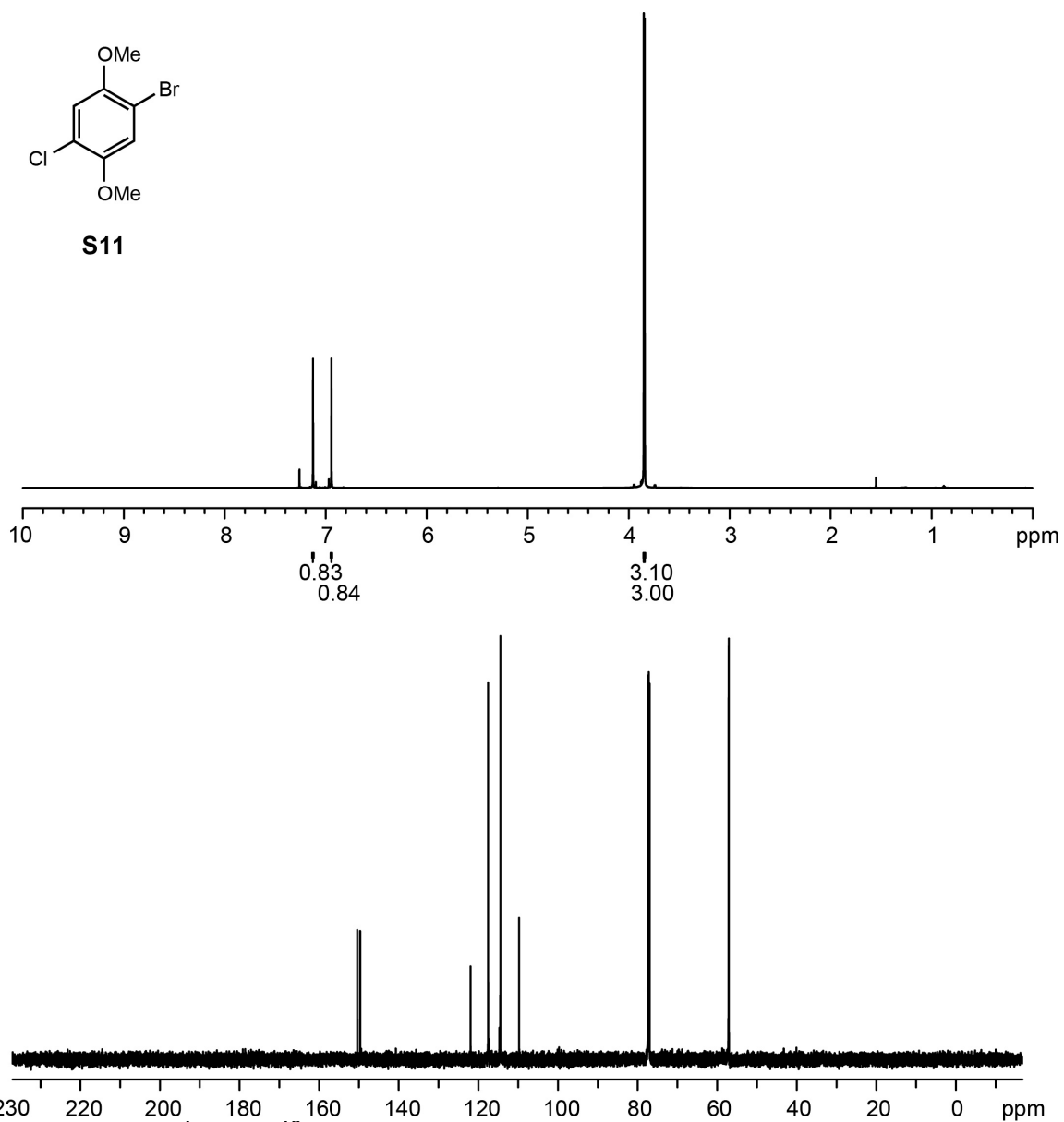
Figure S2-15. ^{1}H and ^{13}C NMR spectra of **S11**.
^{1}H NMR (700 MHz, CDCl$_3$) δ 7.13 (s, 1H), 6.94 (s, 1H), 3.85 (s, 3H), 3.84 (s, 3H).
^{13}C NMR (176 MHz, CDCl$_3$) δ 150.41, 149.67, 121.94, 117.54, 114.46, 109.75, 57.11, 57.06.

146

V. Initiation Rate Studies

GRIM reaction of monomer 2

After 8 h of GRIM reaction of monomer **2** (see Synthetic Procedure), an aliquot (~0.5 mL) was quenched with 12M HCl (0.5 mL) and then extracted with CH_2Cl_2 (2 x 1.5 mL), dried over $MgSO_4$, filtered, and then concentrated. The sample was redissolved in 1 mL CH_2Cl_2 and analyzed by GC-MS.
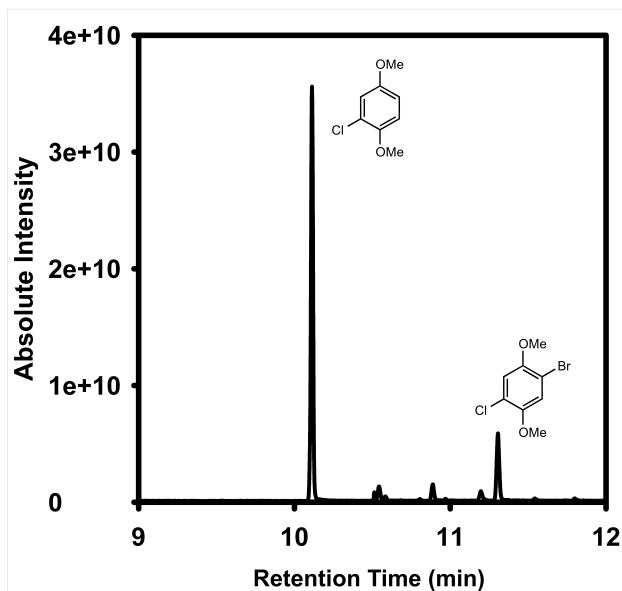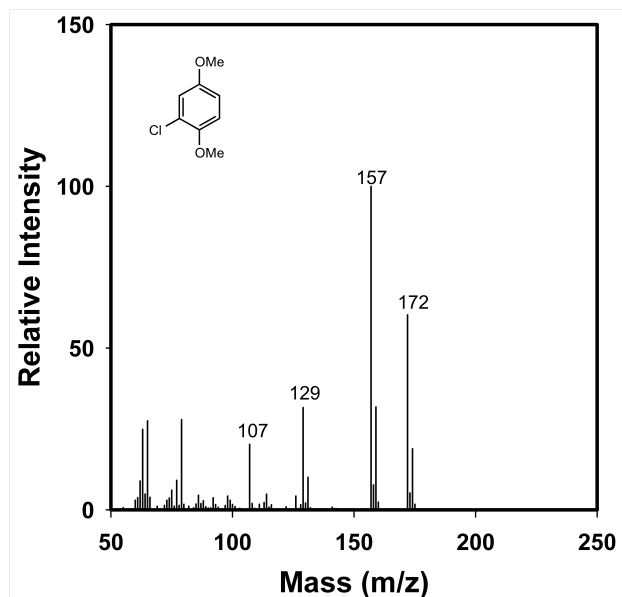
Figure S2-16. GC trace of quenched monomer **2**.

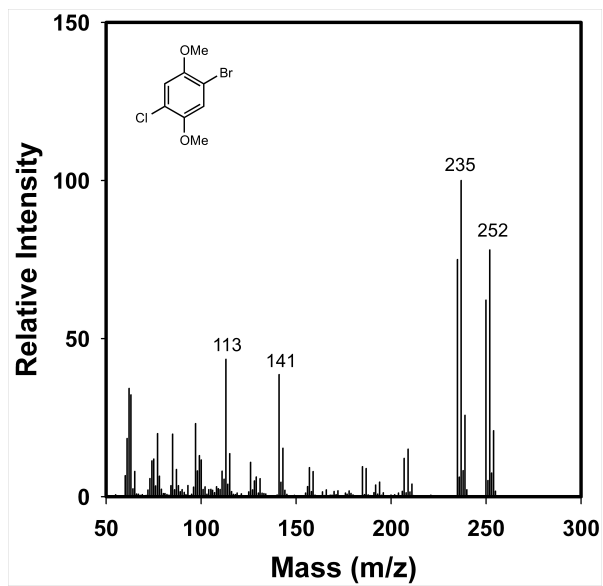**Figure S2-17**. GC-MS trace of peak at 10.11 min for quenched monomer **2**.

**Figure S2-18**. GC-MS trace of peak at 11.31 min for unreacted **S11**.

In a glovebox under N_2 atmosphere, in a 4 mL vial, a nickel stock solution was prepared by dissolving **1b** (19.7 mg, 0.0265 mmol, 1.0 equiv) and PPh_3 (14.9 mg, 0.0568 mmol, 2.1 equiv) in THF (1.0 mL). Then, trifluoromethyl benzene (26 μL, 0.34 M in THF, 0.33 equiv) was added as an internal standard. An NMR tube was charged with this solution (0.8 mL), sealed with a septum, and removed from the glovebox. The tube was cooled to 0 °C in the NMR spectrometer for ~40 min. Immediately prior to acquiring kinetic data, **2** (0.2 mL, 0.2 M in THF, 2.0 equiv, kept at 0 °C) was injected into the tube. The tube was rapidly inverted once and then inserted into the spectrometer at 0 °C. Each ^{19}F NMR spectrum was taken with the following parameters using Varian vnmr 500; acquisition time = 1.5 s, relaxation time = 3.0 s, scan size = 4, and pre-acquisition delay = 120 s.

Representative Procedure for Performing Igor Pro Analysis:
The integrated peak value of **3b** was converted to concentration using an internal standard. The concentration was fit to the equations below using Igor Pro v6.22A. 'CollumKinetic 5000' was used as the master procedure file and the analysis was performed using the same procedure reported in 'Fitting to Differential equations in Igor Pro' provided by the Collum group.[8] The reductive elimination constant is calculated to significant digits that encompass one standard deviation.

$$\frac{d[\textbf{3}]}{dt} = -k_{re}[\textbf{3}] \quad (2)$$
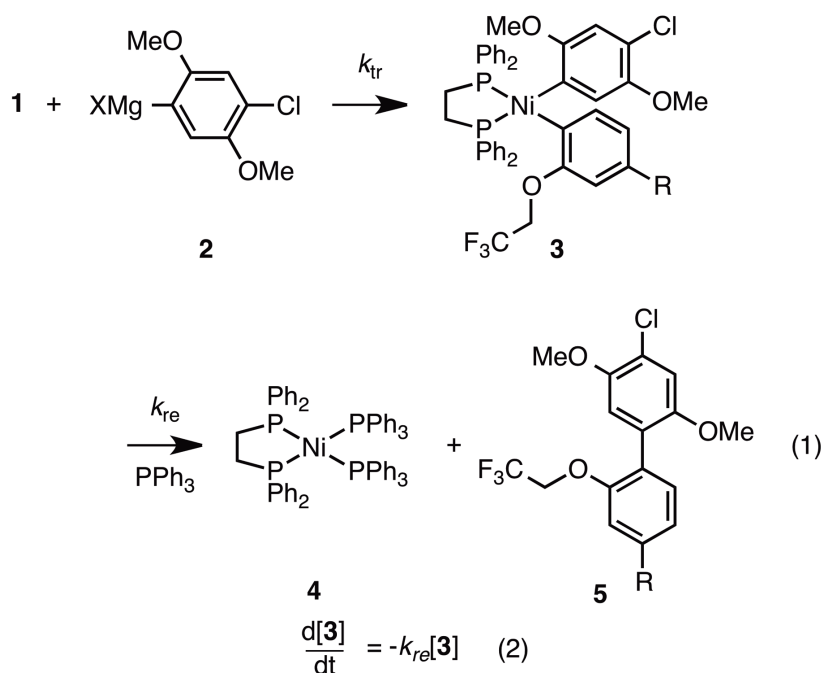
Control experiment

Initiation rate studies were performed with varying [PPh$_3$] to determine its effect on the rate of reductive elimination (temp = 0 °C, [**1b**] = 0.02 M, and [**2**] = 0.04 M).

Table S2-1. Rate data for catalyst **1b** with varying [PPh$_3$].

[PPh$_3$] (M)	k_{re} (s^{-1} x 10^{-3})
0.04	0.671 ± 0.006
0.08	0.69 ± 0.07
0.16	0.72 ± 0.09

Figure S2-19. Plot of concentration versus time for catalyst **3b** generated *in situ* from catalyst **1b** with varying [PPh$_3$], (0.04 M (●), 0.08 M (○), 0.16 M(▼)).
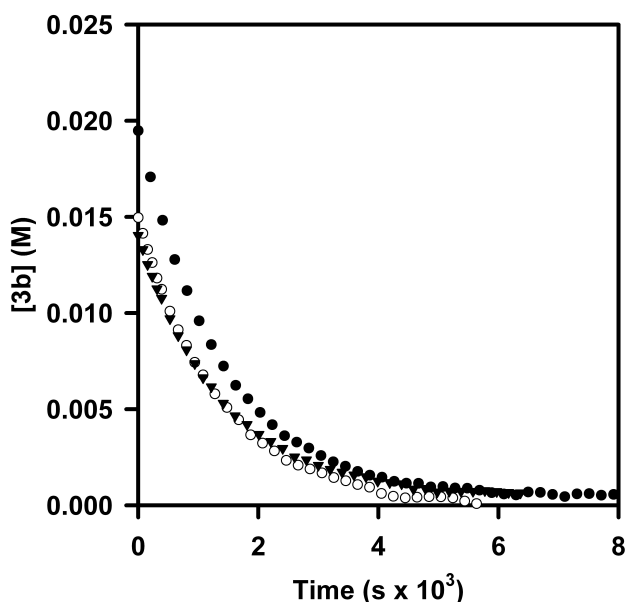
Initiation rate studies were performed with varying [2] to determine its effect on the rate of reductive elimination (temp = 0 °C, [1b] = 0.02 M, and [PPh$_3$] = 0.04 M).

Table S2-2. Rate data for catalyst **1b** with varying [**2**].

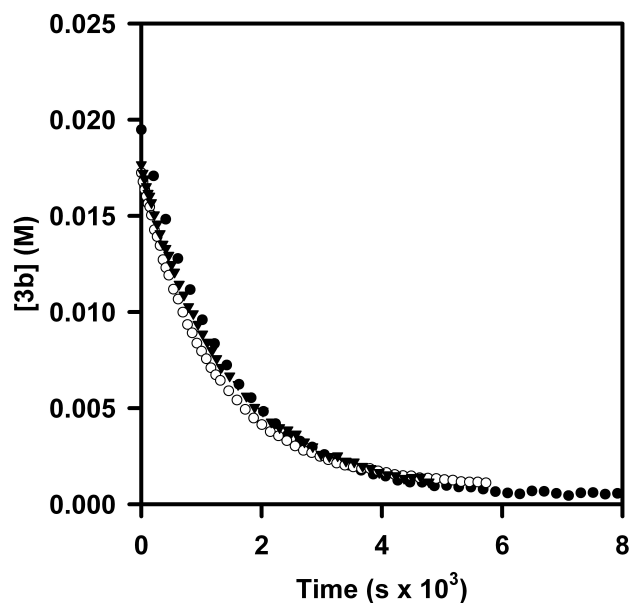| [2] (M)	k_{re} (s^{-1} x 10^{-3})
0.04	0.671 ± 0.006
0.08	0.73 ± 0.01
0.16	0.73 ± 0.10

Figure S2-20. Plot of concentration versus time for catalyst **3b** generated *in situ* from catalyst **1b** with varying [**2**], (0.04 M (●), 0.08 M (○), 0.16 M(▼)).

The catalyst initiation was observed using ^{19}F and ^{31}P NMR spectroscopy to support the peak assignments.
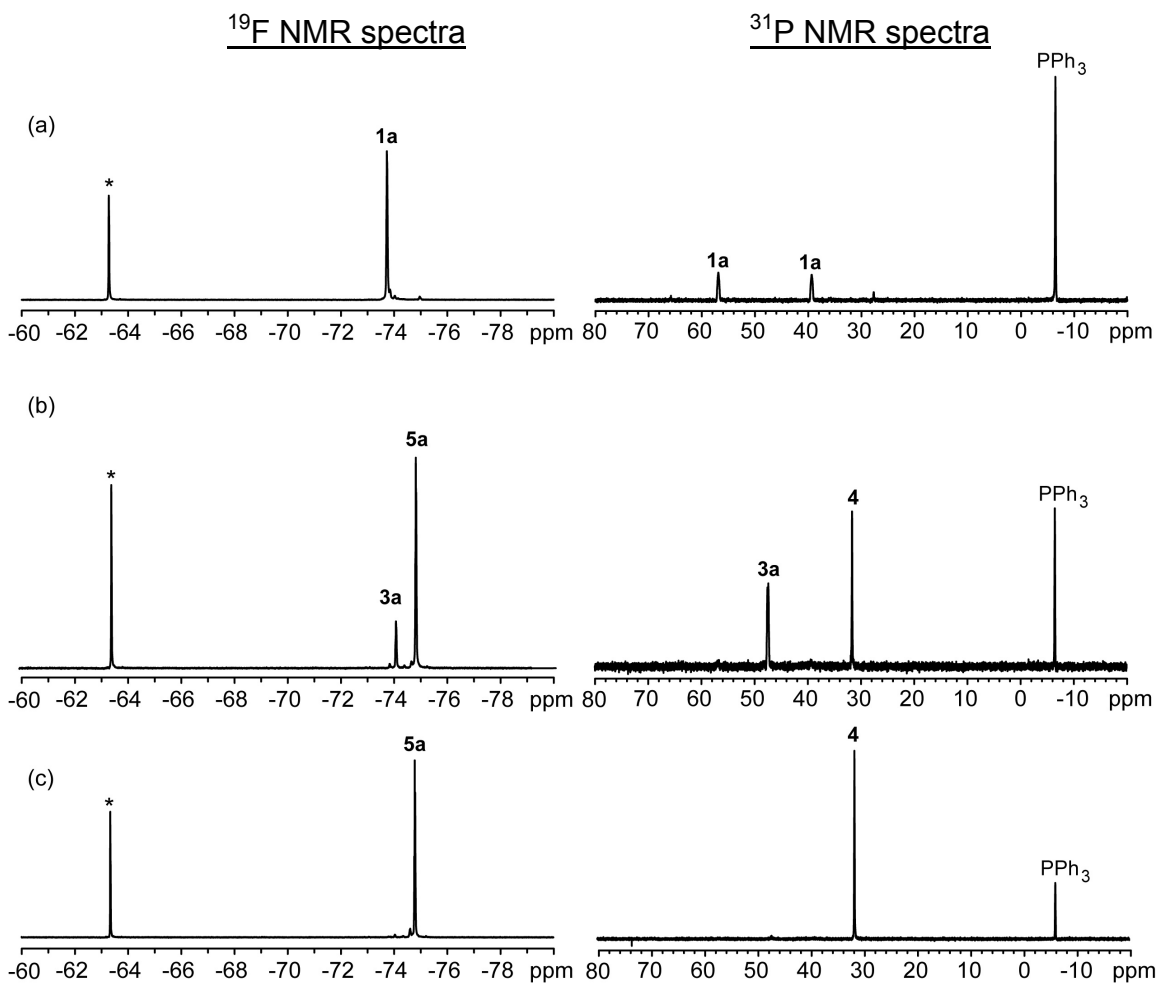
Figure S2-21. Representative ^{19}F and ^{31}P NMR spectra of initiation rate study for catalyst **1a** at the (a) beginning, (b) middle, and (c) end of the reaction.
*Represents the internal standard, trifluoromethyl benzene.
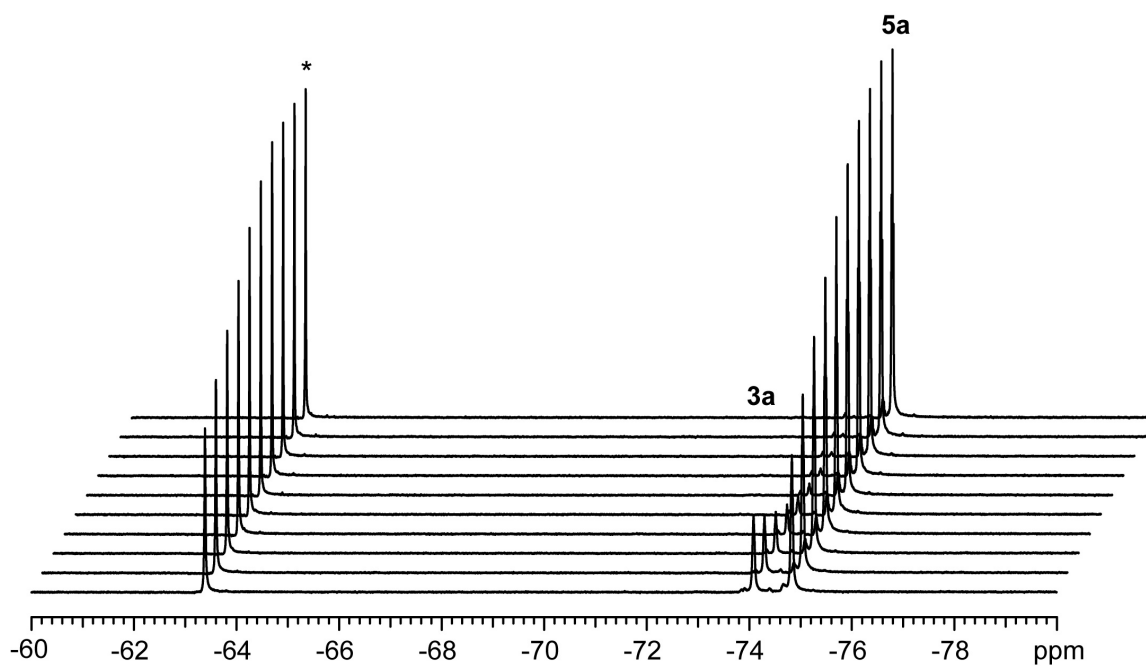
Figure S2-22. Representative ^{19}F NMR spectral array for catalyst **1a**. *Represents internal standard, trifluoromethyl benzene.

Figure S2-23. Plot of concentration versus time for data in Figure S2-22.

Table S2-3. Rate data for catalyst **1a**.

Trial	k_{re} (s^{-1} x 10^{-3})
1	6.84
2	6.92
Average	6.88 ± 0.06

The catalyst initiation was observed using ^{19}F and ^{31}P NMR spectroscopy to support the peak assignments.
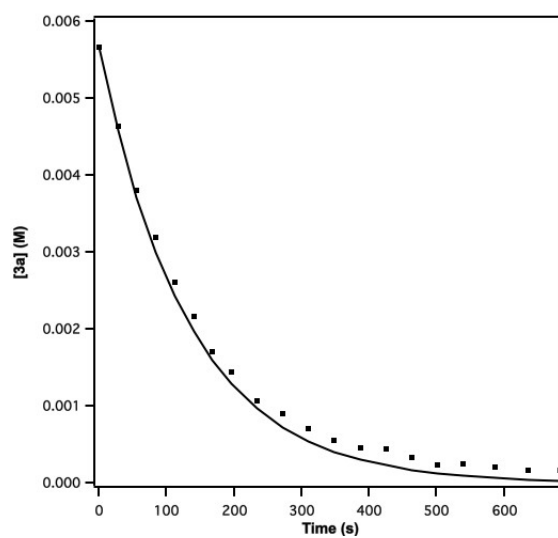
^{19}F NMR spectra ^{31}P NMR spectra
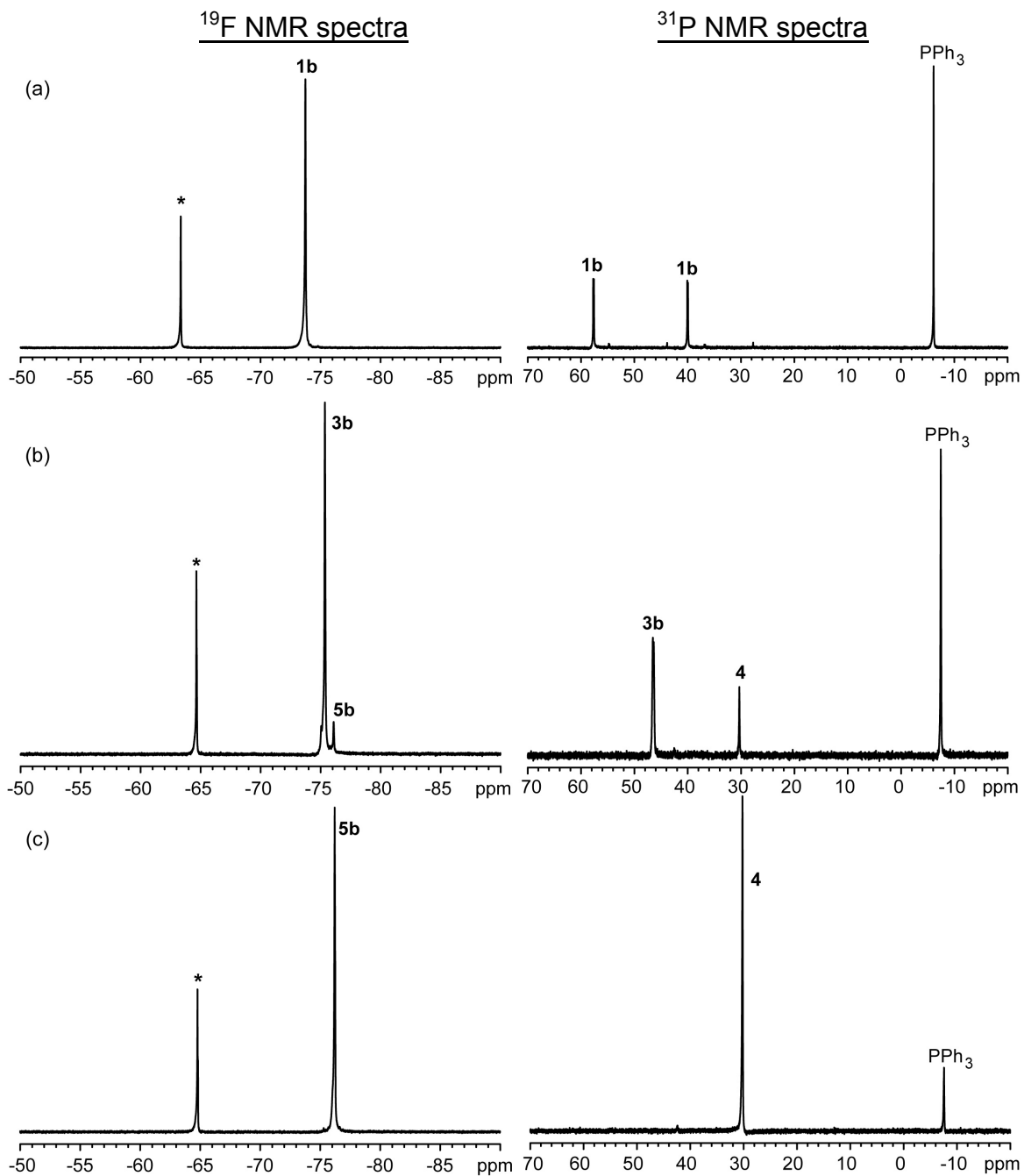
Figure S2-24. Representative ^{19}F and ^{31}P NMR spectra of initiation rate study for catalyst **1b** at the (a) beginning, (b) middle, and (c) end of the reaction. *Represents the internal standard, trifluoromethyl benzene.

Figure S2-25. Representative ^{19}F NMR spectral array for catalyst **1b**. *Represents internal standard, trifluoromethyl benzene.

Figure S2-26. Plot of concentration versus time for data in Figure S2-25.

Table S2-4. Rate data for catalyst **1b**.

Trial	k_{re} (s^{-1} x 10^{-3})
1	0.666
2	0.675
Average	0.671 ± 0.006

The catalyst initiation was observed using ^{19}F and ^{31}P NMR spectroscopy to support the peak assignments.
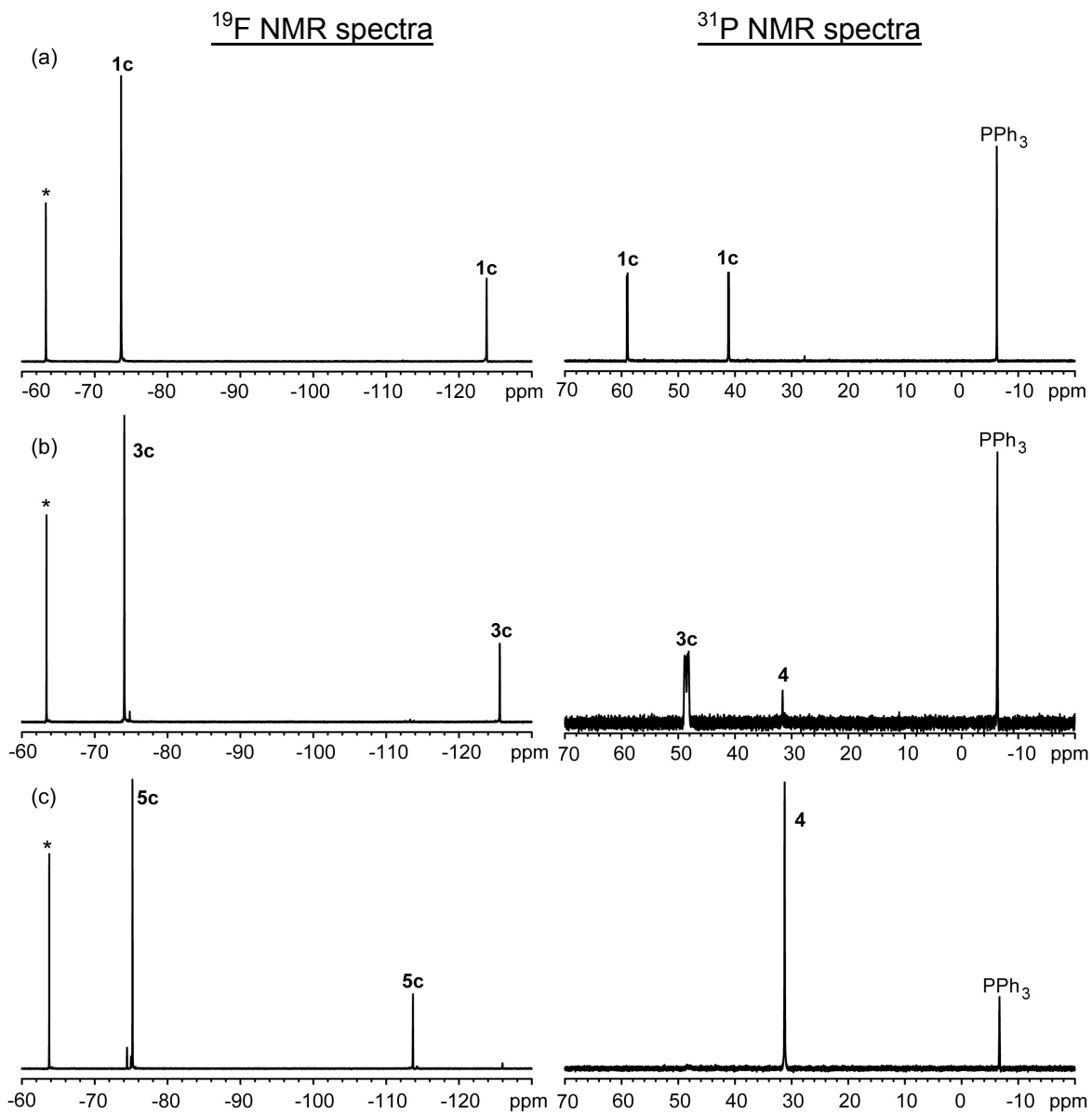
Figure S2-27. Representative ^{19}F and ^{31}P NMR spectra of initiation rate study for catalyst **1c** at the (a) beginning, (b) middle, and (c) end of the reaction.
*Represents the internal standard, trifluoromethyl benzene.

Figure S2-28. Representative ^{19}F NMR spectral array for catalyst **1c**. *Represents internal standard, trifluoromethyl benzene.
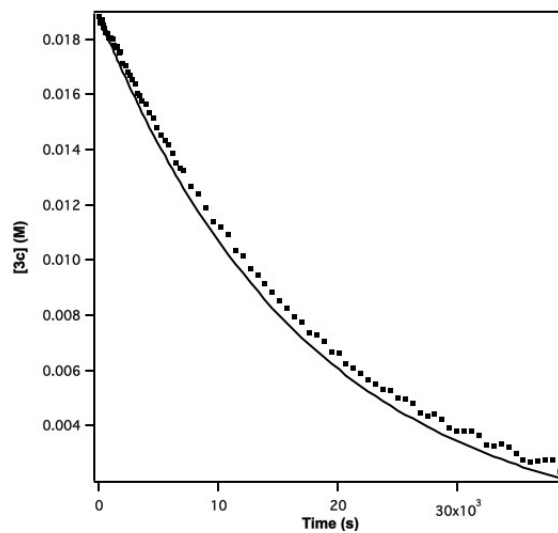
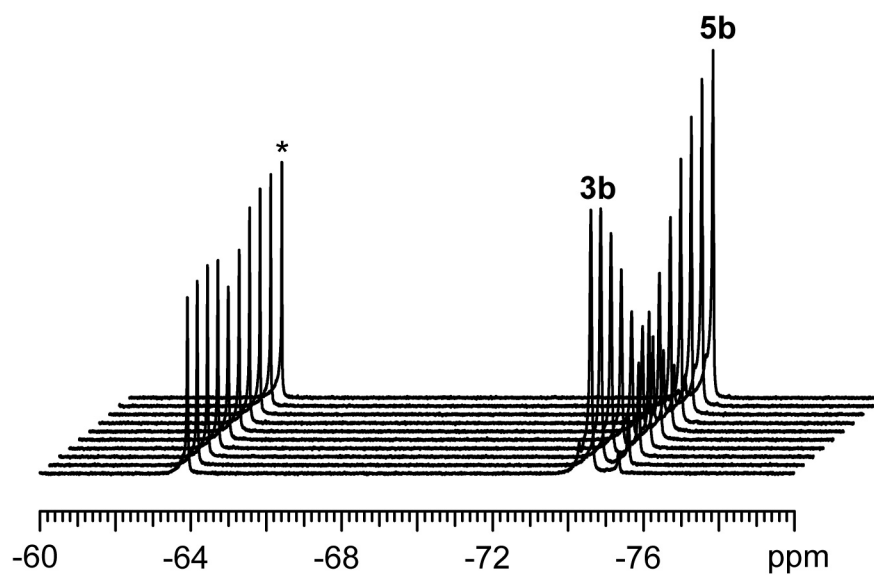**Figure S2-29.** Plot of concentration versus time for data in Figure S2-28.

Table S2-5. Rate data for catalyst **1c**.

Trial	k_{re} (s^{-1} x 10^{-3})
1	0.0519
2	0.0521
Average	0.0520 ± 0.0001

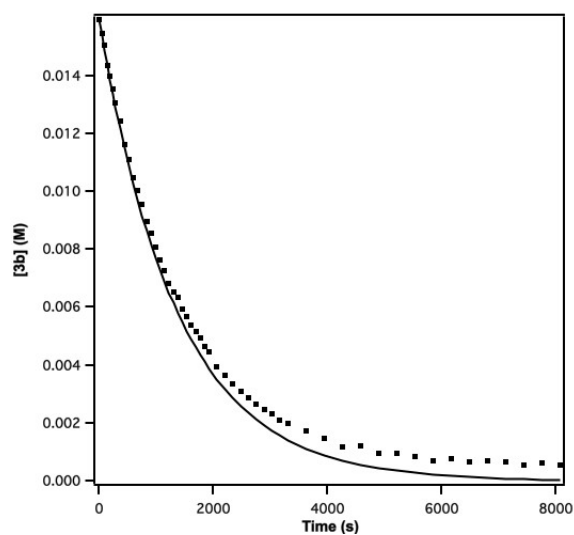The catalyst initiation was observed using ^{19}F and ^{31}P NMR spectroscopy to support the peak assignments.
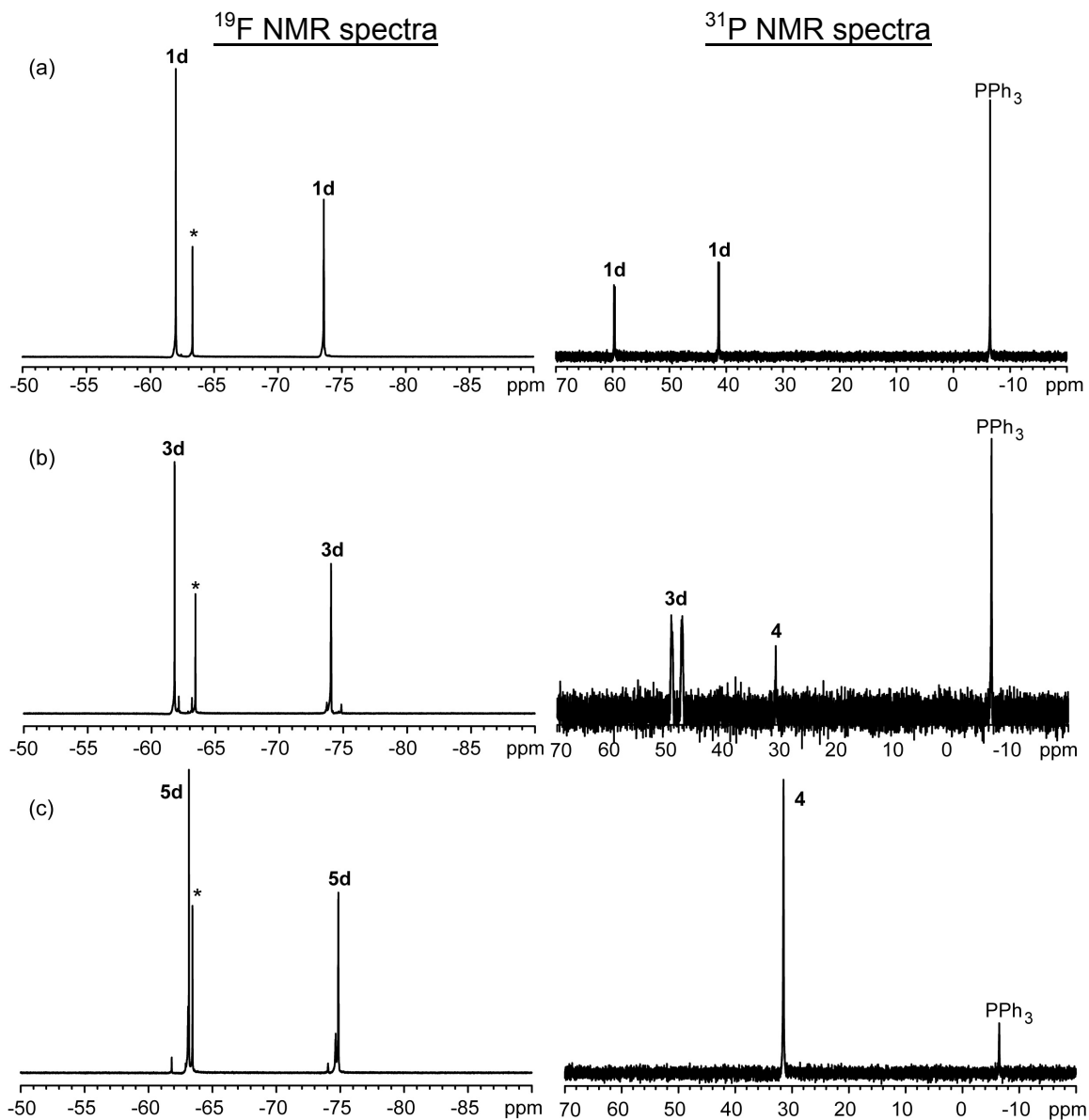
Figure S2-30. Representative ^{19}F and ^{31}P NMR spectra of initiation rate study for catalyst **1d** at the (a) beginning, (b) middle, and (c) end of the reaction. *Represents the internal standard, trifluoromethyl benzene.

Figure S2-31. Representative ^{19}F NMR spectral array for catalyst **1d**. *Represents internal standard, trifluoromethyl benzene.
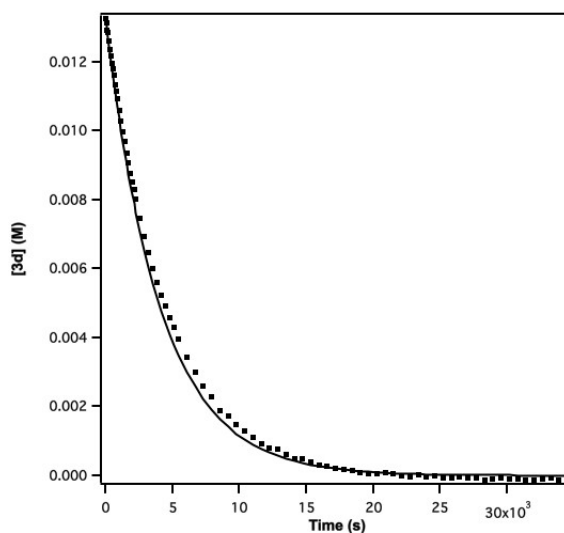
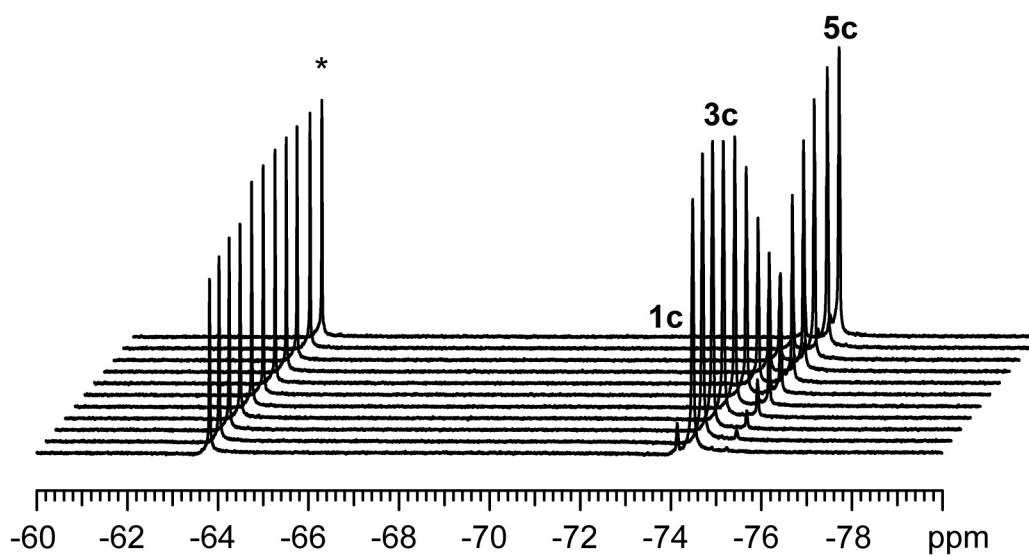**Figure S2-32.** Plot of concentration versus time for data in Figure S2-31.

Table S2-6. Rate data for catalyst **1d**.

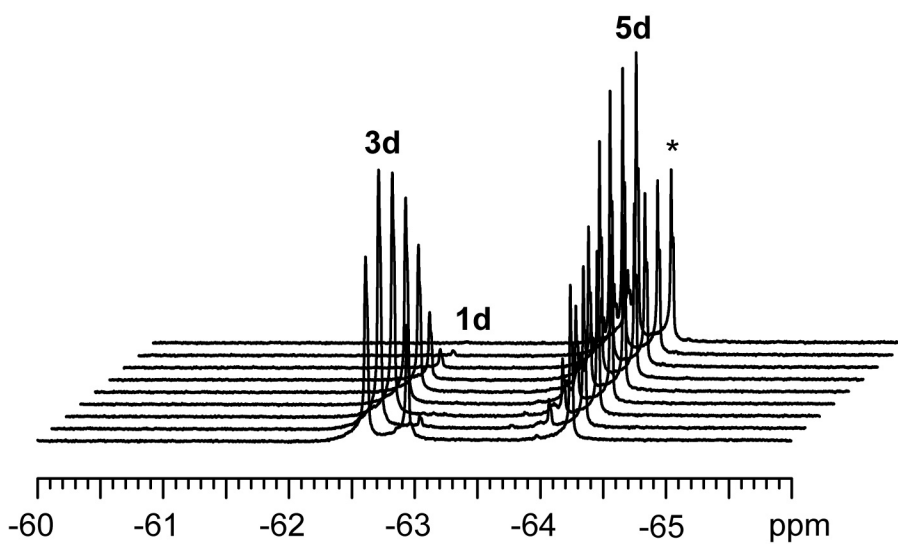| Trial	k_{re} (s^{-1} x 10^{-3})
1	0.2233
2	0.220
Average	0.222 ± 0.002

VI. Polymerization

Representative Procedure for M_n and Đ versus Conversion Studies utilizing React IR:

The IR probe was inserted through an O-ring sealed 14/20 ground glass adapter (custom-made) into an oven-dried 50 mL 2-neck flask equipped with a stir bar. The other neck was fitted with a three-way adapter fitted with a septum for injections/aliquot sampling and an N_2 line. The oven-dried flask was cooled under vacuum. The flask was then filled with N_2 and evacuated again for a total of three cycles. The flask was charged with THF (6.5 mL) and cooled to 0 °C over 15 min. After recording a background spectrum, monomer **6** (2.5 mL, 0.41 M in THF, 1.0 equiv) was added by syringe and allowed to equilibrate for at least 10 min at 0 °C before proceeding. The catalyst solution (1.0 mL, 0.015 M in THF, 0.015 equiv) was then injected and spectra were recorded every 30 s over the entire reaction. To account for mixing and temperature equilibration, spectra recorded in the first 60 s of the reaction were discarded. Aliquots (~0.5 mL) were taken through the three way adapter via syringe and immediately quenched with 12 M HCl (~1 mL). Each aliquot was then extracted with CH_2Cl_2 (2 x 1.5 mL) (with mild heating if polymer had precipitated), dried over $MgSO_4$, filtered, and then concentrated. The samples were dissolved in THF (with heating), and passed through a 0.2 μm PTFE filter for GPC analysis.
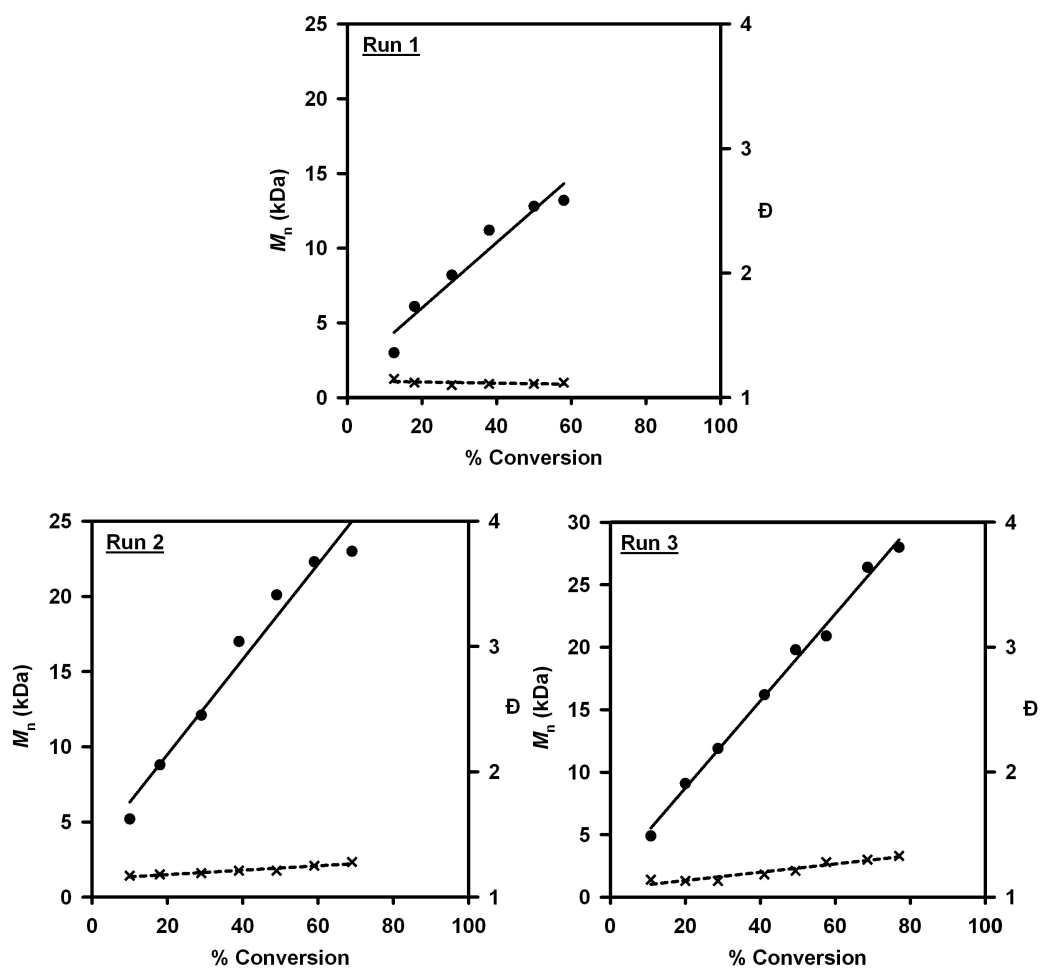
Figure S2-33. Plot of M_n (●) and Đ (**x**) versus conversion for **1a** (temp = 0 °C, [**1a**] = 0.0015 M, [**6**] = 0.10 M (Run 1), 0.10 M (Run 2), 0.01 M (Run 3)).

Table S2-7. Data for the plot in Figure S2-33, Run 1.

% Conversion	M_n (kDa)	Đ
13	3.0	1.15
19	6.1	1.12
28	8.2	1.10
38	11.2	1.11
50	12.8	1.11
58	13.2	1.12

Table S2-8. Data for the plot in Figure S2-33, Run 2.

% Conversion	M_n (kDa)	Đ
10	5.2	1.17
18	8.8	1.18
29	12.1	1.19
39	17.0	1.21
49	20.1	1.21
59	22.3	1.25
69	23.0	1.28

Table S2-9. Data for the plot in Figure S2-33, Run 3.

% Conversion	M_n (kDa)	Đ
11	4.9	1.14
20	9.1	1.13
29	11.9	1.13
41	16.2	1.18
49	19.8	1.21
58	20.9	1.28
69	26.4	1.30
77	28.0	1.33

Figure S2-34. Plot of M_n (●) and Đ (**x**) versus conversion for **1b** (temp = 0 °C, [**1b**] = 0.0015 M, [**6**] = 0.10 M (Run 1), 0.10 M (Run 2)).

Table S2-10. Data for the plot in Figure S2-34, Run 1.

% Conversion	M_n (kDa)	Đ
10	4.3	1.21
18	6.4	1.25
27	8.7	1.26
41	11.3	1.28
49	13.7	1.31
61	15.2	1.32
70	18.2	1.33
81	18.6	1.33

Table S2-11. Data for the plot in Figure S2-34, Run 2.

% Conversion	M_n (kDa)	Đ
11	5.3	1.19
19	8.4	1.22
31	11.1	1.23
40	13.2	1.26
47	14.4	1.26
60	16.6	1.28
72	19.7	1.30
79	17.7	1.39

Figure S2-35. Plot of M_n (●) and Đ (**x**) versus conversion for **1c** (temp = 0 °C, [**1c**] = 0.0015 M, [**6**] = 0.10 M (Run 1), 0.10 M (Run 2)).

Table S2-12. Data for the plot in Figure S2-35, Run 1.

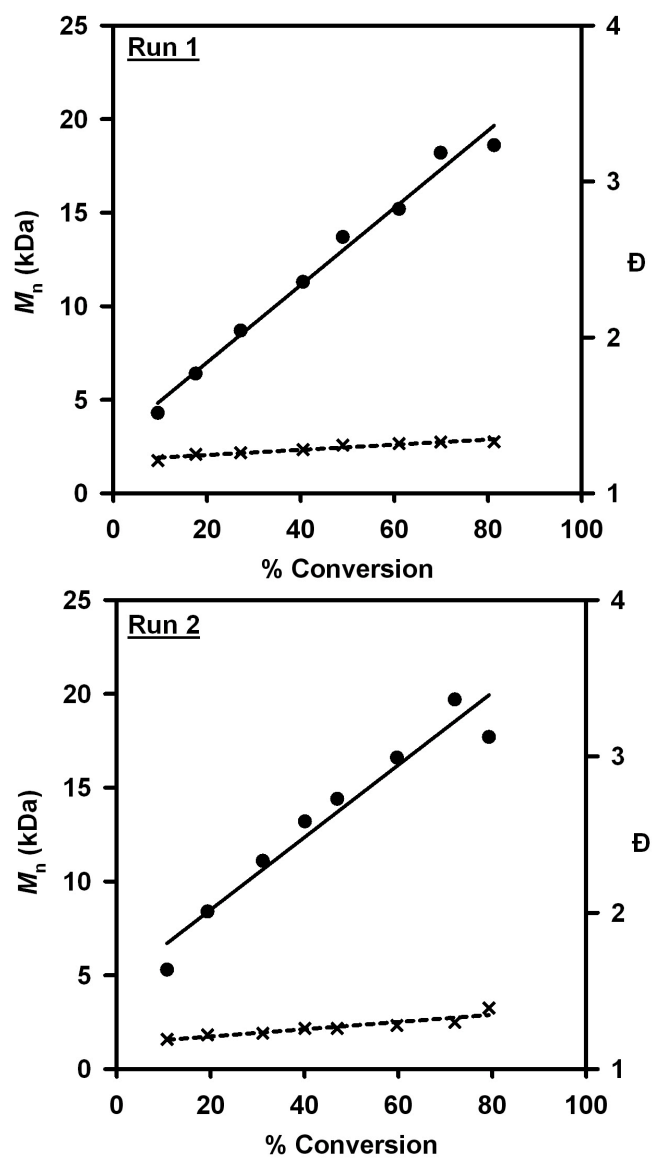| % Conversion	M_n (kDa)	Đ
10	6.4	1.65
24	8.9	1.76
32	11.1	1.96
46	14.3	1.85
59	13.9	2.13
71	14.3	2.18
79	15.3	2.23

Table S2-13. Data for the plot in Figure S2-35, Run 2.

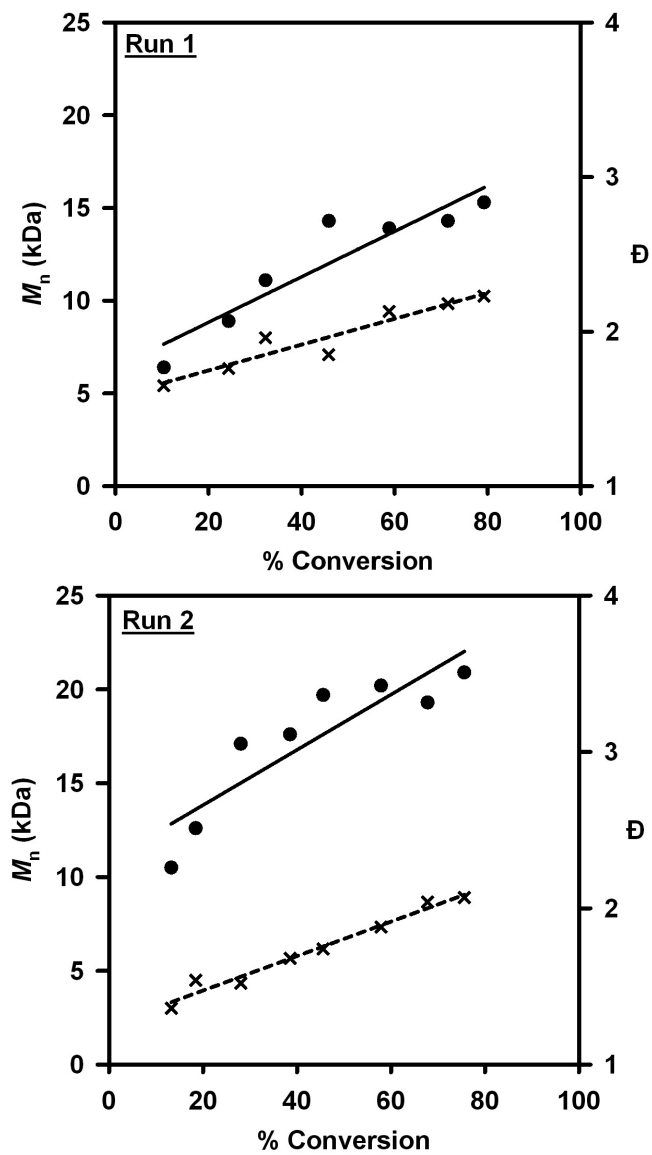| % Conversion	M_n (kDa)	Đ
13	10.5	1.36
18	12.6	1.54
28	17.1	1.52
39	17.6	1.68
46	19.7	1.74
59	20.2	1.88
68	19.3	2.04
76	20.9	2.07

Figure S2-36. Plot of M_n (●) and Đ (x) versus conversion for **1d** (temp = 0 °C, [**1d**] = 0.0015 M, [**6**] = 0.10 M (Run 1), 0.10 M (Run 2)).
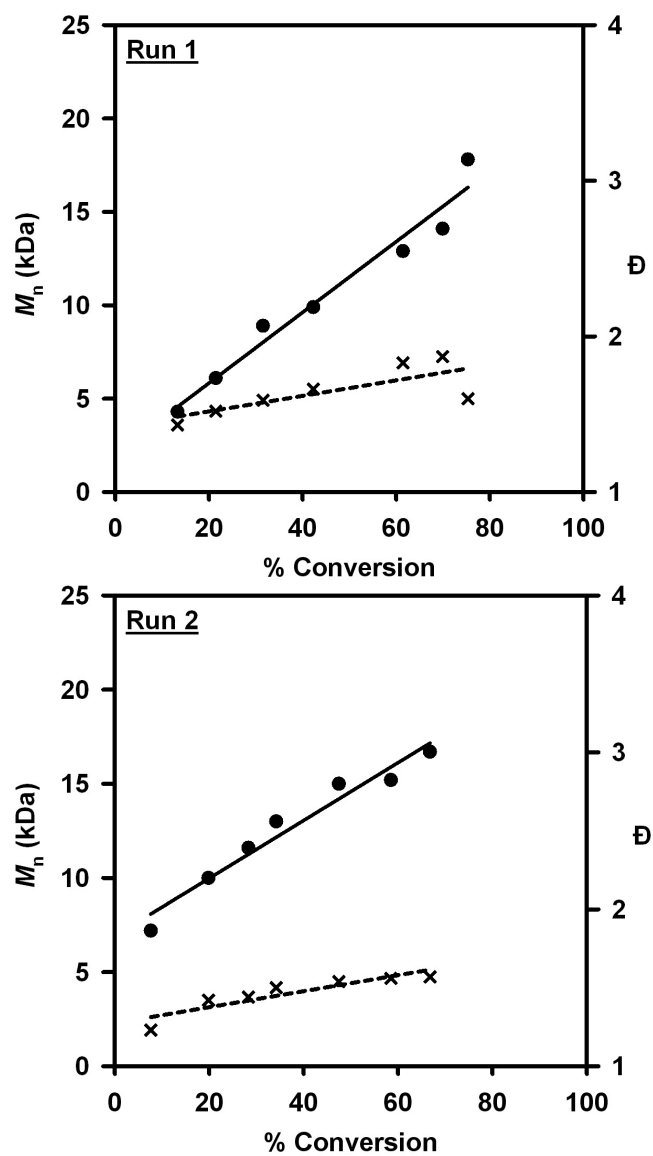
Table S2-14. Data for the plot in Figure S2-36, Run 1.

% Conversion	M_n (kDa)	Đ
13	4.3	1.43
21	6.1	1.52
32	8.9	1.59
42	9.9	1.66
61	12.9	1.83
70	14.1	1.87
75	17.8	1.60

Table S2-15. Data for the plot in Figure S2-36, Run 2.

% Conversion	M_n (kDa)	Đ
8	7.2	1.23
20	10.0	1.42
28	11.6	1.44
34	13.0	1.50
47	15.0	1.54
59	15.2	1.56
67	16.7	1.57
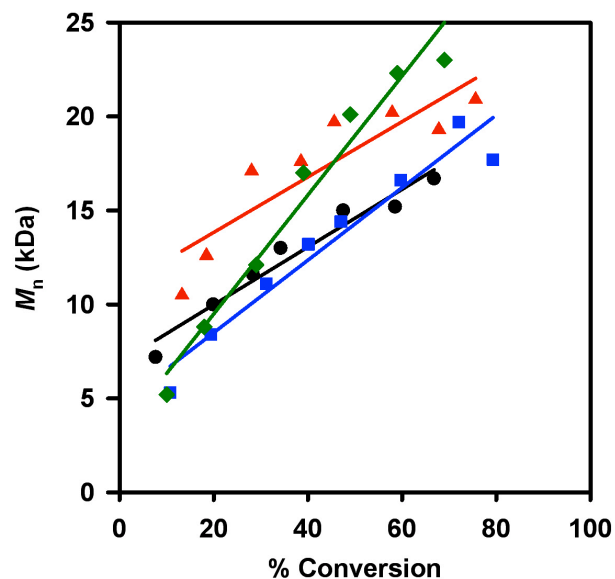
Figure S2-37. Representative plot of M_n versus conversion for all four catalysts. Samples within ±4% of target conversion were included (**1a**(◆); **1b**(■); **1c**(▲); **1d**(●)).
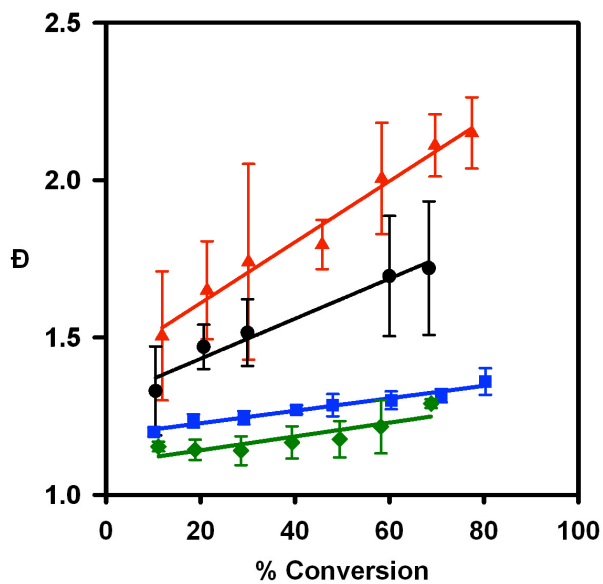
Figure S2-38. Plot of average Đ versus conversion for all four catalysts with error bars. Samples within ±4% of target conversion were included (**1a**(◆); **1b**(■); **1c**(▲); **1d**(●)).

Comparison of propagation and simulated Ni initiator consumption

The React IR was used to determine [**6**] over time. The data for [**1a-d**] was simulated based on rate constant and initiation concentration where [Ni]$_0$ = 0.0015 M using equation (3).

$$[Ni] = [Ni]_0 e^{-k_{re(initiation)}t}$$

$$(3)$$
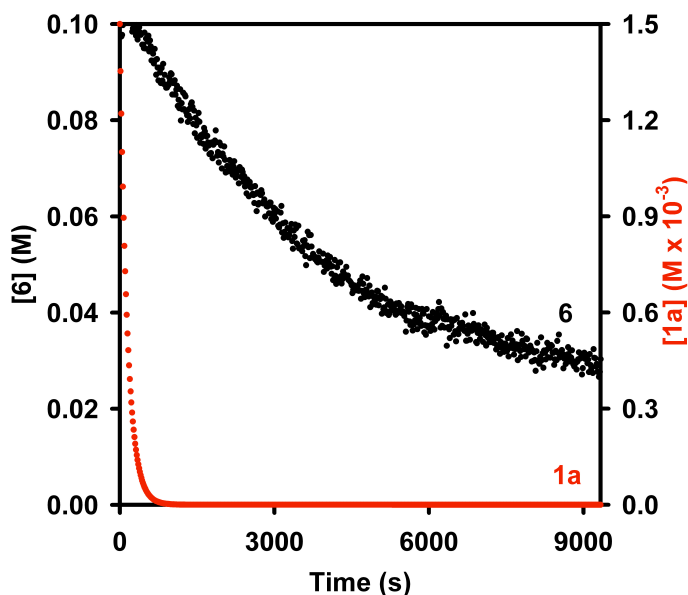
Figure S2-39. Plot of [**6**] (●) and simulated [**1a**] (●) versus time.

Figure S2-40. Plot of [**6**] (●) and simulated [**1b**] (●) versus time.

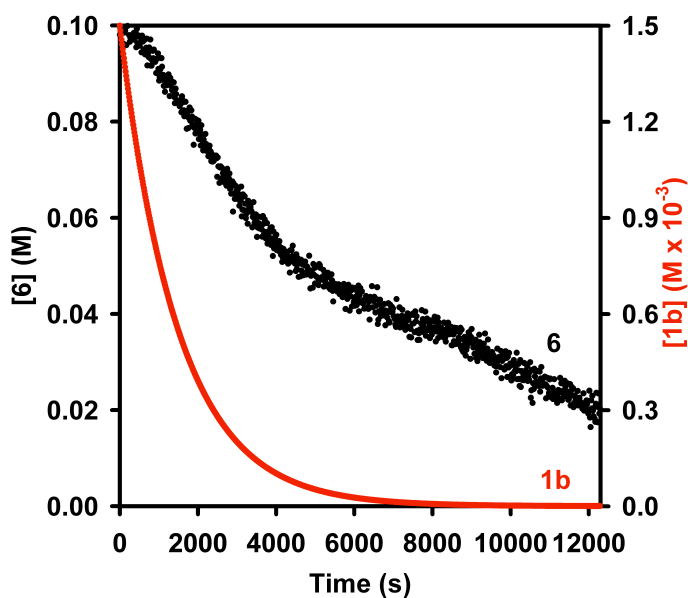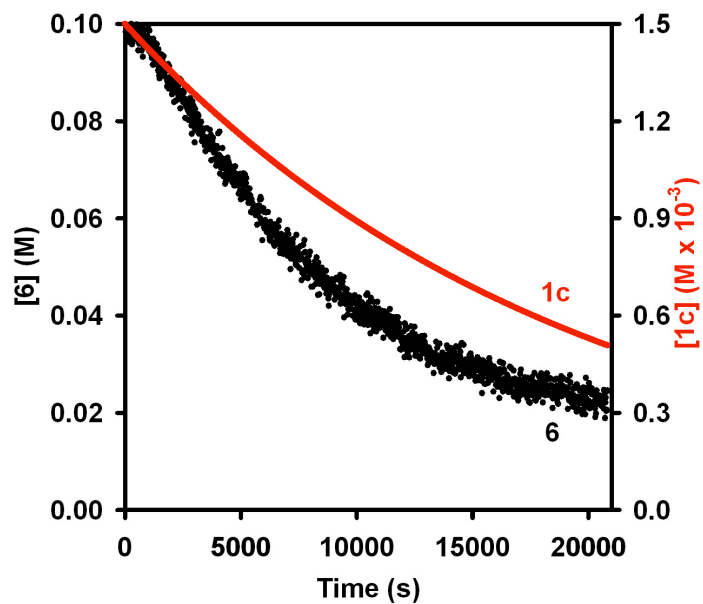**Figure S2-41**. Plot of [**6**] (●) and simulated [**1c**] (●) versus time.
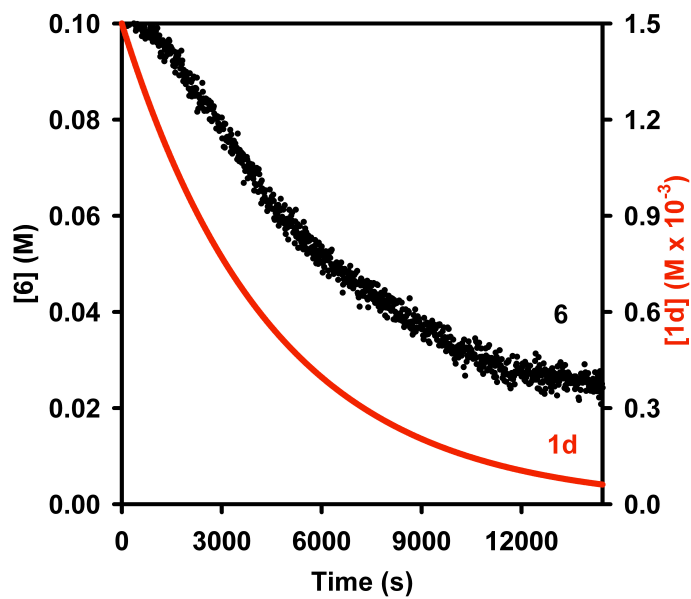
Figure S2-42. Plot of [**6**] (●) and simulated [**1d**] (●) versus time.

All actions were performed in a glovebox under N_2 atmosphere. A 20 mL vial was equipped with a stir bar. Sequentially, **1b** (12 mg, 0.016 mmol, 1 equiv), THF (4.8 mL), and **6** (0.20 mL, 0.46 M, 7 equiv) were added to the flask. After 1.5 h, the reaction was removed from the glovebox and poured into HCl (3 mL, 12 M) and then extracted with CH_2Cl_2 (3 x 5 mL). The combined organic layers were dried over $MgSO_4$ and filtered. The filtrate was concentrated in vacuo. The resulting solid was washed with MeOH (20 mL) to give **P6** as an off-white solid: M_n: 2.1 kDa, Đ: 1.23 (GPC). For the MS sample a small amount of polymer was dissolved in $CHCl_3$ and first filtered through a pipet column of basic, acidic, and neutral alumina to remove residual Ni and the solution was concentrated in vacuo. The general procedure was followed for MALDI-TOF MS sample preparation (see General Experimental pS2).
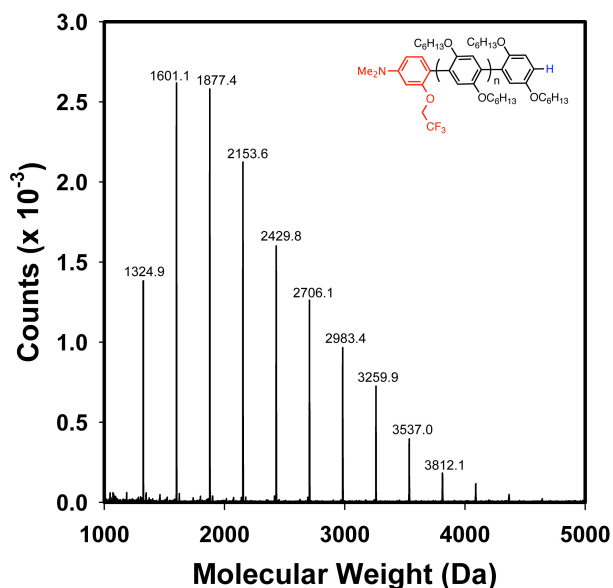
Figure S2-43. MALDI-TOF MS spectrum of **P6a** initiated with **1a**.
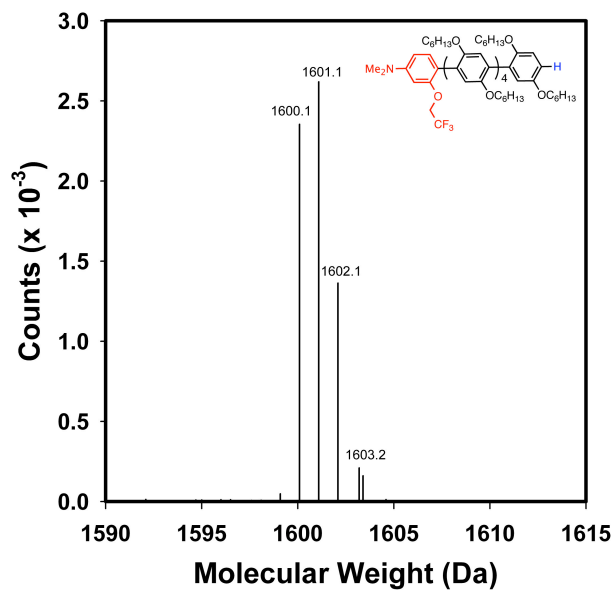
Figure S2-44. Expanded view of Figure S2-43.
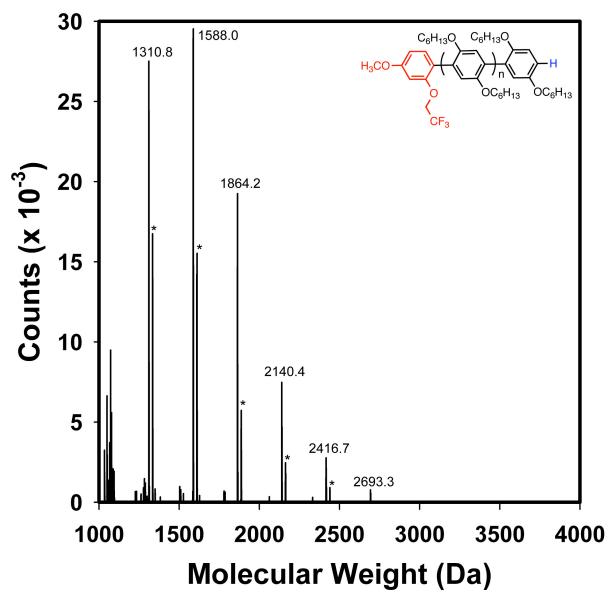
Figure S2-45. MALDI-TOF MS spectrum of **P6b** initiated with **1b**.
*Represents [M + Na]⁺.
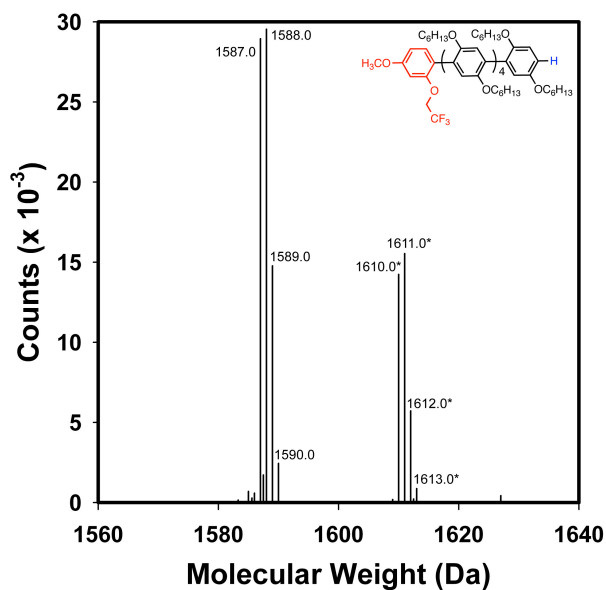
Figure S2-46. Expanded view of Figure S2-45.
*Represents [M + Na]⁺.

Figure S2-47. MALDI-TOF MS spectrum of **P6c** initiated with **1c**.
*Represents [M + Na]+.
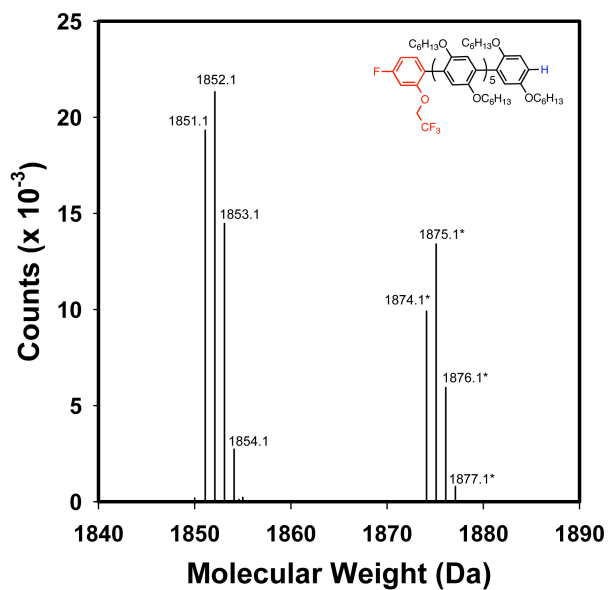
Figure S2-48. Expanded view of Figure S2-47.
*Represents [M + Na]+.
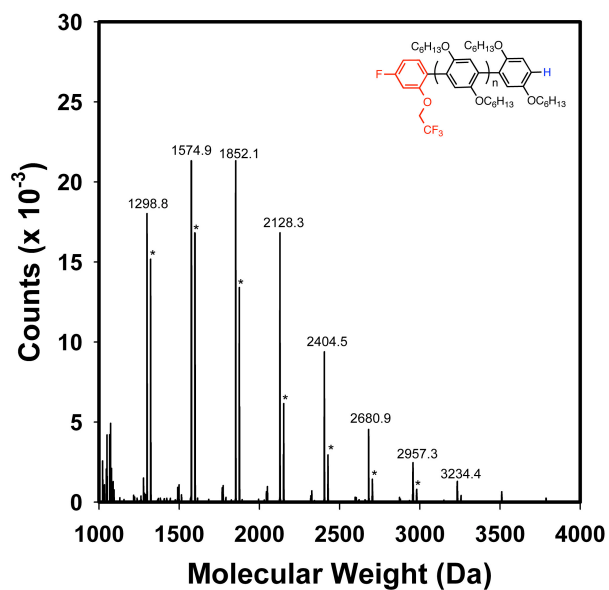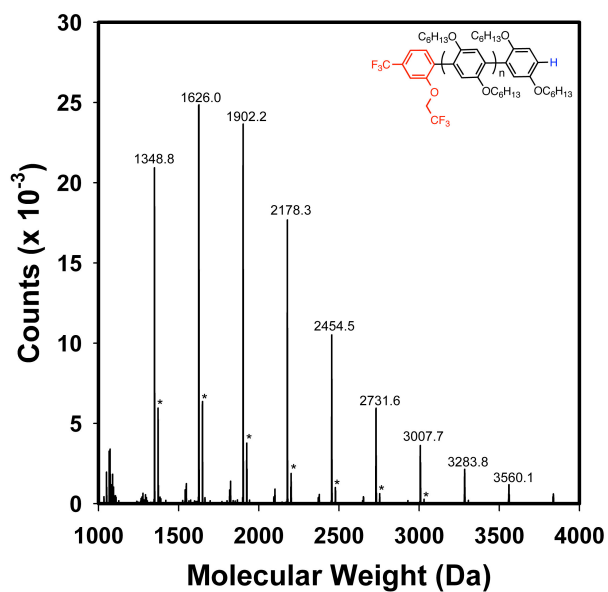
Figure S2-49. MALDI-TOF MS spectrum of **P6d** initiated with **1d**.
*Represents [M + Na]$^+$.
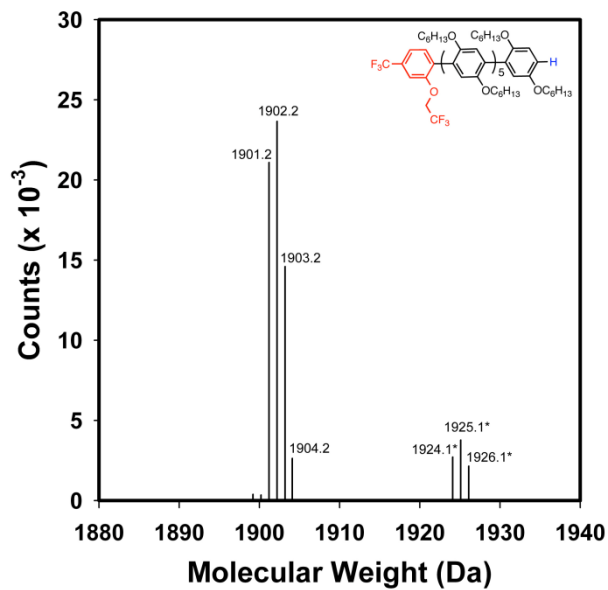
Figure S2-50. Expanded view of Figure S2-49.
*Represents [M + Na]$^+$.

VII. Computational Studies

Transition states (TSs) on the spin-singlet potential energy surface were optimized for the reductive elimination from **3** for 20 substituents (see Table S2-16). For selected substituted systems, we also examined the triplet electronic state, which is at least 30 kcal mol^{-1} higher in energy than the singlet. For R = H, we performed a systematic search of conformations of **3** to identify the low-lying rotamers of the aryl substituents and phosphine substituents. The resulting lowest-lying conformation is depicted in Fig. S2-51, for both **3** and the corresponding TS. Reactants (**3**) and TSs for each of the 20 substituents were then optimized based on this low-lying conformation. Free energy barriers were computed based on the quasi-harmonic-oscillator/rigid-rotor approximation, at a temperature of 273 K. For all reported TSs, there was a single imaginary frequency with an imaginary mode indicative of the forming C–C bond and breaking C–Ni bonds. Optimized Cartesian coordinates for all 20 reactants and TSs are listed at the end of this file.
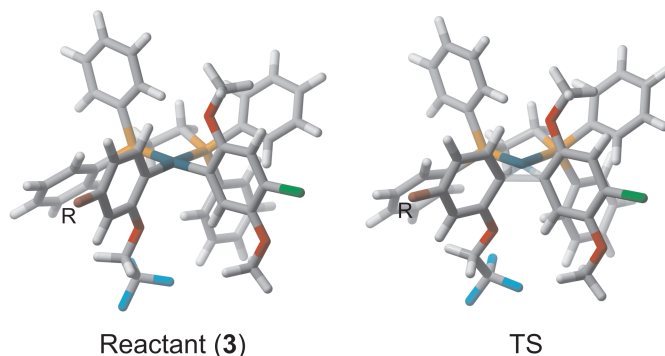
Reactant (**3**)　　　　　　　　TS

Figure S2-51. Structures of the reactant and TS for the reductive elimination of **3**.

The computed free energy barriers are listed in Table S2-16, along with Hammett constants and changes in the charge delocalized on the two aryl rings. As shown in Fig. S2-52, there is essentially no linear correlation between computed barrier heights and either the Hammett σ_p constants or the differences in charges of the reacting carbon atoms.
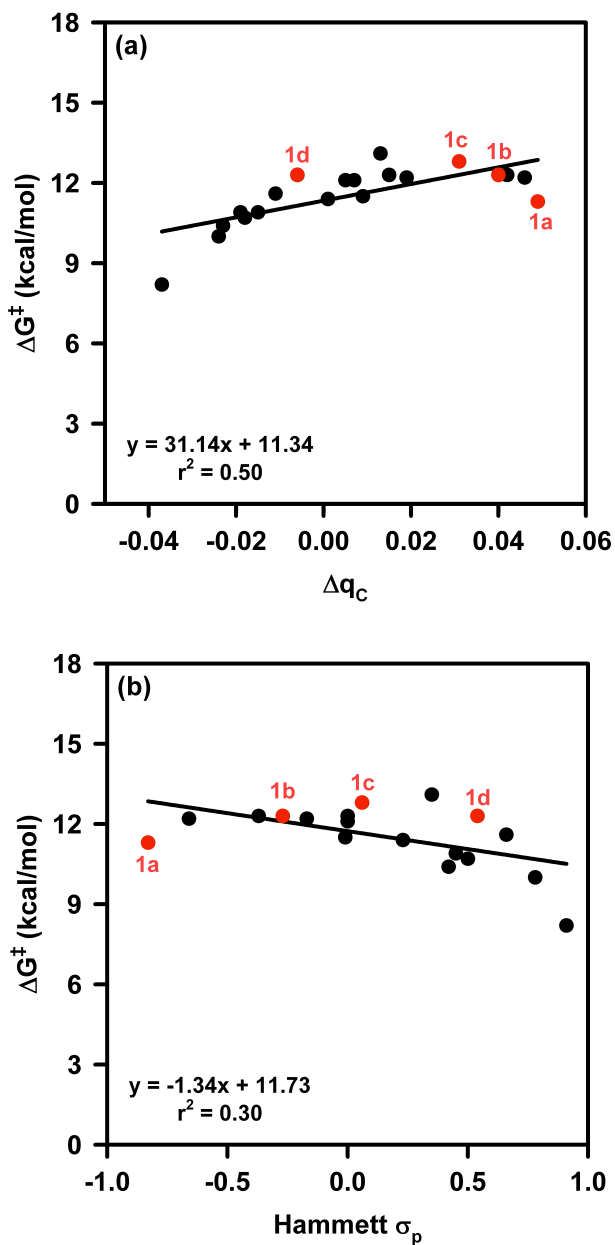
Figure S2-52. Plots of free energy barriers (kcal mol^{-1}) versus (a) the difference in charge between the two reacting carbon atoms (Δq_C) and (b) Hammett σ_p constants.

Changes in the ring charges were calculated to test whether the ability of the aryl rings to delocalize the increasing electron density on the catalyst during the reductive elimination is responsible for the lowering of the reaction barriers. Charges were computed for each atom in the reactants and TSs for all 20 substituted systems based on natural population analyses (NPA). The total charge on the two reacting phenyl rings, excluding the reacting carbons but including all aryl substituents, was calculated for the reactant and TS. The difference in these ring charges (TS – reactant) is reported as ΔCharge in Table S2-16.
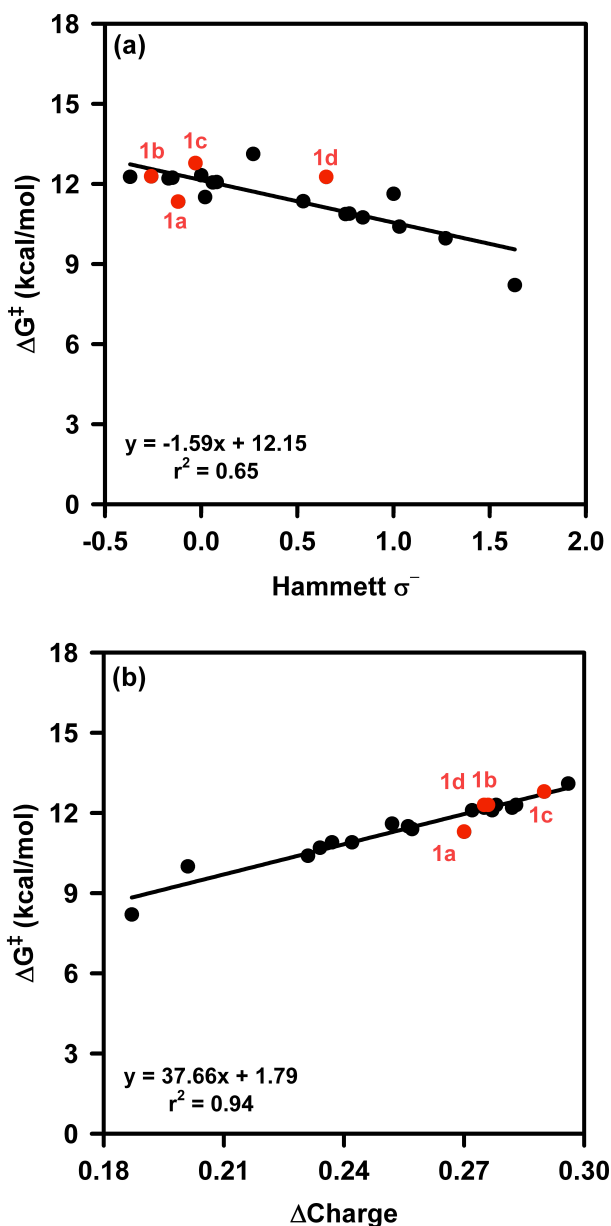
Figure S2-53. Plots of free energy barriers (kcal mol^{-1}) versus (a) Hammett σ^{-} constants and (b) change in charge on two aryl rings between **3** and the transition state, excluding the carbon atoms bound to the Ni.

Table S2-16. Computed free energy barriers ($\Delta G^{\ddagger}$, kcal mol^{-1}), Hammett σ_p and σ^{-} constants, the change in charge on the two aryl rings (ΔCharge), the charges on the reacting carbons [q_{C1} and qc2, where C1 and C2 refer to the carbons on the substituted and monomer rings, respectively], and the difference in charges at the reacting carbons (Δq_C).

R	$\Delta G^{\ddagger}$	σ_p	σ^{-}	ΔCharge	q_{C1}	q_{C2}	Δq_C
NH$_2$	12.2	–0.66	–0.15	0.275	-0.228	-0.182	0.046
N(CH$_3$)$_2$	11.3	–0.83	–0.12	0.270	-0.231	-0.182	0.049
CH$_3$	12.2	–0.17	–0.17	0.282	-0.201	-0.183	0.019
H	12.3	0.00	0.00	0.283	-0.197	-0.182	0.015
OCH$_3$	12.3	–0.27	–0.26	0.276	-0.221	-0.181	0.040
CCH	11.4	0.23	0.53	0.257	-0.183	-0.182	0.001
F	12.8	0.06	–0.03	0.290	-0.214	-0.183	0.031
CF$_3$	12.3	0.54	0.65	0.275	-0.178	-0.184	-0.006
CN	11.6	0.66	1.00	0.252	-0.172	-0.183	-0.011
NO$_2$	10.0	0.78	1.27	0.201	-0.161	-0.184	-0.024
CHO	10.4	0.42	1.03	0.231	-0.161	-0.184	-0.023
COCH$_3$	10.7	0.50	0.84	0.234	-0.166	-0.184	-0.018
SCH$_3$	12.1	0.00	0.06	0.272	-0.188	-0.184	0.005
COOCH$_3$	10.9	0.45	0.75	0.242	-0.168	-0.183	-0.015
NO	8.2	0.91	1.63	0.187	-0.146	-0.183	-0.037
OCF$_3$	13.1	0.35	0.27	0.296	-0.196	-0.183	0.013
OH	12.3	–0.37	–0.37	0.278	-0.224	-0.182	0.042
COOH	10.9	0.45	0.77	0.237	-0.165	-0.184	-0.019
CH$_2$OH	12.1	0.00	0.08	0.277	-0.189	-0.182	0.007
Ph	11.5	–0.01	0.02	0.256	-0.191	-0.182	0.009

VIII. References Cited

(1)   Lanni, E. L.; McNeil, A. J. *Macromolecules* **2010**, *43*, 8039–8044.

(2)   (a) Lanni, E. L.; McNeil, A. J. *J. Am. Chem. Soc.* **2009**, *131*, 16573–16579. (b) Miyakoshi, R.; Shimono, K.; Yokoyama, A.; Yokozawa, T. *J. Am. Chem. Soc.* **2006**, *128*, 16012–16013.

(3)   Leonardi, A.; Motta, G.; Riva, C.; Testa, R. WO/01/09140.

(4)   Xichen, L.; Feng, R.; Yugui, S. WO/2010/145203.

(5)   Maruyama, S.; Kawanishi, Y. *J. Mater. Chem.* **2002**, *12*, 2245–2249.

(6)   Barhate, N. B.; Gajare, A. S.; Wakharkar, R. D.; Bedekar, A. V. *Tetrahedron* **1999**, *55*, 11127–11142.

(7)   Love, B. E.; Jones, E. G. *J. Org Chem.* **1999**, *64*, 3755–3756.

(8)   For the numerical integration procedure, see:
http://www.chem.cornell.edu/dbc6/Site_2/Group_Resources.html. For leading references on this procedure, see: (a) Hoepker, A. C.; Gupta, L.; Ma, Y.; Faggin, M. F.; Collum, D. B. *J. Am. Chem. Soc.* **2011**, *133*, 7135–7151. (b) Ma, Y.; Hoepker, A. C.; Gupta, L.; Faggin, M. F.; Collum, D. B. *J. Am. Chem. Soc.* **2010**, *132*, 15610–15623.

Appendix 3

Supporting Information for Chapter 4
Utilizing Heteroaromatic and Aromatic Reactive Ligands to Selectively Increase
Initiation Rates

Contents   **Page**

I. Materials

i-PrMgCl (2 M in THF) was purchased in 100 mL quantities from Aldrich. Bis(cyclooctadiene)nickel (Ni(cod)$_2$) and 1,2-bis(diphenylphosphino)ethane (dppe) were purchased from Strem. All other reagent grade materials and solvents were purchased from Aldrich, Acros, EMD, or Fisher and used without further purification unless otherwise noted. THF was dried and deoxygenated using an Innovative Technology (IT) solvent purification system composed of activated alumina, copper catalyst, and molecular sieves. N-Bromosuccinimide (NBS) was recrystallized from hot water and dried over P$_2$O$_5$. Flash chromatography was performed on SiliCycle silica gel (40-63 µm) and thin layer chromatography was performed on Merck TLC plates pre-coated with silica gel 60 F254. Compounds **S1–S2**,[1] **S4**,[2] and **4–10** (except **5**)[3] were prepared from modified literature procedures.

II. General Experimental

NMR Spectroscopy: Unless otherwise noted, ^{1}H, ^{13}C, ^{19}F and ^{31}P NMR spectra for all compounds were acquired at rt in CD_2Cl_2 or $CDCl_3$ on a Varian vnmrs 700 operating at 700, 176, 660, and 283 MHz and Varian vnmrs 500 operating at 500, 126, 470, and 202 MHz, respectively. For ^{1}H and ^{13}C spectra in deuterated solvents, the chemical shift data are reported in units of δ (ppm) relative to tetramethylsilane (TMS) and referenced with residual solvent. ^{19}F NMR spectra were referenced to $CFCl_3$ and ^{31}P NMR spectra were referenced to H_3PO_4. For ^{1}H, ^{19}F and ^{31}P NMR spectra in non-deuterated THF, the chemical shift data are reported in units of δ (ppm) and referenced with the THF peak at 3.58 ppm in the ^{1}H NMR spectrum which is then applied to all nuclei. Multiplicities are reported as follows: singlet (s), doublet (d), doublet of doublets (dd), triplet (t), quartet (q), multiplet (m), broad resonance (br), and apparent triplet (at).

Mass Spectrometry: HRMS data were obtained on a Micromass AutoSpec Ultima Magnetic Sector mass spectrometer.

IR Spectroscopy: Samples were recorded using a Mettler Toledo ReactIR iC10 fitted with a Mercury Cadmium Telluride (MCT) detector, and AgX probe (9.5 mm x 1.5 mm) with a SiComp tip. The spectra were processed using icIR 4.0 software and raw absorbances were exported into Microsoft Excel or Sigma Plot 10 for analysis.

MALDI-TOF MS: MALDI-TOF mass spectra were recorded using Bruker AutoFlex Speed in linear mode at mass between 5000 and 15000. The matrix, *trans*-2-[3-(4-*tert*-butylphenyl)-2-methyl-2-propenylidene]malononitrile (DCTB), was prepared at a concentration of 0.1 M in $CHCl_3$ and the matrix, sinapic acid, was prepared as saturated solution in a mixture of 30/70 (v/v) $MeCN/H_2O$ with 0.1% TFA. The instrument was calibrated with a mixture of peptides in the sinapic acid matrix. The polymer sample was dissolved in THF to obtain a ~1 mg/mL solution. A 2 μL aliquot of polymer solution was mixed with 2 μL of the DCTB matrix solution. This mixture (1 μL) was placed on the target plate and then air-dried.

Gel-Permeation Chromatography: Polymer molecular weights were determined by comparison with polystyrene standards (Varian, EasiCal PS-2 MW 580-377,400) on a Waters 1515 HPLC instrument equipped with Waters Styragel® (7.8 x 300 mm) THF HR 0.5, THF HR 1, and THF HR 4 type columns in sequence and analyzed with Waters 2487 dual absorbance detector (254 nm). Samples were dissolved in THF (with mild heating) and passed through a 0.2 μm PTFE filter prior to analysis.

Titrations of the Grignard Reagents: An accurately weighed sample of salicylaldehyde phenylhydrazone[4] (typically between 290–310 mg) was dissolved in THF (5.00 mL). An aliquot (0.50 mL) of this solution was stirred at rt while

ArMgCl in THF was added dropwise using a 500 µL syringe. The initial solution is yellow and turns bright orange at the end-point.

Statistical Analysis: Reported quantitative data represents the average of 2-3 experiments and the error bars represent the standard deviation in these measurements.

III. Synthetic Procedures
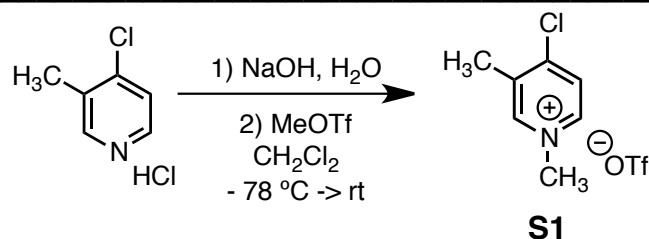
S1. In a 50 mL round-bottom flask, 4-chloro-3-methylpyridine hydrochloride (332 mg, 2.03 mmol, 1.0 equiv) was dissolved H_2O (3.0 mL) and NaOH (2.4 mL, 1.0 M in H_2O) was added dropwise while stirring. The solution turned from clear to yellow. After stirring for 5 min at rt, the reaction was extracted with Et_2O (3 x 3 mL). The combined organic layers were dried over $MgSO_4$, filtered, and transferred into 25 mL oven-dried Schlenk flask equipped with a stir bar. The organic layer was then concentrated in vacuo. The resulting yellow oil was dissolved in dry CH_2Cl_2 (3 mL) and cooled to -78 °C. While stirring, methyl trifluoromethanesulfonate (220 µL, 2.01 mmol, 1.0 equiv) was added dropwise. The mixture was allowed to warm to rt and stirred overnight. The reaction was concentrated in vacuo and the resulting solid was triterated in THF (1 x 3 mL) and Et_2O (2 x 3 mL) to give 444 mg of **S1** as a white solid (76% yield). HRMS (ESI) [M+] Calcd. for C_7H_9ClN, 142.0418; found, 142.0415. [M-] Calc, for CF_3O_3S, 148.9520; found, 148.9520. ^{19}F NMR (470 MHz, CD_2Cl_2) δ -79.15.
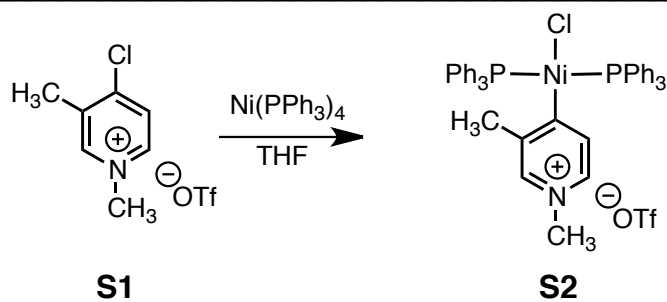
S2. A 20 mL vial was equipped with a stir bar in the glovebox. Sequentially, $Ni(PPh_3)_4$ (122 mg, 0.110 mmol, 1.1 equiv), **S1** (29 mg, 0.10 mmol, 1.0 equiv), and THF (1 mL) were added. The dark red homogeneous solution was stirred at rt overnight. The resulting yellow precipitate in an orange/brown solution was filtered through Celite and washed with toluene (20 mL). The yellow/orange solid was dissolved in CH_2Cl_2 (50 mL), filtered, and dried in vacuo to give 78 mg of **S2** as a yellow solid (89% yield). Elemental Analysis: Calcd for $C_{44}H_{39}ClF_3NNiO_3P_2S$, C, 60.40; H, 4.49; Found C, 60.26; H, 4.74. ^{19}F NMR (470 MHz, CD_2Cl_2) δ -79.03.
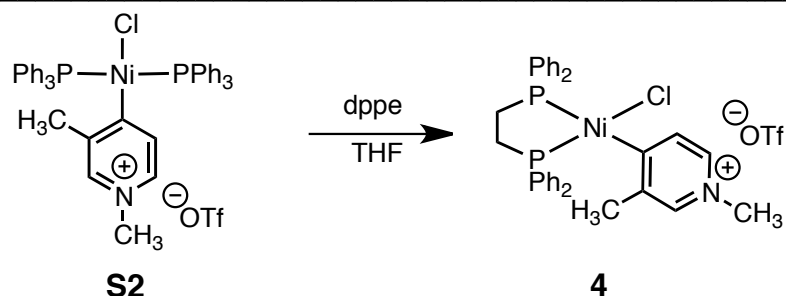
4. A 20 mL vial was equipped with a stir bar in the glovebox. Sequentially, **S2** (89 mg, 0.10 mmol, 1.0 equiv), dppe (44 mg, 0.11 mmol, 1.1 equiv), and THF (2 mL) were added. The solution turned from yellow heterogeneous to orange homogeneous solution in 30 min. The solution was stirred at rt for 2 h. The orange solution was concentrated in vacuo until ~0.5 mL of solution was left. Addition of hexanes (3 mL) led to an orange precipitate. The solid was filtered and washed with hexanes (20 mL). The resulting solid was recrystallized in THF/hexanes to give 54 mg of **4** as an orange solid (72% yield). Elemental Analysis: Calcd for $C_{34}H_{33}ClF_3NNiO_3P_2S$, C, 54.54; H, 4.44; N, 1.87; Found C, 54.78; H, 4.70; N, 1.80. ^{19}F NMR (470 MHz, CD_2Cl_2) δ -78.86.
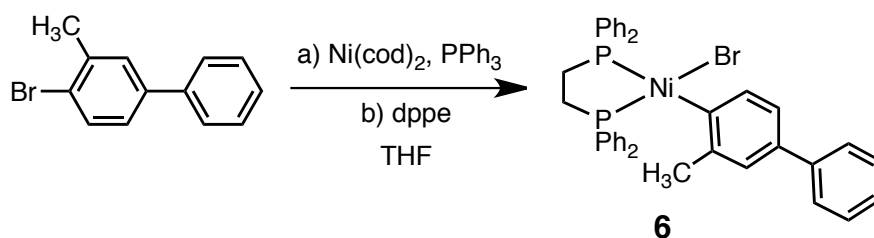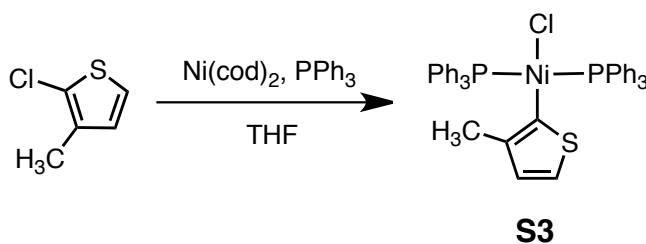

6. A 20 mL vial was equipped with a stir bar in the glovebox. Sequentially, Ni(cod)$_2$ (84 mg, 0.31 mmol, 1.0 equiv), PPh$_3$ (161 mg, 0.615 mmol, 2.0 equiv) and THF (2 mL) were added. The solution was stirred for 5 min and 4-bromo-3-methylbiphenyl (86 mg, 0.35 mmol, 1.1 equiv) and THF (2 mL) were added. The solution was stirred at rt for 2 h. To the deep red solution, dppe (2 mL, 0.17 M in THF, 0.34 mmol, 1.1 equiv) were added. The solution was stirred for another 2 h. The orange solution was concentrated in vacuo until ~1 mL of solution was left. Addition of hexanes (18 mL) led to a yellow orange precipitate. The solid was filtered and washed with hexanes (20 mL). The resulting solid was recrystallized in THF/hexanes to give 106 mg of **6** as an orange solid (50% yield). Elemental Analysis: Calcd for $C_{39}H_{35}BrNiP_2$, C, 66.51; H, 5.01; Found C, 66.57; H, 5.16.
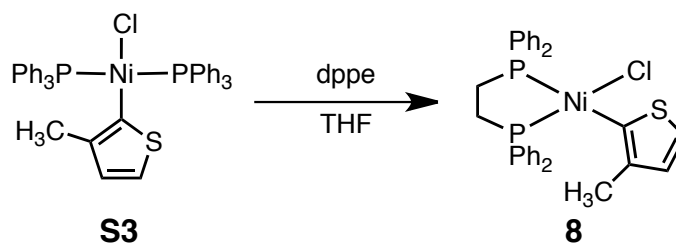
7
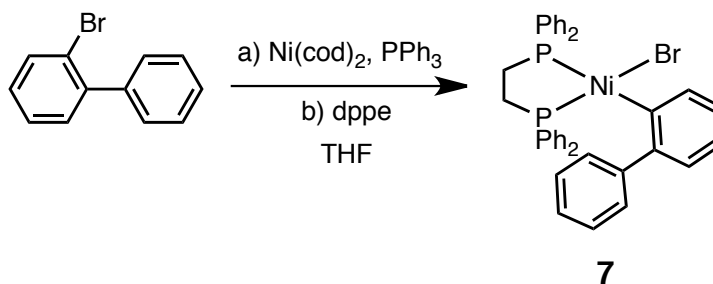
6. A 20 mL vial was equipped with a stir bar in the glovebox. Sequentially, Ni(cod)$_2$ (137 mg, 0.498 mmol, 1.0 equiv), PPh$_3$ (264 mg, 1.01 mmol, 2.0 equiv) and THF (6 mL) were added. The solution was stirred for 5 min and 2-bromobiphenyl (0.13 mL, 0.75 mmol, 1.5 equiv) was added. The solution was stirred at rt for 2 h. To the deep red solution, dppe (4 mL, 0.14 M in THF, 0.55 mmol, 1.1 equiv) were added. The solution was stirred for another 2 h. The orange solution was concentrated in vacuo until ~2 mL of solution was left. Addition of hexanes (18 mL) led to a yellow precipitate. The solid was filtered and washed with hexanes (20 mL). The resulting solid was recrystallized in THF/hexanes to give 288 mg of **6** as a yellow solid (83% yield). Elemental Analysis: Calcd for C$_{38}$H$_{33}$BrNiP$_2$, C, 66.13; H, 4.82; Found C, 66.10; H, 4.98.


S3

S3. A 20 mL vial was equipped with a stir bar in the glovebox. Sequentially, Ni(cod)$_2$ (139 mg, 0.506 mmol, 1.0 equiv), PPh$_3$ (262 mg, 0.999 mmol, 2.0 equiv), toluene (4 mL), and 2-chloro-3-methylthiophene (82 µL, 0.75 mmol, 1.5 equiv) were added. The solution was stirred at rt for 30 min and turned from dark red homogeneous to orange heterogeneous solution. The reaction was removed from the glovebox. Addition of hexanes (30 mL) led to an orange precipitate. The solid was filtered and washed with hexanes (20 mL) and cold MeOH (5 mL). The resulting solid was recrystallized in THF/hexanes to give 299 mg of **S3** as an orange solid (84% yield). Elemental analysis: Calcd for C$_{41}$H$_{35}$ClNiP$_2$S, C, 68.79; H, 4.93; Found C, 68.49; H, 4.88.
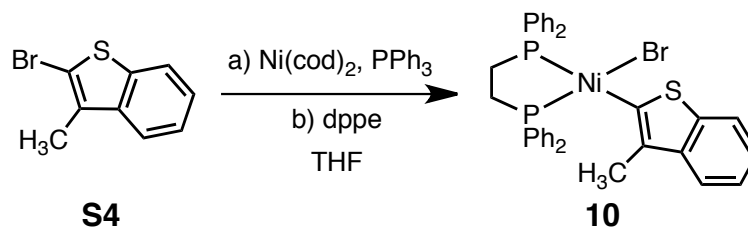
8. A 20 mL vial was equipped with a stir bar in the glovebox. Sequentially, **S2** (144 mg, 0.20 mmol, 1.0 equiv), dppe (89 mg, 0.22 mmol, 1.1 equiv), and THF (4 mL) were added. The solution was stirred at rt for 1 h. The heterogeneous orange solution was concentrated in vacuo until ~1 mL of solution was left. Addition of hexanes (18 mL) led to an orange precipitate. The solid was filtered and washed with hexanes (20 mL). The resulting solid was recrystallized in THF/hexanes to give 78 mg of **7** as an orange solid (66% yield). The product is air-sensitive and prone to decomposition.
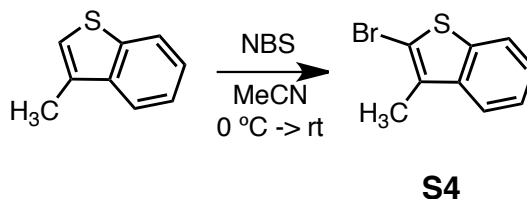

S4. A 10 mL round-bottom flask was equipped with a stir bar and cooled to 0 °C with ice bath. Sequentially, 3-methylbenzothiophene (402 μL, 3.00 mmol, 1.0 equiv), MeCN (3.5 mL), and NBS (561 mg, 3.15 mmol, 1.05 equiv) were added. The ice bath was removed after 5 min and the solution was stirred at rt for 30 min. The reaction was quenched with water (15 mL) and extracted with CH_2Cl_2 (3 x 10 mL). The combined organic layers were dried over $MgSO_4$, filtered, and concentrated in vacuo. The resulting oil was purified with silica gel chromatography, using 100% hexanes as the eluent to give 618 mg of **S4** as a clear liquid (91% yield). HRMS (EI): [M+] Calcd for C_9H_7BrS, 225.9452; found, 225.9450.

S4 → **10**

a) Ni(cod)$_2$, PPh$_3$

b) dppe

THF

9. A 20 mL vial was equipped with a stir bar in the glovebox. Sequentially, Ni(cod)$_2$ (82 mg, 0.30 mmol, 1.0 equiv), PPh$_3$ (158 mg, 0.602 mmol, 2.0 equiv) and THF (3 mL) were added. The solution was stirred for 5 min and **S4** (104 mL, 0.46 mmol, 1.5 equiv) and THF (1 mL) were added. The solution was stirred at rt for 1.5 h. To the deep red solution, dppe (2 mL, 0.17 M in THF, 0.33 mmol, 1.1 equiv) were added. The solution was stirred for another 2 h. The orange solution was concentrated in vacuo until ~1 mL of solution was left. Addition of hexanes (18 mL) led to a yellow precipitate. The solid was filtered and washed with hexanes (5 mL). The resulting solid was recrystallized in THF/hexanes to give 133 mg of **9** as a dark orange solid (65% yield). Elemental Analysis: Calcd for C$_{35}$H$_{31}$BrNiP$_2$S, C, 61.44; H, 4.57; Found C, 61.33; H, 4.68.
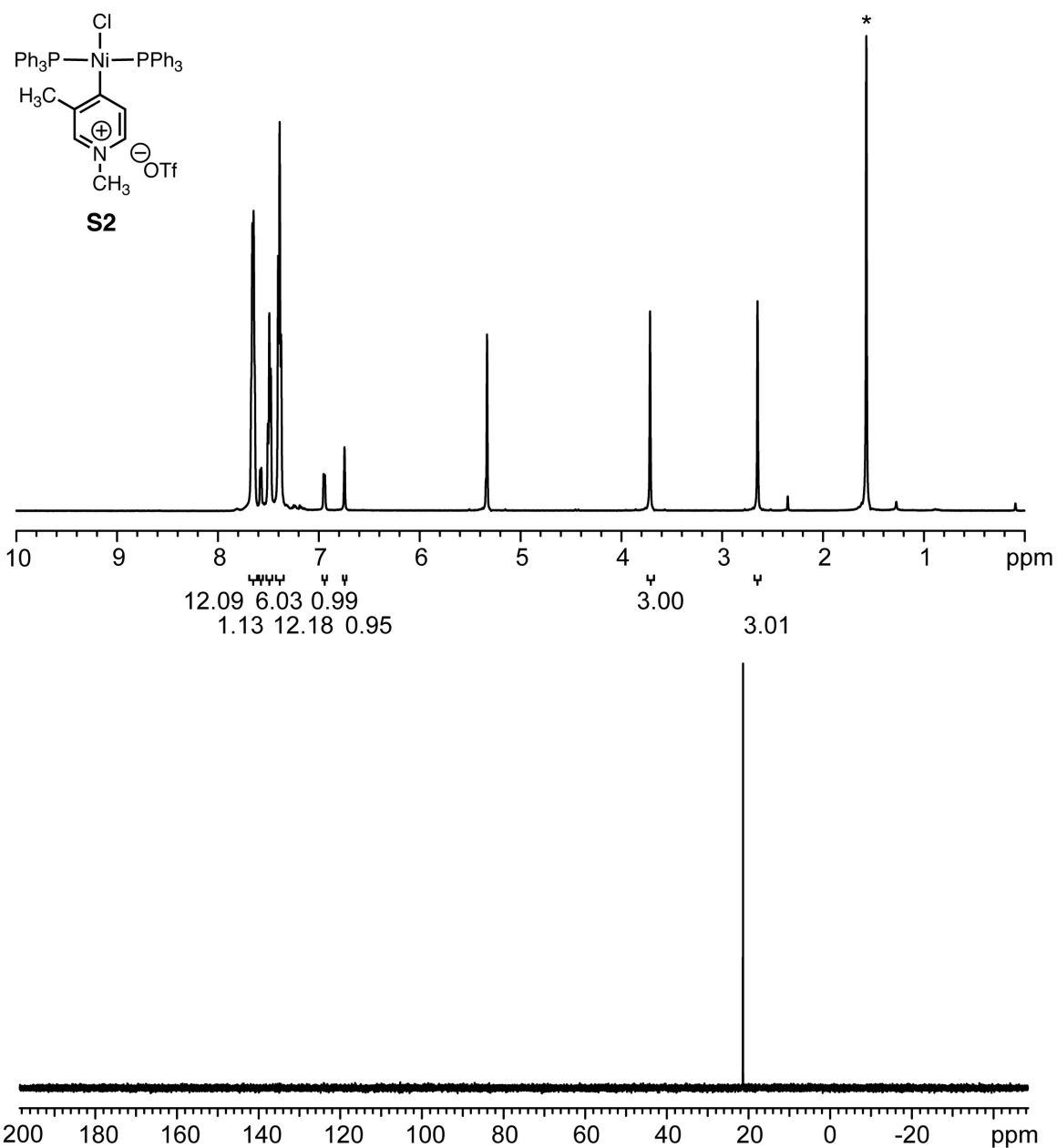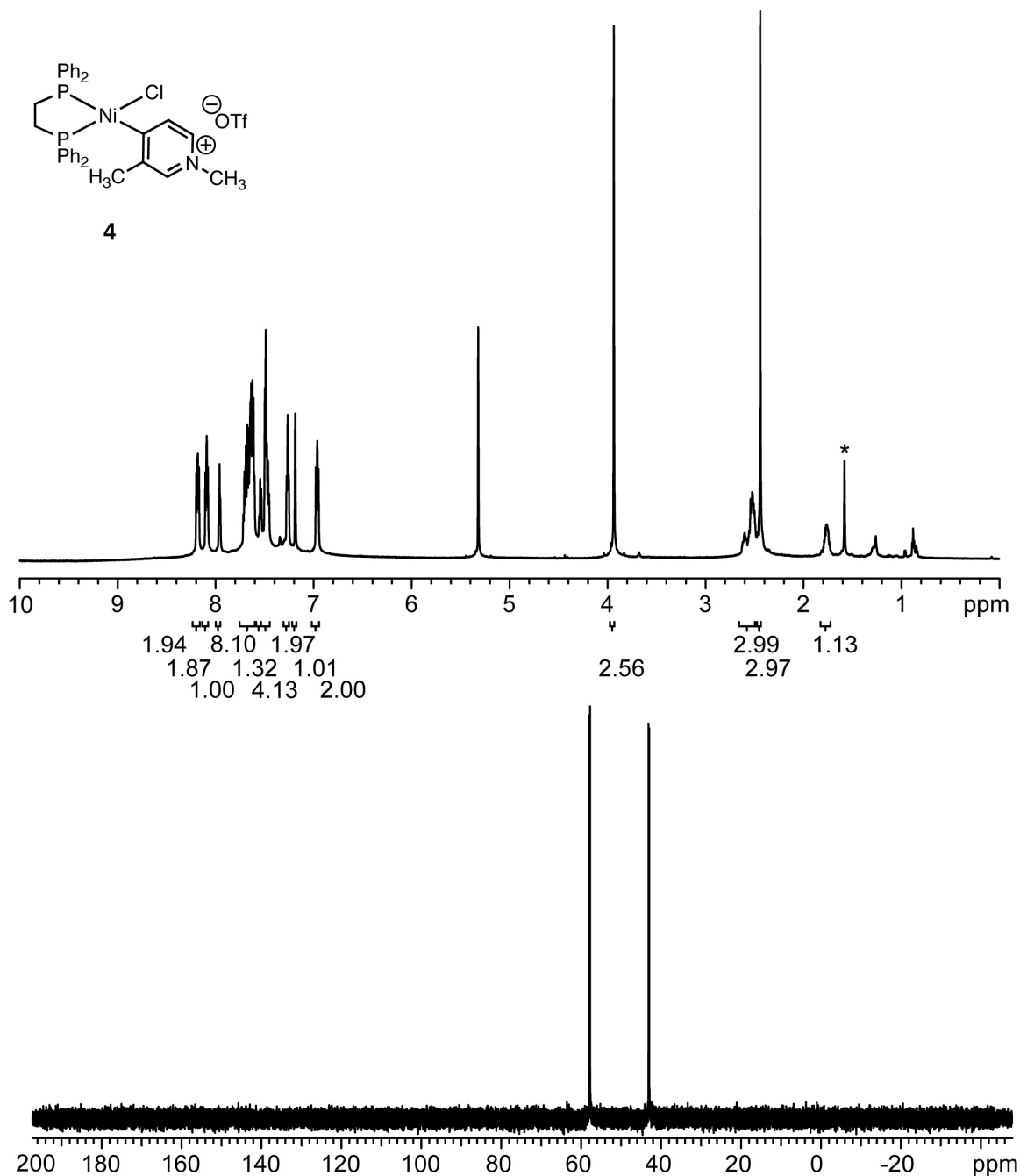
IV. NMR Spectra
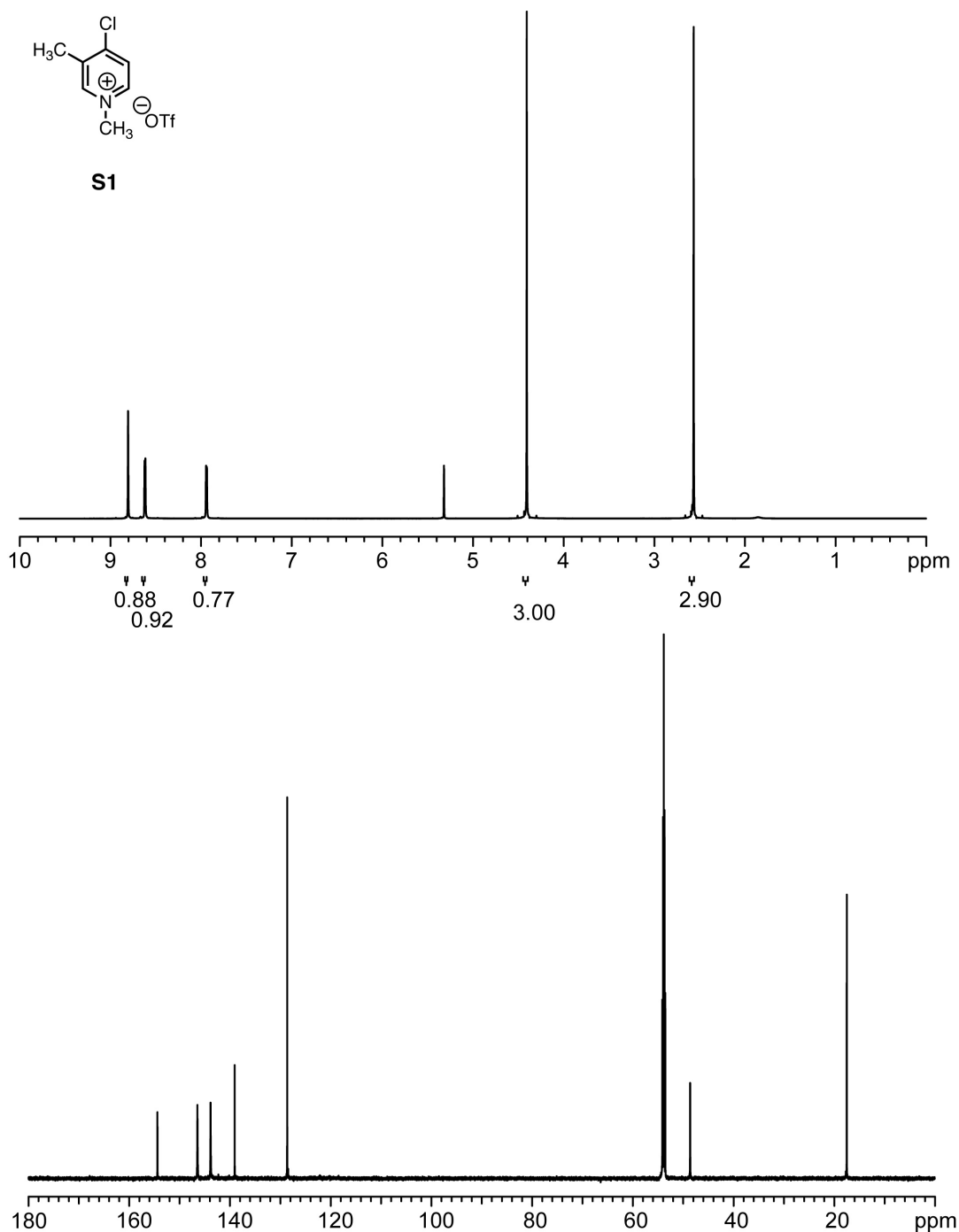
Figure S3-1. ^{1}H and ^{13}C NMR spectra of **S1**.
^{1}H NMR (700 MHz, CD$_2$Cl$_2$) δ 8.81 (s, 1H), 8.62 (d, J = 6.3 Hz, 1H), 7.94 (d, J = 6.3 Hz, 1H), 4.41 (s, 3H), 2.57 (s, 1H). ^{13}C NMR (176 MHz, CDCl$_3$) δ 154.39, 146.45, 143.84, 139.05, 128.63, 48.61, 17.51. *^{13}C peaks for CF$_3$ of triflate counterion was expected at around 115 ppm as a quartet[5] but it is often unobserved.[1]

194

Figure S3-2. ^{1}H and ^{31}P NMR spectra of **S2**.

^{1}H NMR (500 MHz, CD$_2$Cl$_2$) δ 7.65 (q, J = 6.0 Hz, 12H), 7.57 (d, J = 6.0 Hz, 1H), 7.49 (at, J = 7.5 Hz, 6H), 7.39 (at, J = 7.5 Hz, 12H), 6.93 (d, J = 5.5 Hz, 1H), 6.73 (s, 1H), 3.70 (s, 3H), 2.64 (s, 3H). *residual H$_2$O. ^{31}P NMR (202 MHz, CD$_2$Cl$_2$) δ 21.35.

195

Figure S3-3. ^{1}H and ^{31}P NMR spectra of **4**.
^{1}H NMR (700 MHz, CD_2Cl_2) δ 8.20–8.17 (m, 2H), 8.09 (at, J = 8.4 Hz, 2H), 7.96 (at, J = 5.5 Hz, 1H), 7.72–7.60 (m, 8H), 7.56–7.53 (m, 1H), 7.50–7.46 (m, 4H), 7.26 (at, J = 7.4 Hz, 2H), 7.19 (s, 1H), 6.96 (at, J = 8.4 Hz, 2H), 3.94 (s, 3H), 2.62–2.50 (m, 3H), 2.44 (s, 3H), 1.82–1.73 (m, 1H). *residual H_2O. ^{31}P NMR (283 MHz, CD_2Cl_2) δ 57.84 (d, J = 39.1 Hz), 43.03 (d, J = 40.2 Hz).
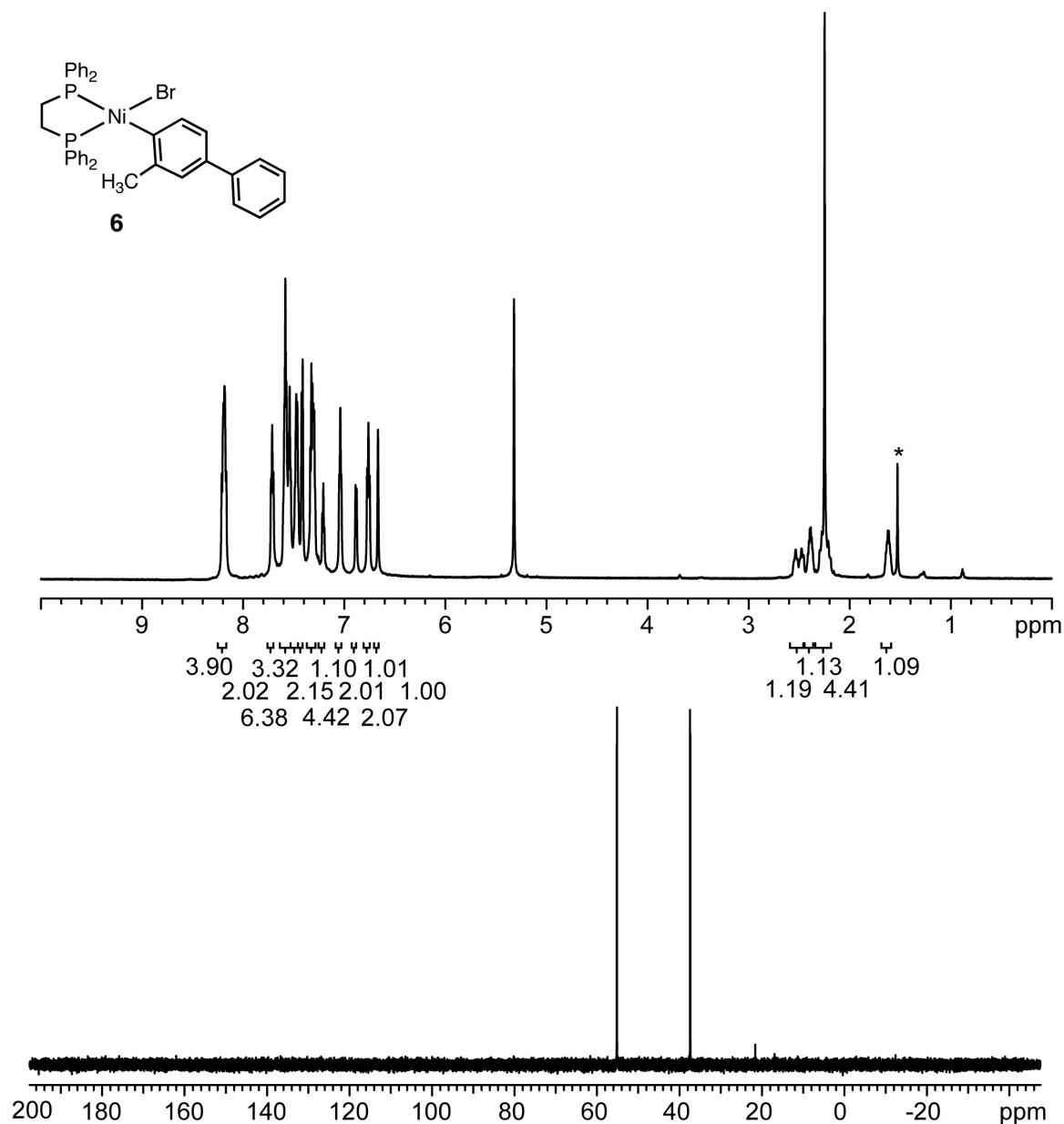
Figure S3-4. ^{1}H and ^{31}P NMR spectra of **6**.
^{1}H NMR (700 MHz, CD$_2$Cl$_2$) δ 8.21–8.17 (m, 4H), 7.71 (at, J = 9.1 Hz, 2H), 7.59–7.41 (m, 12H), 7.34–7.30 (m, 4H), 7.21 (at, J = 7.0 Hz, 1H), 7.04 (at, J = 6.3 Hz, 1H), 6.88 (d, J = 7.7 Hz, 1H), 6.76 (at, J = 9.8 Hz, 2H), 6.67 (s, 1H), 2.51 (dt, J = 40.6, 13.3 Hz, 1H), 2.41–2.37 (m, 1H), 2.28–2.22 (m, 4H), 1.63–1.62 (m, 1H). *residual H$_2$O. ^{31}P NMR (283 MHz, CD$_2$Cl$_2$) δ 55.16 (d, J = 19.0 Hz), 37.4 (d, J = 20.1 Hz).

197
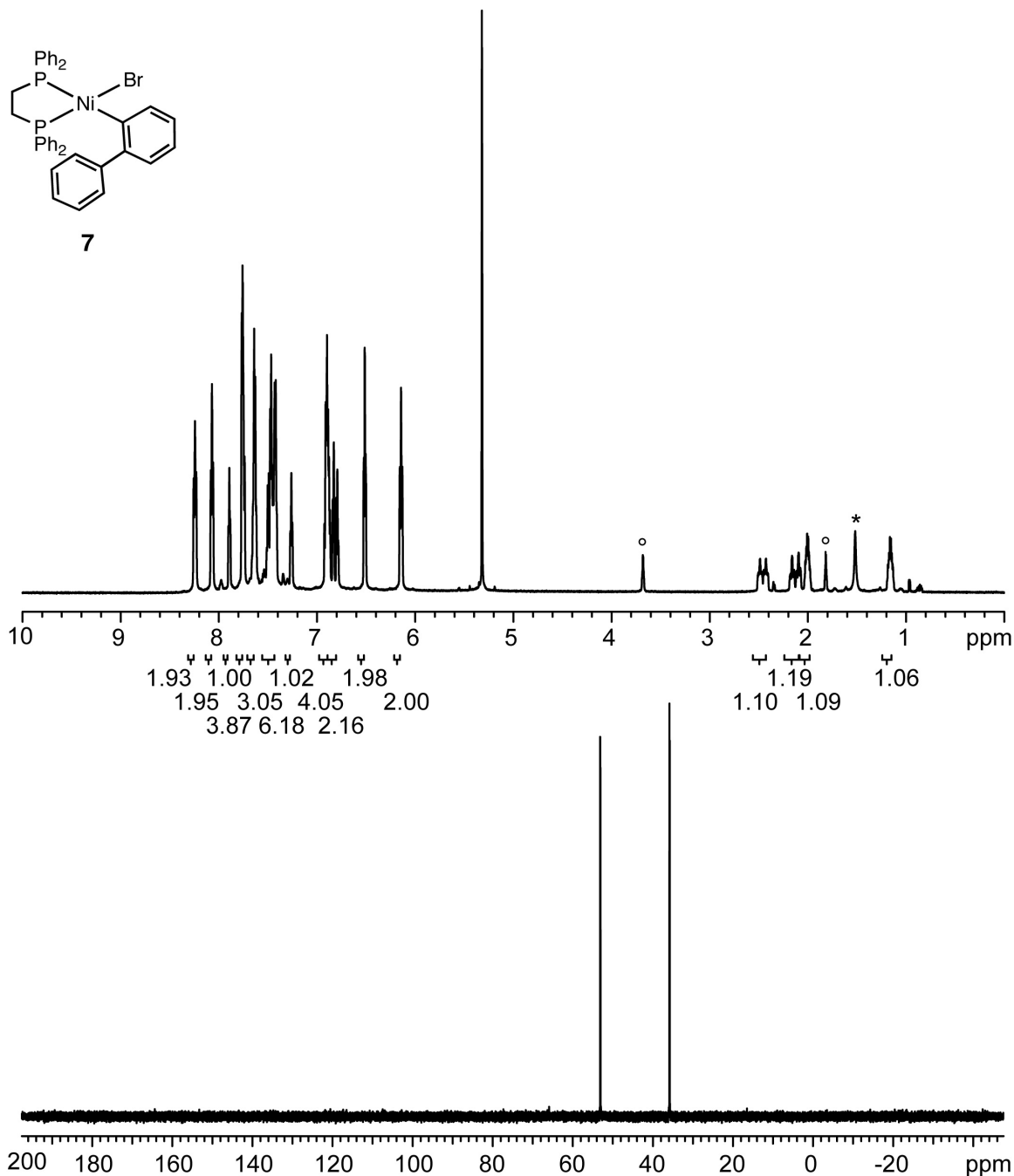
Figure S3-5. ^{1}H and ^{31}P NMR spectra of **7**.

^{1}H NMR (700 MHz, CD$_2$Cl$_2$) δ 8.24 (at, J = 9.1 Hz, 2H), 8.07 (at, J = 8.0 Hz, 2H), 7.89 (at, J = 8.2 Hz, 1H), 7.77–7.74 (m, 4H), 7.65–7.62 (m, 3H), 7.51–7.41 (m, 6H), 7.26 (at, J = 7.3 Hz, 1H), 6.92–6.87 (m, 4H), 6.84–6.78 (m, 2H), 6.52–6.50 (m, 2H), 6.15 (at, J = 8.6 Hz, 2H), 2.46 (dt, J = 42.0, 11.9 Hz, 1H), 2.12 (dt, J = 56.7, 14.0 Hz, 1H), 2.02–1.98 (m, 1H), 1.18–1.14 (m, 1H). residual *H$_2$O and °THF. ^{31}P NMR (283 MHz, CD$_2$Cl$_2$) δ 53.10 (d, J = 22.4 Hz), 35.82 (d, J = 22.4 Hz).
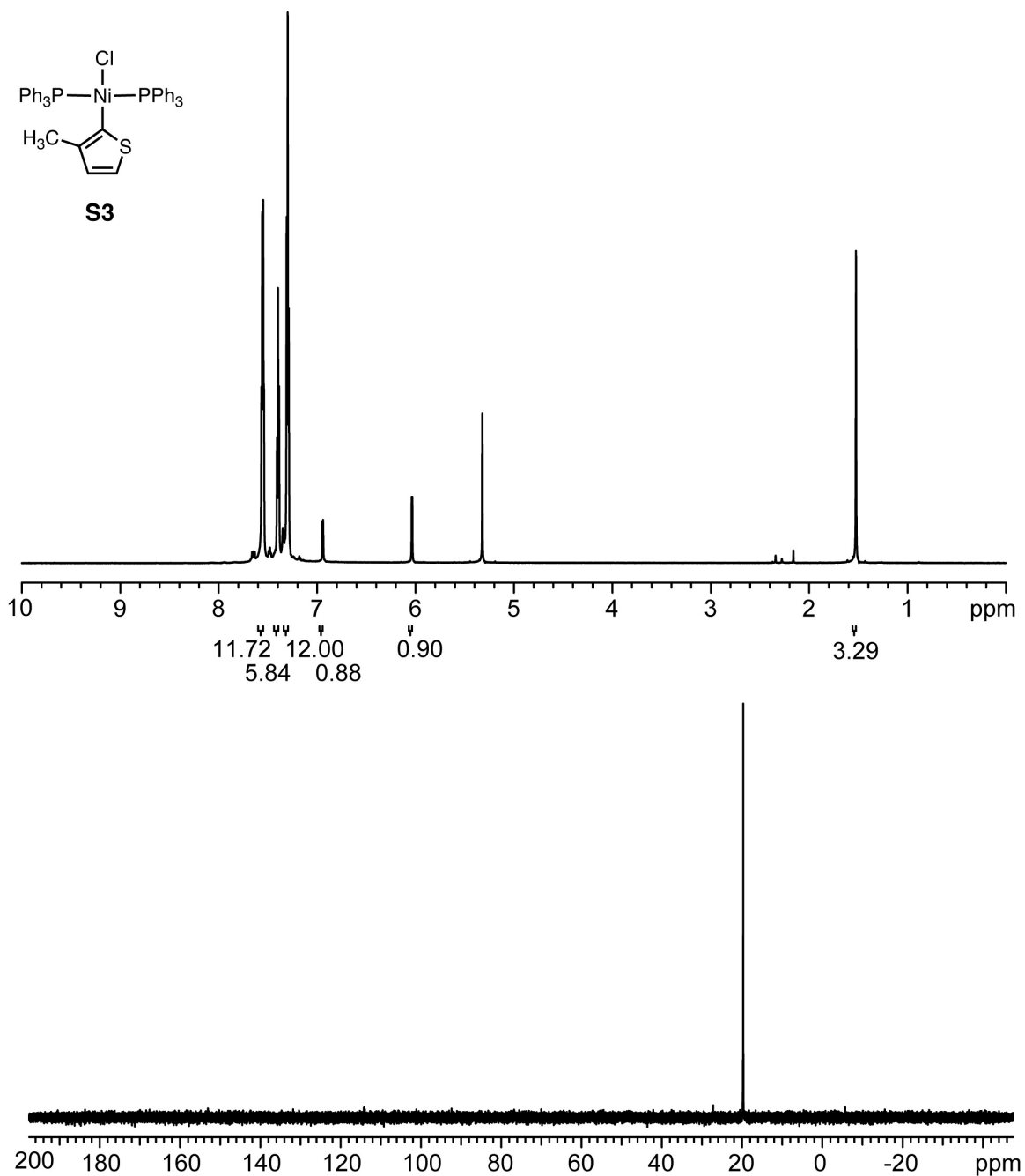
Figure S3-6. ^{1}H and ^{31}P NMR spectra of **S3**.
^{1}H NMR (700 MHz, CD$_2$Cl$_2$) δ 7.55 (q, J = 5.8 Hz, 12H), 7.40 (at, J = 7.7 Hz, 6H), 7.30 (at, J = 7.7 Hz, 12H), 6.94 (d, J = 4.2 Hz, 1H), 6.04 (d, J = 4.2 Hz, 1H), 1.52 (s, 3H). ^{31}P NMR (283 MHz, CD$_2$Cl$_2$) δ 19.69.
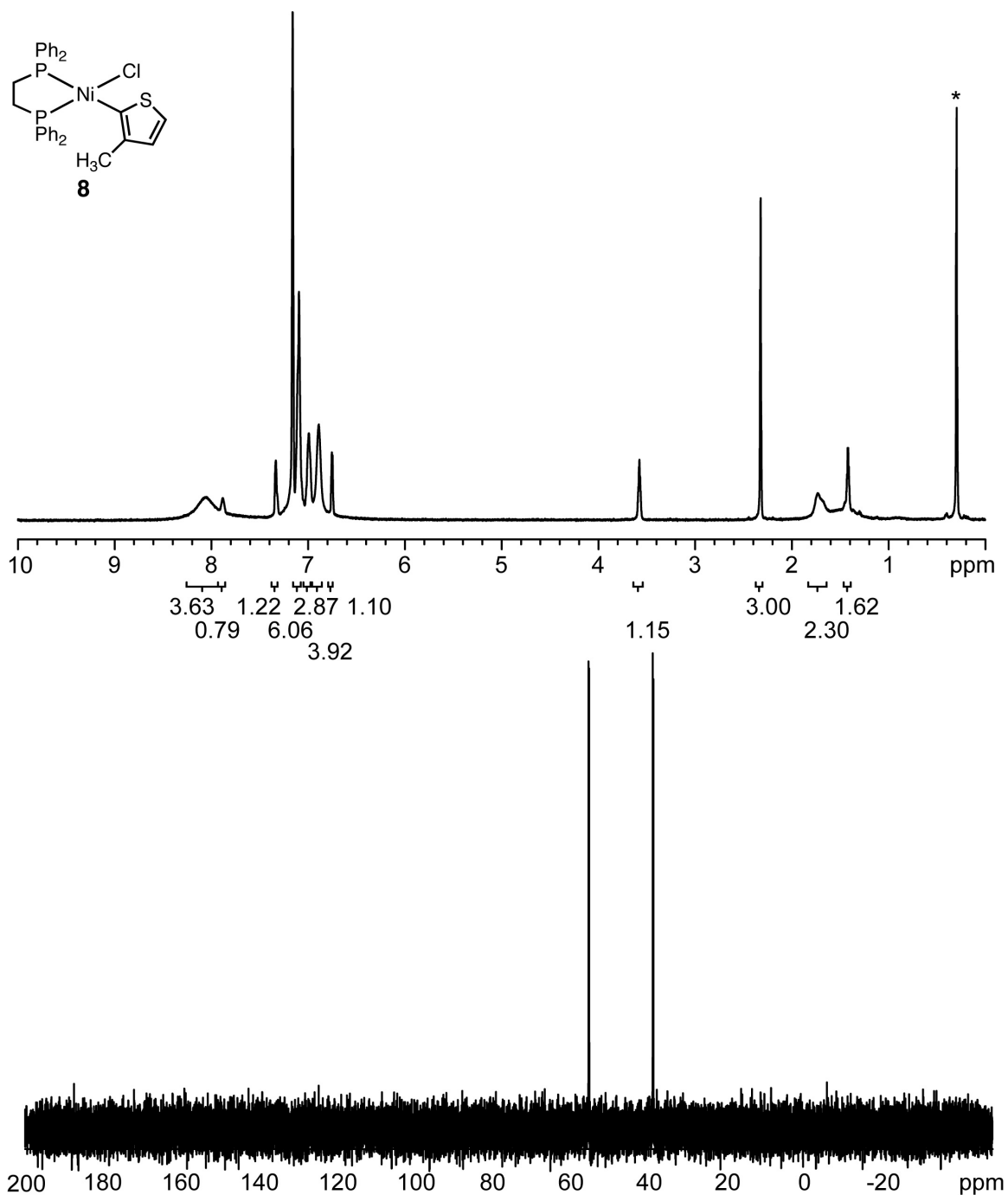
Figure S3-7. ^{1}H and ^{31}P NMR spectra of **8**.
^{1}H NMR (500 MHz, C_6D_6) δ 8.05 (bs, 4H), 7.88 (bs, 1H), 7.35–7.31 (m, 1H), 7.14–7.06 (m, 6H), 7.20–6.96 (m, 3H), 6.89 (bs, 4H), 6.77–6.74 (bs, 1H), 3.60–3.56 (m, 1H), 2.33 (s, 3H), 1.73 (bs, 2H), 1.44–1.41 (m, 1H). *residual grease from C_6D_6. ^{31}P NMR (202 MHz, C_6D_6) δ 54.59 (d, J = 33.5 Hz), 38.20 (d, J = 33.5 Hz).
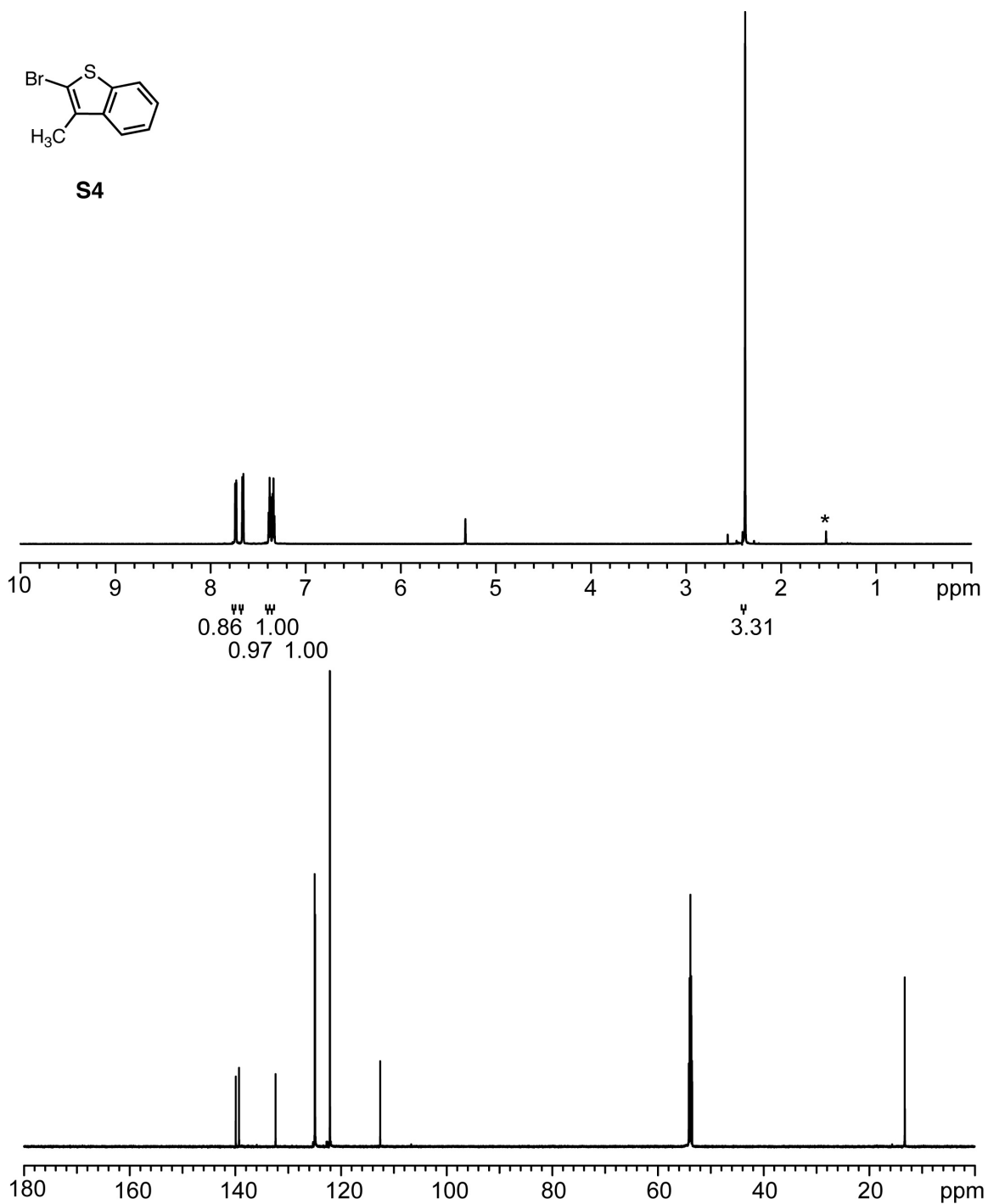
Figure S3-8. ¹H and ¹³C NMR spectra of **S4**.
¹H NMR (700 MHz, CD₂Cl₂) δ 7.74 (d, *J* = 7.7 Hz, 1H), 7.66 (d, *J* = 8.4 Hz, 1H), 7.38 (at, *J* = 7.7 Hz, 1H), 7.34 (at, *J* = 7.7 Hz, 1H), 2.21 (s, 3H). *residual H₂O.
¹³C NMR (176 MHz, CD₂Cl₂) δ 139.91, 139.29, 132.39, 124.98, 124.90, 122.10, 112.58, 13.28.
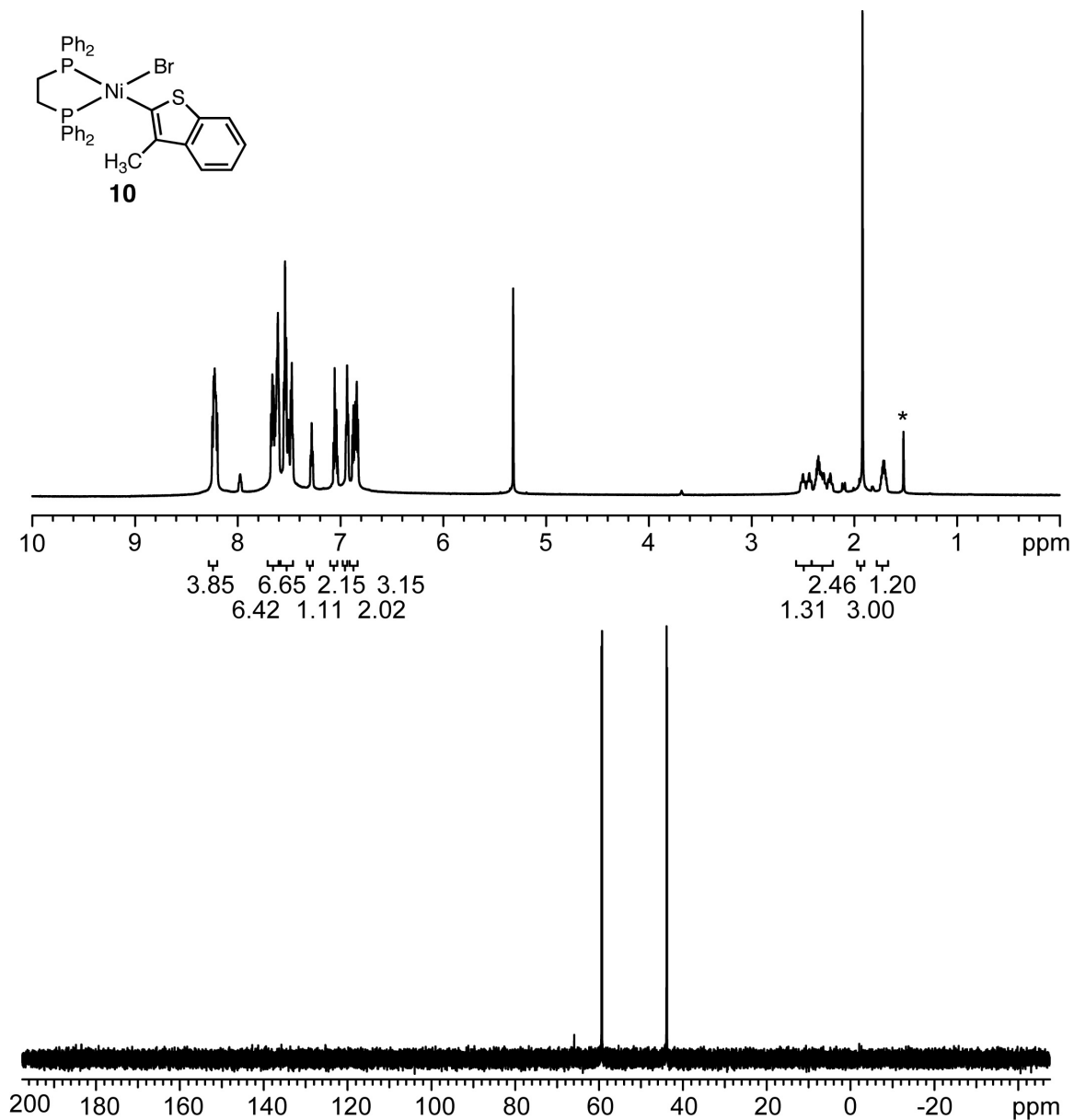
Figure S3-9. ^{1}H and ^{31}P NMR spectra of **10**.
^{1}H NMR (700 MHz, CD_2Cl_2) δ 8.25–8.20 (m, 4H), 7.68–7.61 (m, 6H), 7.55–7.46 (m, 6H), 7.28 (at, J = 7.3 Hz, 1H), 7.07–7.03 (m, 2H), 6.94 (at, J = 7.7 Hz, 2H), 6.89–6.83 (m, 3H), 2.47 (td, J = 42.7, 11.2 Hz, 1H), 2.38–2.22 (m, 2H), 1.92 (s, 3H), 1.74–1.69 (m, 1H). *residual H_2O. ^{31}P NMR (283 MHz, CD_2Cl_2) δ 59.32 (d, J = 35.9 Hz), 43.82 (d, J = 35.9 Hz).

V. Initiation Rate Studies

Representative Procedure for Performing React IR Initiation Rate Studies:
The IR probe was inserted through an O-ring sealed 14/20 ground glass adapter (custom-made) into an oven-dried 50 mL 2-neck flask equipped with a stir bar. The other neck was fitted with a three-way adapter with a septum for injections/aliquot sampling and an N_2 line. The oven-dried flask was cooled under vacuum. The flask was then filled with N_2 and evacuated again for a total of three cycles. The flask was charged with THF (6.7 mL) and cooled to 0 °C over 15 min. After recording a background spectrum, monomer **1** (2.3 mL, 0.44 M in THF, 1.0 equiv) was added by syringe and allowed to equilibrate for at least 5 min at 0 °C before proceeding. The catalyst solution (1.0 mL, 0.015 M, 0.015 equiv) was then injected and spectra were recorded every 15 s over the entire reaction. To account for mixing and temperature equilibration, spectra recorded in the first 60 s of the reaction were discarded and the initial rate was calculated from 10% monomer conversion after the first 60s.

Representative Procedure for Preparing Pre-Initiated Ni(dppe)Cl$_2$ Stock Solution:
A 4 mL vial was equipped with a stir bar in the glovebox. Sequentially, Ni(dppe)Cl$_2$ (13.5 mg, 0.0256 mmol, 1.0 equiv), THF (1.1 mL), and **1** (0.58 mL, 0.44 M, 10 equiv) were added to the flask. The reaction mixture was stirred for 10 min until homogeneous. The final catalyst solution concentration was 0.015M.
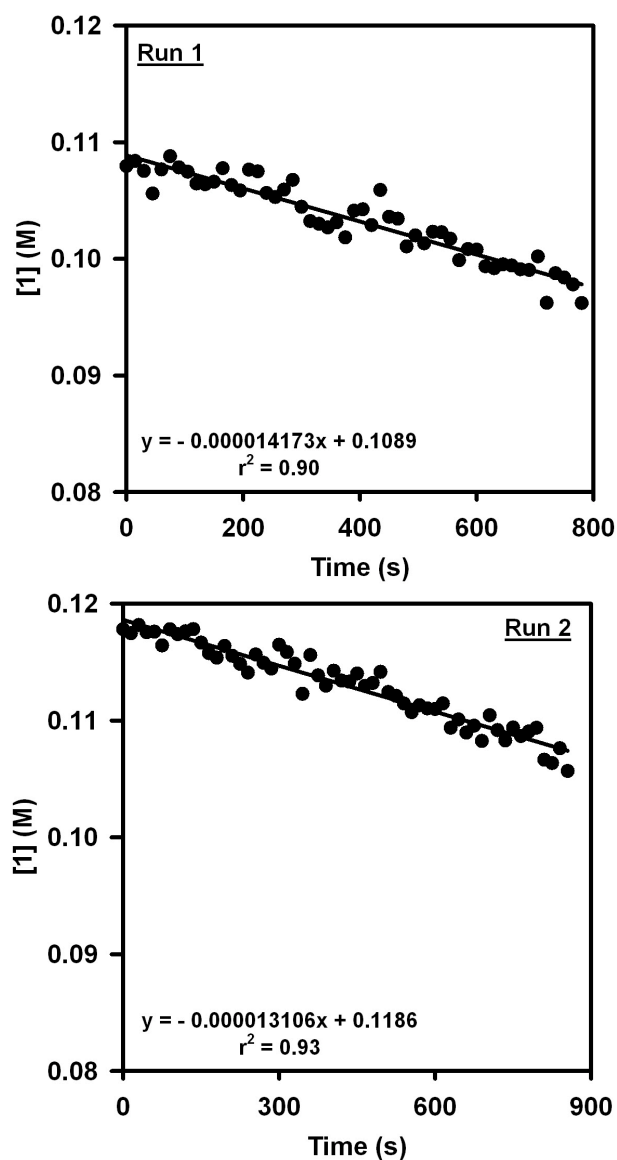
Figure S3-10. Plot of [monomer] versus time for the polymerization catalyzed by **4**. (temp = 0 °C, [**4**] = 0.0015 M, [**1**] = 0.11 M (Run 1), 0.12 M (Run 2)).

Table S3-1. Table of data for the plot in Figure S3-10.

Run	Initial rate (M s^{-1})	k_{obs} (s^{-1})	Time (s)	Calculated k_i (s^{-1})
1	14.2 x 10^{-6}	9.45 x 10^{-3}	780	1.53 x 10^{-3}
2	13.1 x 10^{-6}	8.74 x 10^{-3}	855	1.21 x 10^{-3}
average	13.6 ± 0.8 x 10^{-6}	9.1 ± 0.5 x 10^{-3}		1.4 ± 0.2 x 10^{-3}

Figure S3-11. Plot of [monomer] versus time for the polymerization catalyzed by **6**. (temp = 0 °C, [**6**] = 0.0015 M, [**1**] = 0.11 M (Run 1), 0.11 M (Run 2)).

Table S3-2. Table of data for the plot in Figure S3-11.

Run	Initial rate $(M\ s^{-1})$	k_{obs} (s^{-1})	Time (s)	Calculated k_i (s^{-1})
1	23.5×10^{-6}	15.7×10^{-3}	420	_[a]
2	17.3×10^{-6}	11.5×10^{-3}	555	3.44×10^{-3}
average	$20 \pm 4 \times 10^{-6}$	$14 \pm 3 \times 10^{-3}$		

[a]Mathematica solve function does not work when k_{obs} is greater than the k_p.
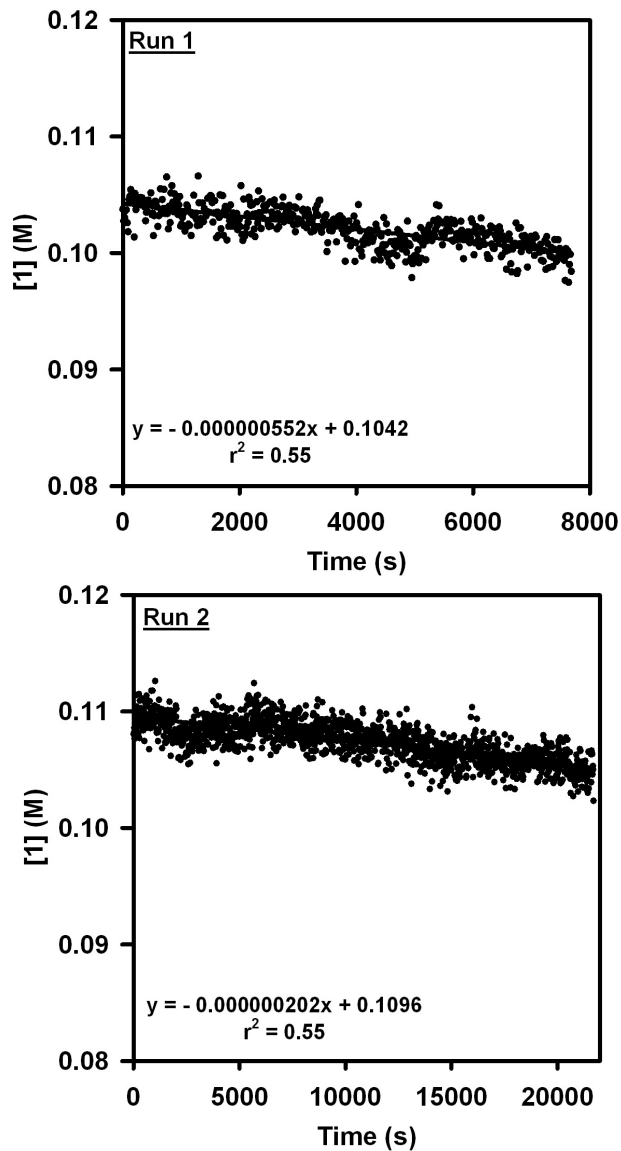
Figure S3-12. Plot of [monomer] versus time for the polymerization catalyzed by **7**. (temp = 0 °C, [**7**] = 0.0015 M, [**1**] = 0.10 M (Run 1), 0.11 M (Run 2)).
*Due to low solubility of precatlyst **7**, the catalyst solution (2.0 mL, 0.0075 M, 0.015 equiv) was used.

Table S3-3. Table of data for the plot in Figure S3-12.

Run	Initial rate $(M\ s^{-1})^*$	k_{obs} (s^{-1})	Time (s)	Calculated k_i (s^{-1})
1	0.552×10^{-6}	0.368×10^{-3}	7680	3.73×10^{-6}
2	0.202×10^{-6}	0.135×10^{-3}	21705	0.483×10^{-6}
average	$0.4 \pm 0.2 \times 10^{-6}$	$0.3 \pm 0.2 \times 10^{-3}$		$2 \pm 2 \times 10^{-6}$

*for 5% monomer conversion. The initiation may be so slow that the induction period is significantly affected by any small amount of catalyst undergoing propagation, thus, making it difficult to get an accurate rate at 5% conversion. Additionally, increased reaction time will result in quenching of the Grignard monomer, which affects the % monomer conversion.
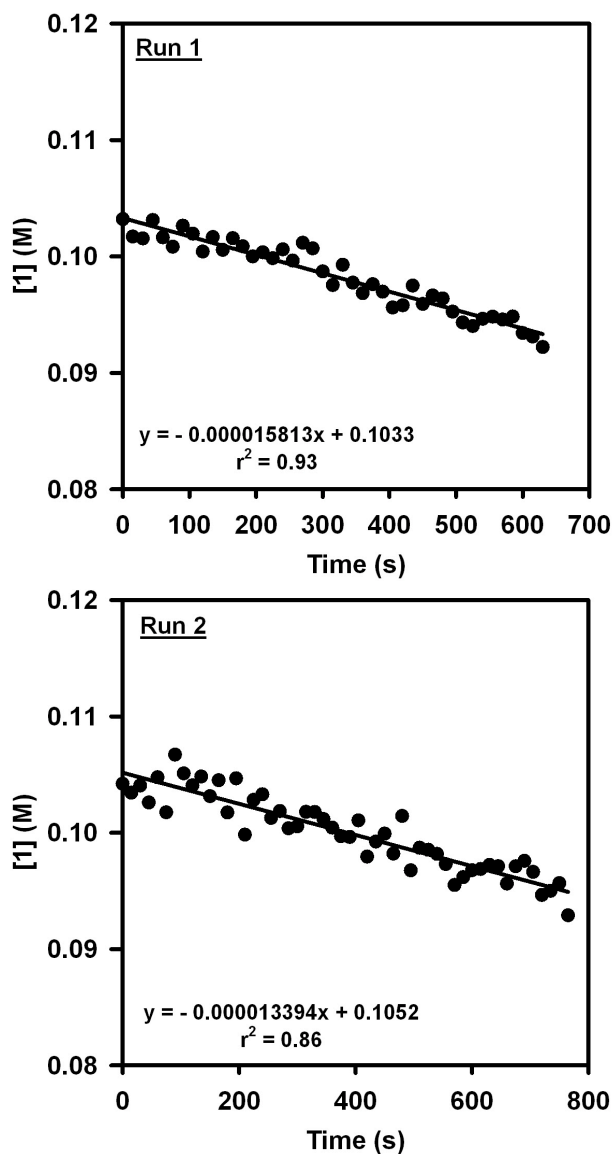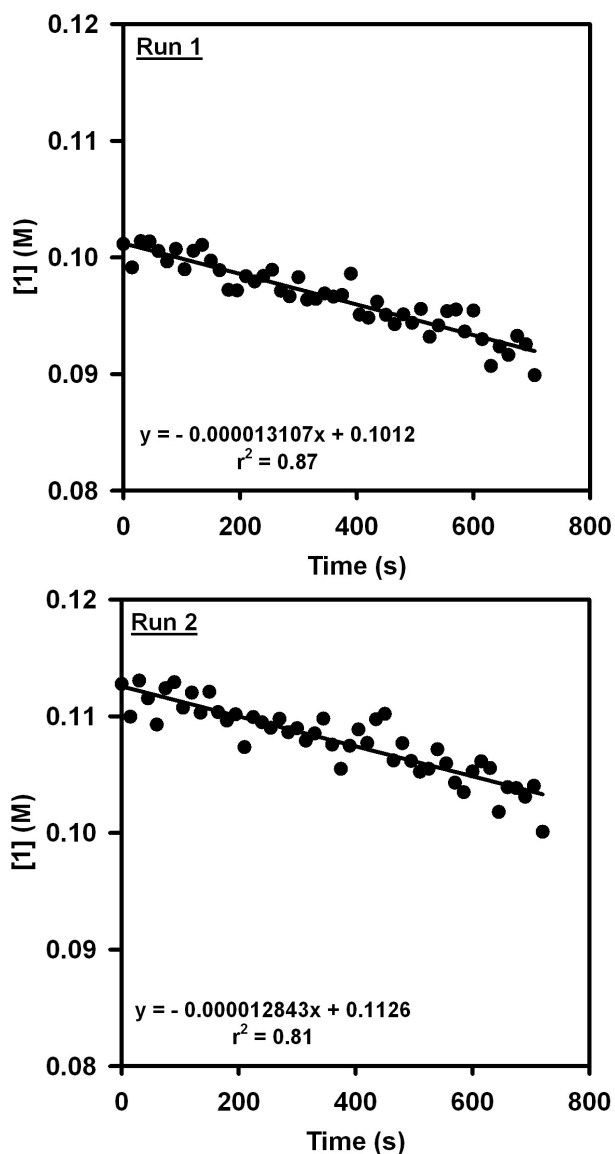
Figure S3-13. Plot of [monomer] versus time for the polymerization catalyzed by **8**. (temp = 0 °C, [**8**] = 0.0015 M, [**1**] = 0.10 M (Run 1), 0.10 M (Run 2)).

Table S3-4. Table of data for the plot in Figure S3-13.

Run	Initial rate $(M\ s^{-1})$	k_{obs} (s^{-1})	Time (s)	Calculated k_i (s^{-1})
1	15.8×10^{-6}	10.5×10^{-3}	630	2.35×10^{-3}
2	13.4×10^{-6}	8.93×10^{-3}	765	1.39×10^{-3}
average	$15 \pm 2 \times 10^{-6}$	$10 \pm 1 \times 10^{-3}$		$1.9 \pm 0.7 \times 10^{-3}$

Figure S3-14. Plot of [monomer] versus time for the polymerization catalyzed by **10**. (temp = 0 °C, [**10**] = 0.0015 M, [**1**] = 0.10 M (Run 1), 0.11 M (Run 2)). *Due to low solubility of precatlyst **10**, the catalyst solution (2.0 mL, 0.0075 M, 0.015 equiv) was used.

Table S3-5. Table of data for the plot in Figure S3-14.

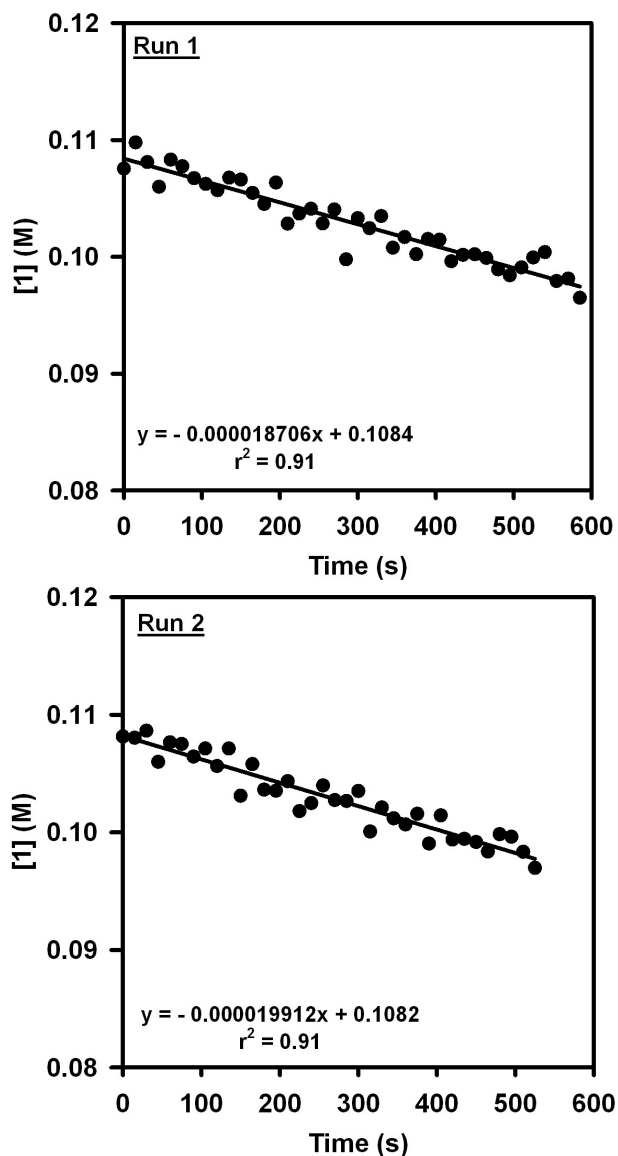| Run	Initial rate (M s^{-1})	k_{obs} (s^{-1})	Time (s)	Calculated k_i (s^{-1})
1	13.1 x 10^{-6}	8.56 x 10^{-3}	630	1.38 x 10^{-3}
2	12.8 x 10^{-6}	8.74 x 10^{-3}	765	1.41 x 10^{-3}
average	13.0 ± 0.2 x 10^{-6}	8.7 ± 0.1 x 10^{-3}		1.40 ± 0.02 x 10^{-3}

Figure S3-15. Plot of [monomer] versus time for the polymerization catalyzed by **12**. (temp = 0 °C, [**12**] = 0.0015 M, [**1**] = 0.11 M (Run 1), 0.11 M (Run 2)).

Table S3-6. Table of data for the plot in Figure S3-15.

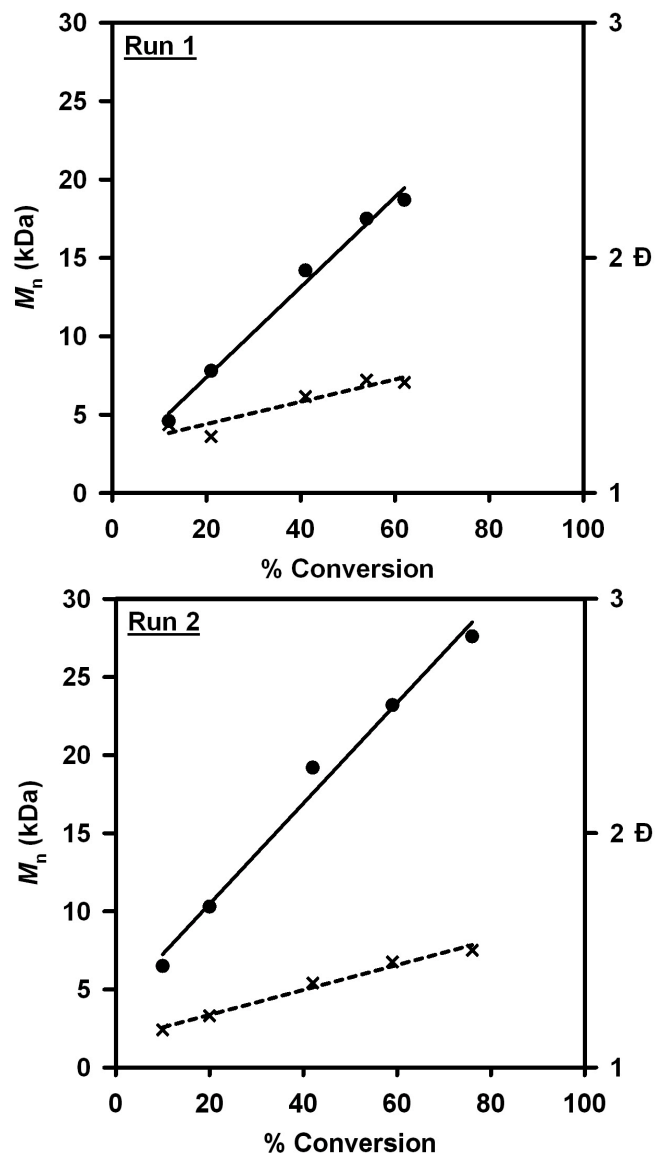| Run	Initial rate $(M\,s^{-1})$	k_{obs} (s^{-1})
1	18.7×10^{-6}	12.5×10^{-3}
2	19.9×10^{-6}	13.3×10^{-3}
average	$19.3 \pm 0.9 \times 10^{-6}$	$12.9 \pm 0.6 \times 10^{-3}$

VI. Polymerization

Representative Procedure for M_n and Đ versus Conversion Studies utilizing in situ React IR Spectroscopy:
The IR probe was inserted through an O-ring sealed 14/20 ground glass adapter (custom-made) into an oven-dried 50 mL 2-neck flask equipped with a stir bar. The other neck was fitted with a three-way adapter with a septum for injections/aliquot sampling and an N_2 line. The oven-dried flask was cooled under vacuum. The flask was then filled with N_2 and evacuated again for a total of three cycles. The flask was charged with THF (6.7 mL) and cooled to 0 °C over 15 min. After recording a background spectrum, monomer **1** (2.3 mL, 0.44 M in THF, 1.0 equiv) was added by syringe and allowed to equilibrate for at least 5 min at 0 °C before proceeding. The catalyst solution (1.0 mL, 0.015 M, 0.015 equiv) was then injected and spectra were recorded every 15 s over the entire reaction. To account for mixing and temperature equilibration, spectra recorded in the first 60 s of the reaction were discarded. Aliquots (~0.5 mL) were taken through the three-way adapter via syringe and immediately quenched with 12 M HCl (~1 mL). Each aliquot was then extracted with CH_2Cl_2 (2 x 1.5 mL) (with mild heating if polymer had precipitated), dried over $MgSO_4$, filtered, and then concentrated. The samples were dissolved in THF (with heating), and passed through a 0.2 μm PTFE filter for GPC analysis.
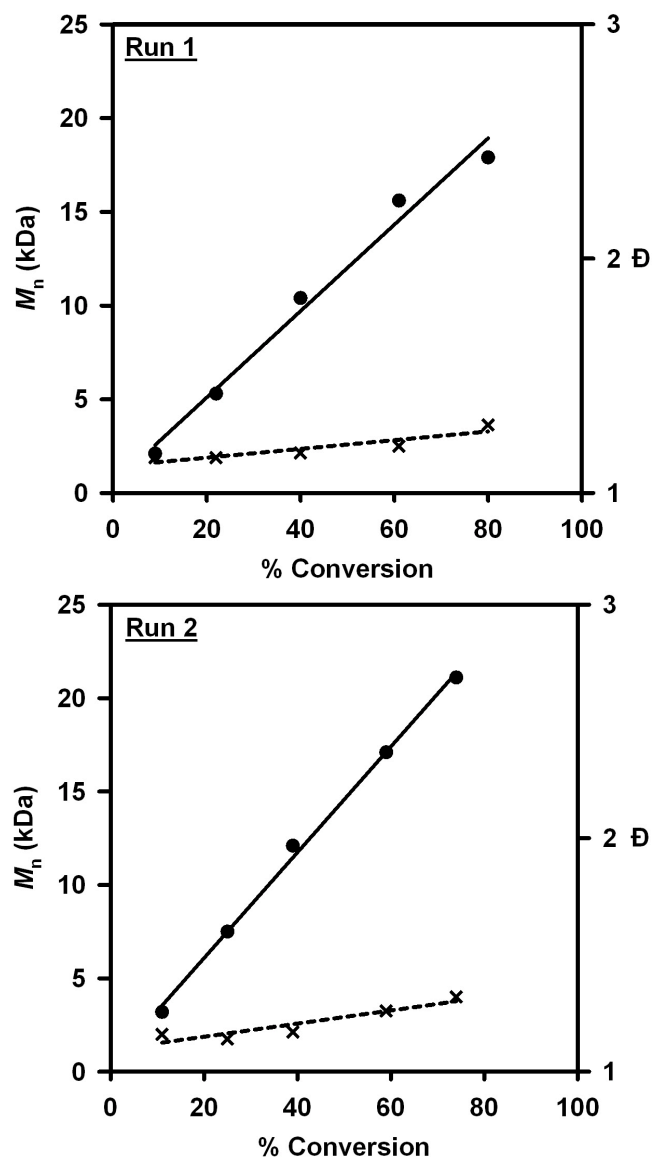
Figure S3-16. Plot of M_n (●) and Đ (**x**) versus conversion for precatalyst **4** (temp = 0 °C, [**4**] = 0.0015 M, [**1**] = 0.11 M (Run 1), 0.12 M (Run 2)).

Table S3-7. Data for the plot in Figure S3-16, Run 1.

% Conversion	M_n (kDa)	Đ
12	4.6	1.29
21	7.8	1.24
41	14.2	1.41
54	17.5	1.48
62	18.7	1.47

Table S3-8. Data for the plot in Figure S3-16, Run 2.

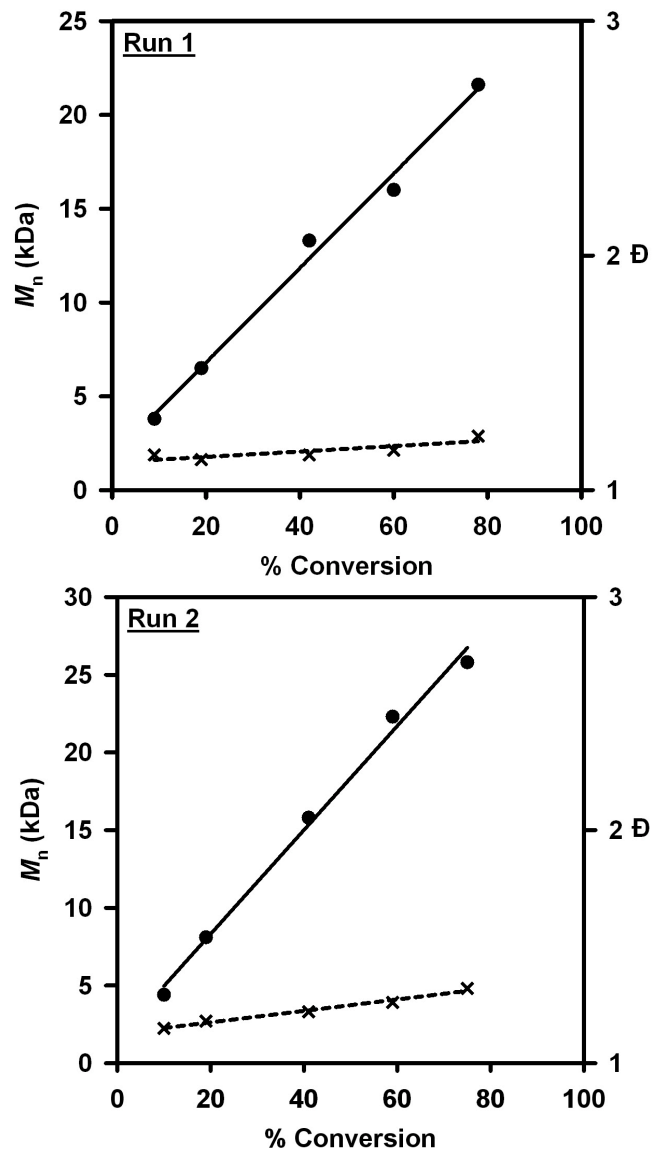| % Conversion	M_n (kDa)	Đ
10	6.5	1.16
20	10.3	1.22
42	19.2	1.36
59	23.2	1.45
76	27.6	1.50

Figure S3-17. Plot of M_n (●) and Đ (**x**) versus conversion for precatalyst **6** (temp = 0 °C, [**6**] = 0.0015 M, [**1**] = 0.11 M (Run 1), 0.11 M (Run 2)).

Table S3-9. Data for the plot in Figure S3-17, Run 1.

% Conversion	M_n (kDa)	Đ
9	2.1	1.15
22	5.3	1.15
40	10.4	1.17
61	15.6	1.20
80	17.9	1.29

Table S3-10. Data for the plot in Figure S3-17, Run 2.

| % Conversion	M_n (kDa)	Đ
11	3.2	1.16
25	7.5	1.14
39	12.1	1.17
59	17.1	1.26
74	21.1	1.32

Figure S3-18. Plot of M_n (●) and Đ (**x**) versus conversion for precatalyst **8** (temp = 0 °C, [**8**] = 0.0015 M, [**1**] = 0.10 M (Run 1), 0.10 M (Run 2)).

Table S3-11. Data for the plot in Figure S3-18, Run 1.

% Conversion	M_n (kDa)	Đ
9	3.8	1.15
19	6.5	1.13
42	13.3	1.15
60	16.0	1.17
78	21.6	1.23

Table S3-12. Data for the plot in Figure S3-18, Run 2.

% Conversion	M_n (kDa)	Đ
10	4.4	1.15
19	8.1	1.18
41	15.8	1.22
59	22.3	1.26
75	25.8	1.32
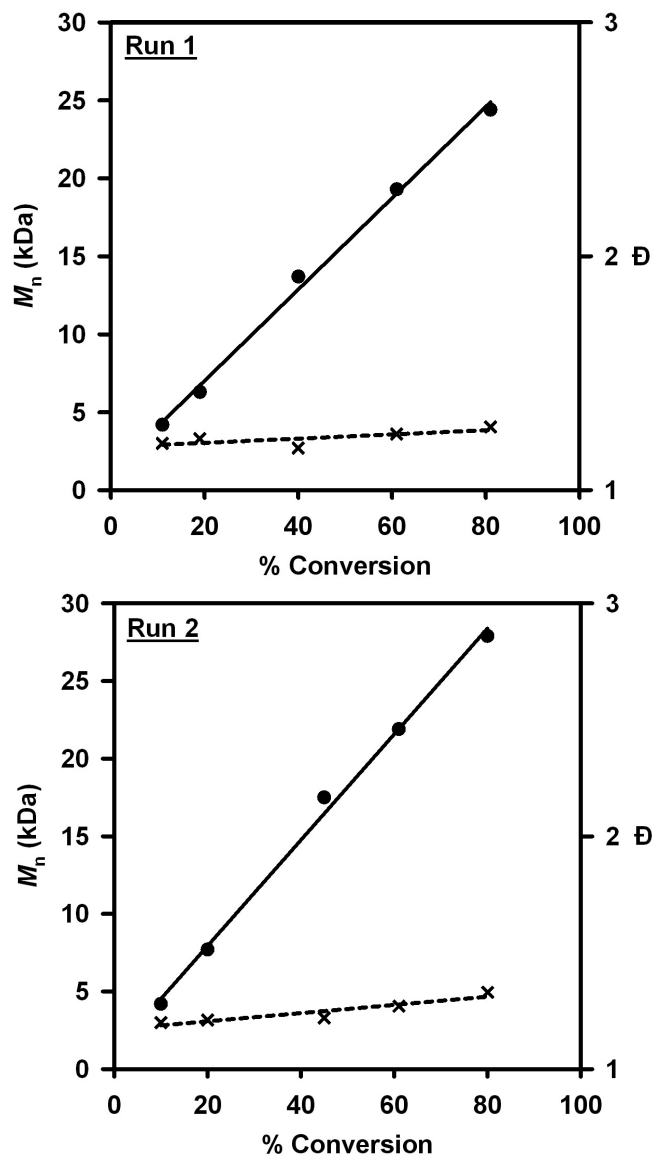
Figure S3-19. Plot of M_n (●) and Đ (**x**) versus conversion for precatalyst **10** (temp = 0 °C, [**10**] = 0.0015 M, [**1**] = 0.10 M (Run 1), 0.11 M (Run 2)).
*Due to low solubility of precatlyst **10**, the catalyst solution (2.0 mL, 0.0075 M, 0.015 equiv) was used.

Table S3-13. Data for the plot in Figure S3-19, Run 1.

% Conversion	M_n (kDa)	Đ
11	4.2	1.20
19	6.3	1.22
40	13.7	1.18
61	19.3	1.24
81	24.4	1.27

Table S3-14. Data for the plot in Figure S3-19, Run 2.

| % Conversion	M_n (kDa)	Đ
10	4.2	1.20
20	7.7	1.21
45	17.5	1.22
61	21.9	1.27
80	27.9	1.33

The aliquot obtained from the M_n and Đ versus conversion study was used for MALDI-TOF MS analysis in linear mode. The sample at 20 or 40% conversion was dissolved in THF (~1 mg/mL).
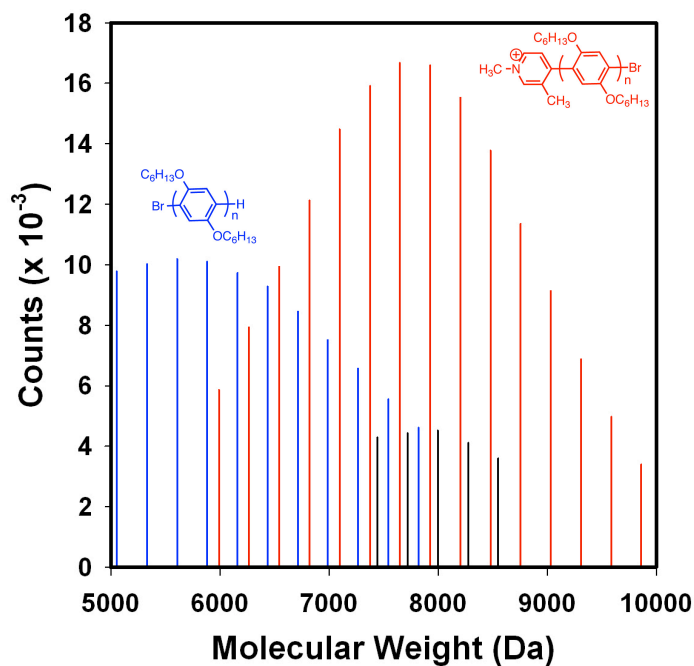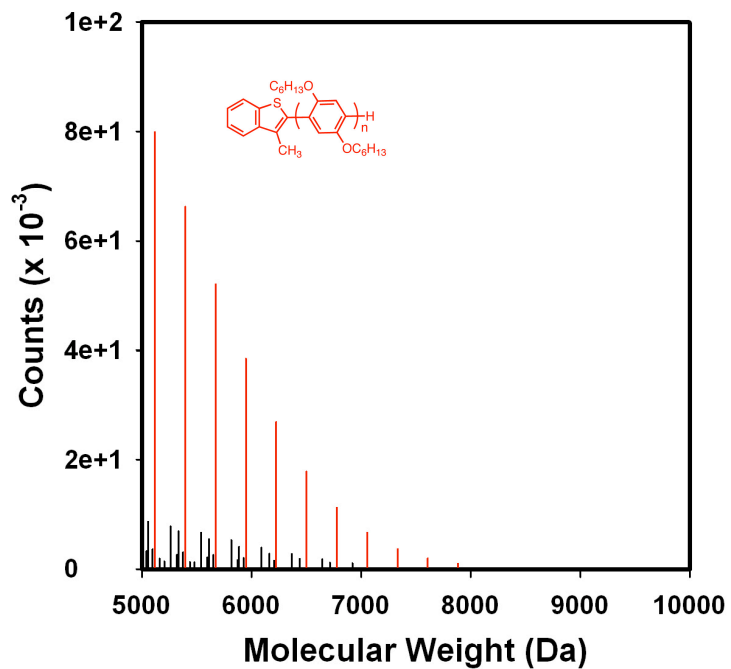

Figure S3-20. MALDI-TOF MS spectrum of **P1** initiated with precatalyst **4** at 20% monomer conversion.
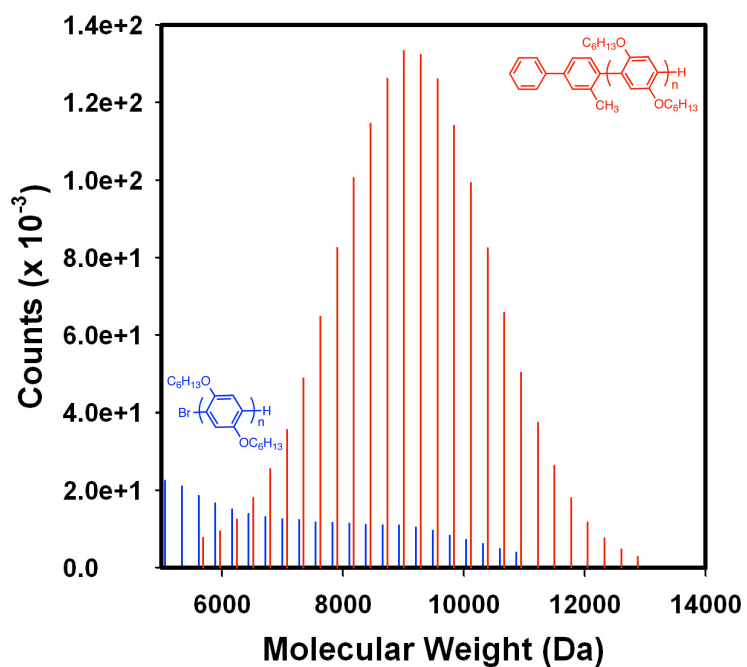
Figure S3-21. MALDI-TOF MS spectrum of **P1** initiated with precatalyst **6** at 40% monomer conversion
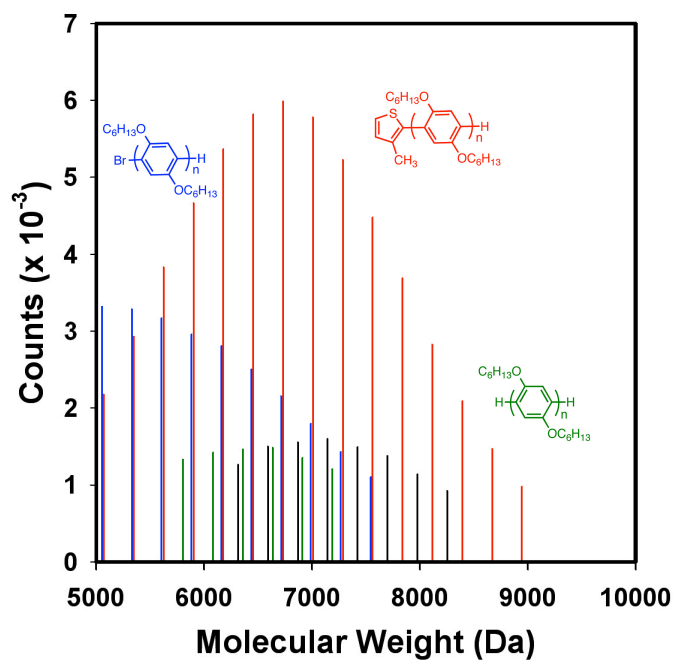
Figure S3-22. MALDI-TOF MS spectrum of **P1** initiated with precatalyst **8** at 20% monomer conversion.

Figure S3-23. MALDI-TOF MS spectrum of **P1** initiated with precatalyst **10** at 20% monomer conversion.

VII. References Cited

(1)   Stander-Grobler, E.; Schuster, O.; Heydenrych, G.; Cronje, S.; Tosh, E.; Albrecht, M.; Frenking, G.; Raubenheimer, H. G. *Organometallics* **2010**, *29*, 5821–5833.

(2)   Collins, E. A.; Garcia-Losada, P.; Hamdouchi, C.; Hipskind, P. A.; Lu, J.; Takakuwa, T. WO/2006/107784 A1.

(3)   Lee, S. R.; Bloom, J. W. G.; Wheeler, S. E.; McNeil, A. J. *Dalton Trans.*, **2013**, *42*, 4218–4222.

(4)   Love, B. E.; Jones, E. G. *J. Org Chem.*, **1999**, *64*, 3755–3756.

(5)   Structurally similar compound, N-Trimethylsilylpyridinium trifluoromethanesulfonate, with reported ^{13}C NMR at 115 ppm (q, J = 320 Hz). For reference, see Klumpp, D. A.; Olah, G. A. *Synthesis* **1997**, *7*, 744–746.